Distribution Agreement

In presenting this thesis or dissertation as a partial fulfillment of the requirements for an advanced degree from Emory University, I hereby grant to Emory University and its agents the non-exclusive license to archive, make accessible, and display my thesis or dissertation in whole or in part in all forms of media, now or hereafter known, including display on the world wide web. I understand that I may select some access restrictions as part of the online submission of this thesis or dissertation. I retain all ownership rights to the copyright of the thesis or dissertation. I also retain the right to use in future works (such as articles or books) all or part of this thesis or dissertation.

Signature:

_____ _____

Yu Hou Date

Chiral Materials and Water Oxidation Catalysts from Transition-Metal-Substituted Polyoxometalates

By

Yu Hou
Doctor of Philosophy

Chemistry

_____
Craig L. Hill
Advisor

_____
Karl S. Hagen
Committee Member

_____
Cora MacBeth
Committee Member

Accepted:

_____
Lisa A. Tedesco, Ph.D.
Dean of the James T. Laney School of Graduate Studies

_____
Date

Chiral Materials and Water Oxidation Catalysts from Transition-Metal-Substituted Polyoxometalates

By

Yu Hou
B.A., Jilin Normal University, China, 2001
M.Sc., Northeast Normal University, China, 2004

Advisor: Craig L. Hill, Ph.D.

An Abstract of
A dissertation submitted to the Faculty of the James T. Laney School of Graduate Studies of Emory University in partial fulfillment of the requirements for the degree of
Doctor of Philosophy in Chemistry

2010

Abstract

Chiral Materials and Water Oxidation Catalysts from Transition-Metal-Substituted Polyoxometalates

By Yu Hou

Polyoxometalates (POMs) are of great importance to both fundamental studies and practical applications, particularly, catalysis. The focus of this thesis is to explore the structural features of polyoxometalates that are closely related to their catalytic properties.

Attempting to synthesize chiral POMs using a lacunary Keggin ligand produced a chiral POM, $[Hf(PW_{11}O_{39})_2]^{10-}$ without chiral organic molecules in the structure. Compound $[Hf(PW_{11}O_{39})_2]^{10-}$ crystallizes in a chiral space group as a conglomerate of two enantiomerically pure crystals in the absence of any chiral source.

Efforts toward synthesizing a ruthenium-containing POM water oxidation catalyst yielded a diruthenium substituted polytungtosilicate, $Cs_6[\{Ru_2O_2(OH_2)_2\}(\gamma\text{-}SiW_{10}O_{36})]\cdot 25H_2O$. Attempts to grow crystals of this compound were unsuccessful. Instead, the polyoxoanion, $[Ru^{IV}{}_4O_4(OH)_2(H_2O)_4(\gamma\text{-}SiW_{10}O_{36})_2]^{10-}$, was obtained by other group members and shown to be capable of oxidizing water to dioxygen in the presence of $[Ru(bpy)_3]^{3+}$ as an oxidant in buffered aqueous solution at *ca.* pH 7. In order to elucidate the mechanism of water oxidation, one-electron-oxidized form with a formula $H_2Ce_{2.5}K(NH_4)_{0.5}[\{Ru^{V}Ru^{IV}{}_3O_6(OH_2)_4\}(\gamma\text{-}SiW_{10}O_{36})_2]\cdot 33H_2O$ was isolated and characterized by single X-ray crystallography, elemental analysis, infrared spectroscopy, UV-vis spectroscopy, and cyclic voltammetry. Its properties are also compared to those of $K_2Rb_8[Ru^{IV}{}_4O_4(OH)_2(H_2O)_4(\gamma\text{-}SiW_{10}O_{36})_2]\cdot 25H_2O$. In addition, the effect of Li^+, Na^+ and K^+ cations on the cyclic voltammograms are also presented in this thesis. In order to obtain less expensive and more efficient water oxidation based on abundant metal elements, polytungstophosphates $Na_2M_2(PW_9O_{34})_2{}^{12-}$ (M = Co, Ni, Mn and Zn) were obtained. Dissolving $Na_2M_2(PW_9O_{34})_2{}^{12-}$ into 1M aqueous LiCl forms $Li_2M_2(PW_9O_{34})_2{}^{12-}$ (M = Co, Ni, Mn and Zn). The use of high valent manganese starting materials produces a new polyoxometalate, $Na_{13}[Mn^{III}(HPW_7O_{28})_2]\cdot 39H_2O$, which exhibits a novel sandwich structure. It also demonstrates that heptatungstate can ligate a 3d metal and represents a rare case of polyoxometalate-based sandwich complex with a single bridging metal.

Chiral Materials and Water Oxidation Catalysts from Transition-Metal-Substituted Polyoxometalates

By

Yu Hou
B.A., Jilin Normal University, China, 2001
M.Sc., Northeast Normal University, China, 2004

Advisor: Craig L. Hill, Ph.D.

A dissertation submitted to the Faculty of the James T. Laney School of Graduate Studies of Emory University in partial fulfillment of the requirements for the degree of Doctor of Philosophy in Chemistry

2010

Acknowledgments

I would like to acknowledge many people for helping me during my doctoral work. My deepest gratitude goes first and foremost to my advisor, Professor Craig L. Hill, for his constant encouragement, patient guidance, invaluable advice and unconditional support. Working with him is a great experience in my whole life.

Secondly, my special thanks go to Dr. Yurii V. Geletii and Dr. Xikui Fang for their generous guidance in research. Dr. Geletii is the person who always gives me instructive suggestions in the research and the one that I can always count on to discuss the tiniest details of a problem. Dr. Fang helped me a lot not only in research but also in daily life.

I am also indebted to the exceptional research committee I have and wish to thank Professor Cora MacBeth and Professor Karl S. Hagen for their continual support, encouragement and precious advice for my research and career development.

I am very grateful for the help from Dr. Kenneth I. Hardcastle, Director of the X-Ray Center at Emory, and the service instructors, Rui Cao and Sheri Lense, for solving the crystal structures. Special thanks also goes to Drs. Wang and Wu for their help in collecting NMR data.

I also thank Dr Lin Xu, our collaborator, for his help in collecting and interpreting magnetic data for my compounds.

I extend many thanks to the previous and current members of the Hill group. Thanks James Wesley Vickers for the thesis proof reading. I would also like to thank Leslie Chauvin for being so organized and helpful to the group.

Last but not least, my thanks would also go to my beloved parents and elder sister, Ye Hou, for their boundless love and whole-hearted support over all these past years. Most importantly, I wish to thank my husband, Song Li, for his love and support through all these years.

Table of Contents

List of Figures

Chapter 1

Chapter 2

Chapter 3

Chapter 4

Chapter 5

List of Schemes

List of Tables

List of Abbreviations

Å	Angstrom
a, *b*, *c*	unit cell axial lengths
An	actinide
anal.	analysis
n-Bu	*n*-butyl
ºC	degrees Celsius
calcd.	calculated
CD	circular dichroism
CIF	crystallographic information file
cm^{-1}	reciprocal centimeter (wavenumber)
DMA	dimethyl acetamide
equiv	equivalent
F(000)	structure factor for the unit cell; it is equal to the total number of electrons in the unit cell
FT-IR	Fourier transform infrared spectroscopy
g	gram(s)
h	hour(s)
Hz	Hertz
J	coupling constant in Hertz
L	ligand
Ln	lanthanide
m	medium (IR)
M	molarity
Me	methyl
mg	milligram(s)
MHz	megahertz
min	minute(s)
mL	milliliter(s)
mmol	millimole
mol	mole
Mr	molecular weight
nm	nanometer
NMR	nuclear magnetic resonance spectroscopy
POM	polyoxometalate
ppm	part per million
R	discrepancy index for crystal structure refinement
s	strong (IR)
sh	shoulder (IR)
TBA	tetrabutylammonium
THA	tetraheptylammonium
TGA	thermal gravimetric analysis
UV	ultraviolet
vs	very strong (IR)
w	weak (IR)

Z	number of molecules per unit cell
α, β, γ	interaxial angles between unit cell vector **b** and **c**, **a** and **c**, and **a** and **b**, respectively
δ	chemical shift (expressed in ppm for NMR)
ε	molar extinction (or absorption) coefficient
θ	the glancing angle of the X-ray beam to the "reflecting plane"
λ	wavelength
μ	the total linear absorption coefficient (with unit of cm^{-1})
χ_m	mass magnetic susceptibility
K	Kevin
pH	potential of hydrogen, a measure of the acidity or alkalinity of a solution

CHAPTER

1

Introduction: Structures and Features of Typical Plenary and Lacunary Polyoxometalates

1.1 Overview of polyoxometalates

Polyoxometalates (POMs for convenience) are early-transition-metal oxygen anion clusters. More specifically, they are oligomeric aggregates that are formed by the linkage of metal cations (primarily the d^0 species V(V), Nb(V), Ta(V), Mo(VI), and W(VI)) with oxygen atoms by self-assembly processes.[1] They have been known for almost 200 years since the discovery of the first heteropolyanion compound by Berzelius in 1826.[2] In the intervening years, advances in structural and analytical techniques have greatly aided the research in this field, enabling the relation between solid-state and solution species, and the link between structural and reactivity properties to be established.[3] The chemically robust nature of POMs, coupled with their highly tunable physicochemical properties (acidity, thermal stability, redox potentials, solubility, size, shape, and charge), lead to their applications beyond the traditional uses as catalysts and inorganic materials. They now contribute to developments in areas ranging from microelectronics to medical diagnosis.[4,5]

POMs have now become a large and rapidly growing class of inorganic clusters that facilitate a range of basic research efforts (from electron transfer and ion pairing to self-assembly) as well as applied studies in the areas of analytical chemistry, electron microscopy, medicine, catalysis and solid state materials.[6] The expansion in POM chemistry has accelerated dramatically, which can be clearly demonstrated by the fast growth of the POM literature in the past three decades. As a result, the syntheses, structures, properties and applications of POMs have been extensively reviewed. [1,6-24]

1.2 Plenary and Lacunary Keggin POMs

Keggin type POM, $[XW_{12}O_{40}]^{n-}$, as a member of the heteropolyoxometalates, was first structurally determined by Keggin in the 1930s using X-ray powder diffraction.[25,26] This structure was later proved by numerous structural characterizations.[27] It consists of a central XO_4 tetrahedron surrounded by four M_3O_{13} triads at each of its vertices. These triads are linked by corner-sharing or edge-sharing with each other. The corner versus edge sharing is dependent upon the isomerism of the molecule. Geometrically, five isomers have been proposed by Baker and Figgis (**Figure 1.1**).[28] The α isomer, which has the overall T_d symmetry, is the most prevalent and thermodynamic stable isomer. Rotating one of the triads by 60° forms the β-Keggin, and the overall symmetry changes from T_d to C_{3v}. The γ, δ and ε isomers are formed by successive 60° rotation of two, three or four W_3O_{13} groups, respectively. Generally, they are less stable than the α- and β-isomers due to the increasing numbers of coulombically-unfavorable edge-shared contacts of two highly charged metal ions. Once all four triads are rotated, the overall symmetry of the resulting ε-isomer goes back to T_d.

The application of Keggin POMs have been extensively documented in numerous patents and applied literatures, in which 80-85% claim or investigate POMs for their catalytic activity. Their popularity can be attributed to the abundant study and their commercial availability.[4]

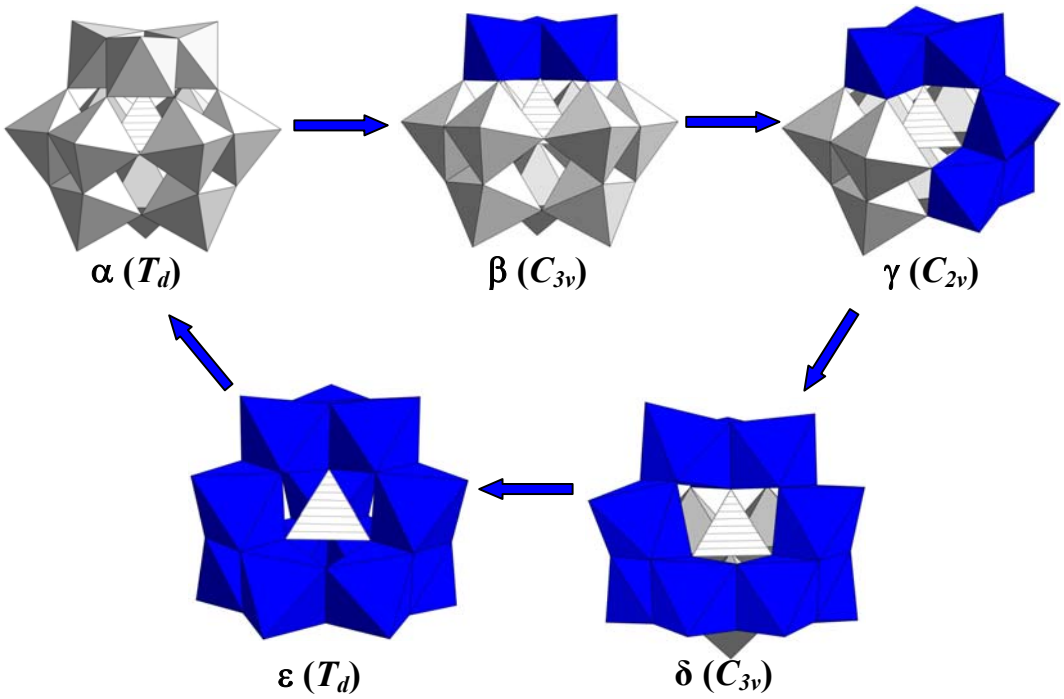

Figure 1.1. The five Baker-Figgis isomers of the Keggin anion $(XO_4)W_{12}O_{36}^{n-}$ in polyhedral representation

Controlled hydrolysis of many heteropolyanion species with base under certain conditions (temperature, ionic strength, etc) can form "defect" structures where one or more addenda atoms have been removed from the "complete" anions along with the oxygen atoms that are not shared by other addenda atoms. This "defect" structure is commonly referred to as a "lacunary" species. Keggin complexes are very convenient for preparing the lacunary species. Like several other POM structural families, Keggin POMs are also not stable at high pH, where a complex series of hydrolysis reactions occur. The generated lacunary POMs are typically stable in a certain pH range and can be used as building locks for constructing larger metal oxide structures or incorporate various transition metals to generate new POMs with modified properties. For the

Keggin type POMs, mono-, bi- and tri-lacuanry species can be formed under different hydrolysis conditions.

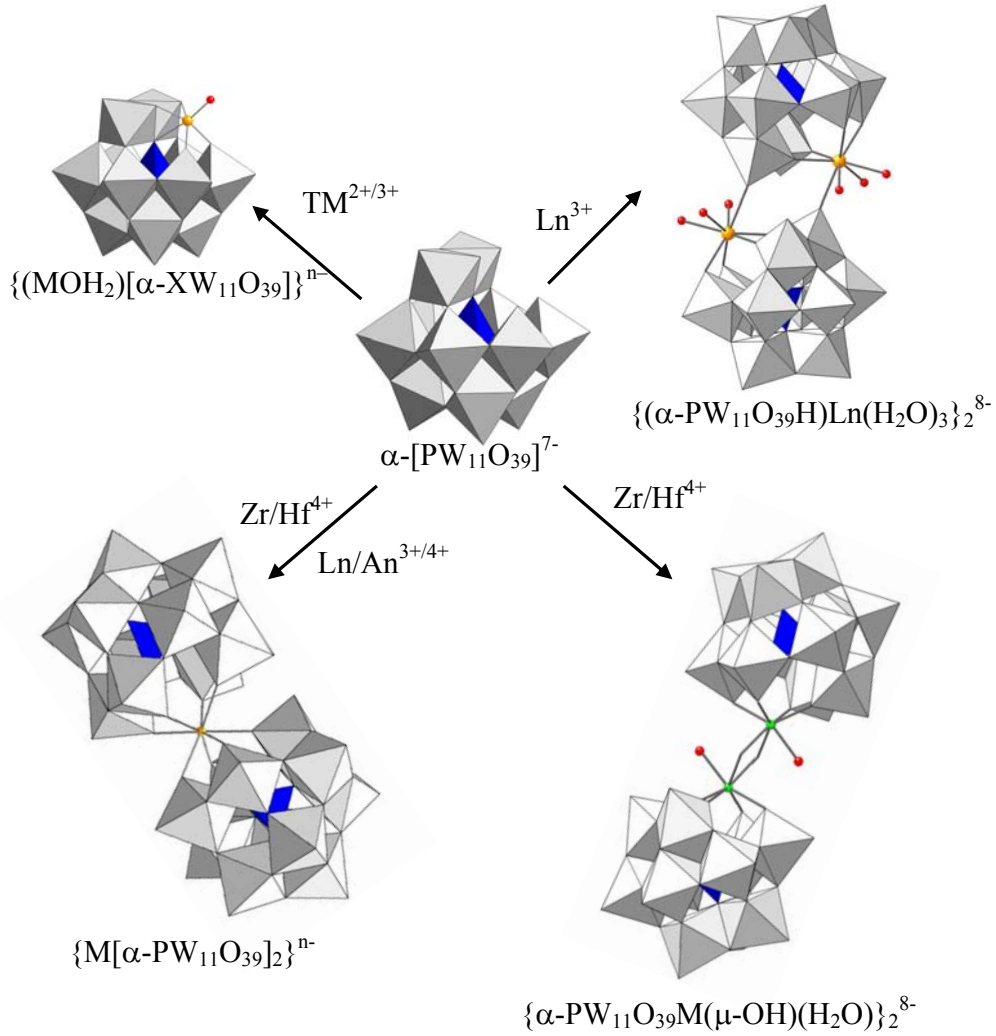

Figure 1.2. The monovacant Keggin polytungstate and its coordination chemistry.

Several mono-lacunary species can be formed depending on the isomerism and heteroatom identity. Only the mono-lacunary α isomer is observed for Keggin type polytungstophosphate, while four monolacunary Keggin polytungstosilicate isomers can be obtained. Reaction of the monovacant Keggin with most of the transition metal ions ($TM^{2+/3+}$) can form a series of compounds with a general formula $\{(MOH_2)[\alpha\text{-}XW_{11}O_{39}]\}^{n-}$. The tetrabutylammonium (TBA) salts of several first-row transition metal substituted $\{PW_{11}\}$ derivatives, e.g. $[(n\text{-}C_4H_9)_4N]_4H[(MOH_2)PW_{11}O_{39}]$ ($M = Mn^{II}$, Co^{II}), have been proven to be remarkably effective catalysts for many reactions, such as the epoxidation of alkenes and sulfoxidation.[29,30] However, some of the chemistry of these complexes remains unclear because of the difficulty to obtain crystal structures of these compounds. This is largely a consequence of their tendency to crystallize in the high symmetry cubic system. Reaction of monovacant Keggin with lanthanide (Ln) and actinide (An) atoms forms 1:2-type compounds, $M[XW_{11}O_{39}]_2\}^{n-}$ (XW_{11} could be α-PW_{11}, α-SiW_{11} and β_2-SiW_{11}), which were first proposed by Peacock and Weakley.[31] In the 1:2-type complexes, one Ln or An atom is coordinated by two tetradentate $\{PW_{11}\}$ anionic ligands in approximately square-antiprism geometry. In addition, 2:2 dimeric complexes can also be obtained for Ln metal ions.[32] 1:2-type and 2:2 type compounds can also be isolated by the reaction of Zr^{4+} and Hf^{4+} with monovacant Keggin species.[33,34] The 1:2-type compounds for Zr^{4+} and Hf^{4+} are isostructural to the Weakley-type complexes, while the structures of the 2:2 type for Zr^{4+} and Hf^{4+} are quite different. In the 2:2 type Zr^{4+} and Hf^{4+} compounds, two Zr^{4+} or Hf^{4+} ions not only coordinate to the monovacant Keggin ligand but also are bridged with each other by two oxygens. In contrast, Ln ions in 2:2 type compounds do not link with each other. Instead, each of

them connects to two manovacant Keggin ligands. Moreover, one-dimensional 1:1-type POM-based Ln derivatives have also been reported, which prove the existence of the 1:1 structural type put forward by Peacock and Weakley.[31]

Trivacant Keggin POMs are another class of widely used lacunary Keggin polytungstates, which are formed by removing three neighboring WO_6 octahedra and are classified as A-type and B-type. The A-isomer refers to the removal of three WO_6 octahedra, one from each of the separate M_3 triads of edge-shared octahedra, so that the face of the central XO_4 tetrahedron faces the vacancy. For B-isomer, one whole M_3 triad of three edge-shared octahedra is removed, so that the apex of the central XO_4 tetrahedron faces the vacancy. Both the A- and B-trivacant POMs have strongly reactive open coordination sites consisting of nucleophilic oxygen atoms. In the very few reported X-ray structures of trivacant polyoxotungstates, the unsaturated positions of the lacunary anions are often occupied with counter cations, such as Na^+ or K^+ atoms.[36,37] It has also been observed that the interaction between the trivacant species and alkali metal cations is dependent on the protonation state of the trivacant species. Such behavior is believed to play a role in solution as well and must be considered in order to control the formation of metal complexes derived from such trivacant precursors.

The solid-state isomerization from $[A\text{-}PW_9O_{34}]^{9-}$ to $[B\text{-}PW_9O_{34}]^{9-}$ can take place on heating $[A\text{-}PW_9O_{34}]^{9-}$ at 150 ºC for 2 days to a week. The thermal transformation can be easily monitored by IR spectroscopy. Unheated $Na_8H[PW_9O_{34}]$ is predominantly, but not exclusively, $[A\text{-}PW_9O_{34}]^{9-}$ and the thermolyzed product is mainly $[B\text{-}PW_9O_{34}]^{9-}$.[38] Neither $[A\text{-}PW_9O_{34}]^{9-}$ nor $[B\text{-}PW_9O_{34}]^{9-}$ are stable in aqueous solution: they decompose to other polytungstate species upon dissolution, including mono tungstate WO_4^{2-}, [α-

$PW_{11}O_{39}]^{7-}$ and PO_4^{3-} (the latter two species can be confirmed by its characteristic chemical shift in ^{31}P NMR spectroscopy).

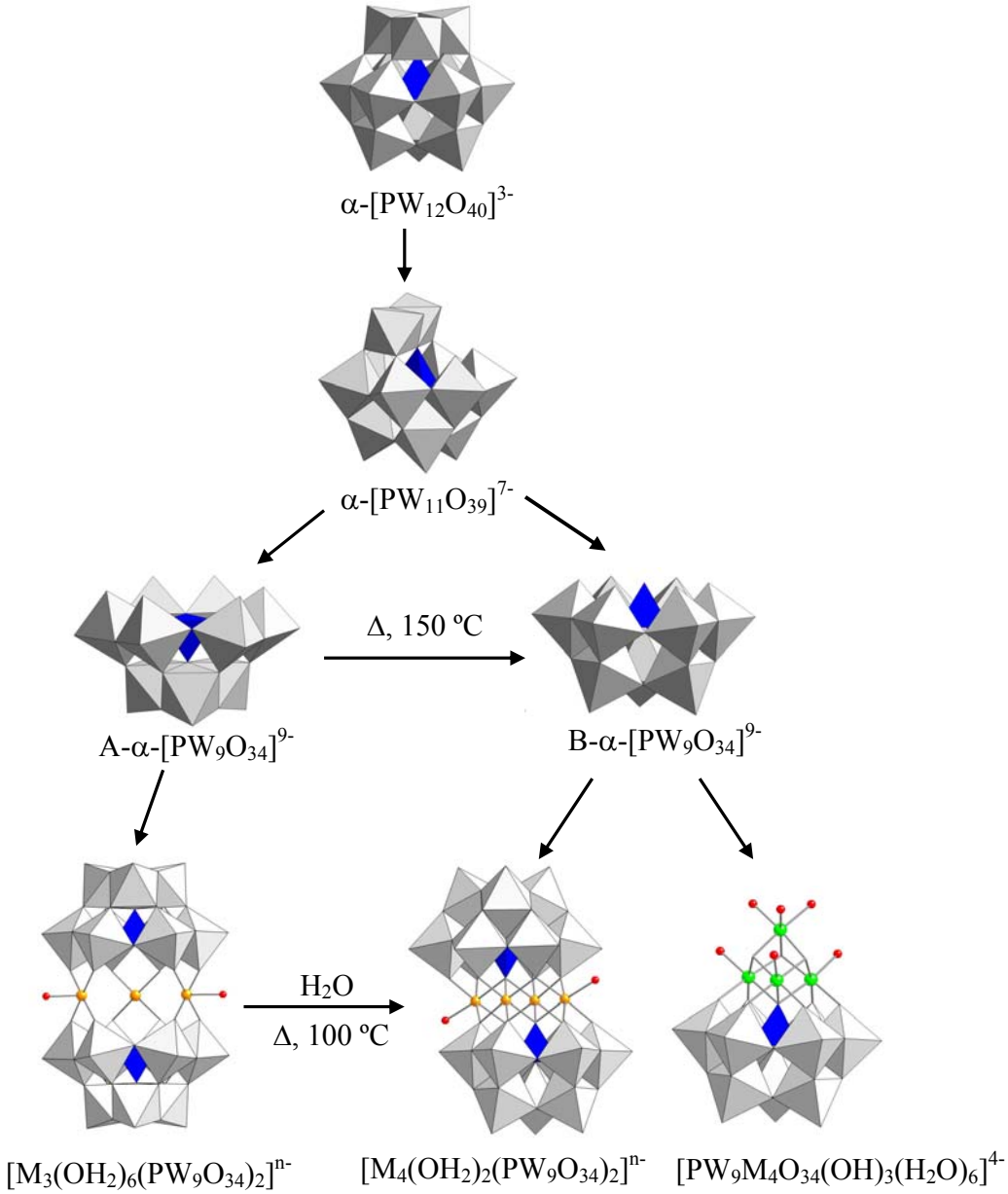

Figure 1.3. Trivacant Keggin polytungstates and their coordination chemistry.

When A- and B-trivacant POMs react with transition metals, the structural difference between them leads to different coordination chemistry. Reactions of A-type tricavant POMs with transition or main group metals commonly form structures with a single substituted POM unit such as those with the formula $[A\text{-}M_3(H_2O)_3XW_9O_{37}]^{n-}$ [39-49] or those with a sandwich-type structure, such as $[M_3(H_2O)_3(A\text{-}XW_9O_{34})_2]^{n-}$.[50-54] Another structural class of sandwich-type POMs from A-type is the dimer which consists of two trisubstituted A-type Keggins linked together by three μ-oxo or μ-hydroxo bridges and is known to exist for both Si and P heteroatoms.[55-57] Interestingly, A-type sandwich POMs with C_{3h} symmetry are capable of incorporating an anion, such as NO_3^- or CO_3^{2-}, into the central cavity surrounded by the three transition metals and the polytungstate frameworks.[51,58] These anions are believed to act as a template in the formation of these sandwich structures and considerably increase the stability of the whole structure in both solution and solid state. In contrast, B-trivacant POMs generally incorporate four transition metals to form $[M_4(OH_2)_2(B\text{-}XW_9O_{34})_2]^{n-}$. Three transition metals can also be sandwiched between two B-trivacant POMs with sodium ion in the free coordination site, for example, $[Ni_3Na(H_2O)_2(PW_9O_{34})_2]^{11-}$. [59] Another interesting example is the compound, in which a cubane like four nickel core is stabilized by $\{B\text{-}PW_9O_{34}\}$ ligand.[60]

Recently, much research has focused on the di-vacant $[\gamma\text{-}XW_{10}O_{36}]^{n-}$ (X = P, Si, Ge) ligand due to its application in H_2O_2 or O_2 based oxidation.[61-63] Among these three divant polyanion, $[\gamma\text{-}SiW_{10}O_{36}]^{8-}$ has been the most studied. The polyanion $[\gamma\text{-}SiW_{10}O_{36}]^{8-}$ was originally synthesized and characterized by Tézé etal. and it has been reported as a catalyst in the reaction of H_2O_2-based epoxidation of alkenes.[64] This lacunary polyanion has also been widely used as ligand to yield transition metal substuted

POMs with unique structures and catalytic reactivities. The polyanion $[\gamma\text{-}GeW_{10}O_{36}]^{8-}$, synthesized in a similar way to $[\gamma\text{-}SiW_{10}O_{36}]^{8-}$, was reported by Kortz and coworkers in 2006.[65] Its coordination chemistry is also very similar to $[\gamma\text{-}SiW_{10}O_{36}]^{8-}$. When $[\gamma\text{-}XW_{10}O_{36}]^{n-}$ binds to two metal ions, two coordination patterns have been observed, namely out-of-pocket and in-pocket. Usually, the in-pocket structure forms a monomer in solution, while out-of-pocket structure yields dimer and trimer, which is consistent with the considerable structural differences between these two coordination patterns. Polyanion $[\{Fe_2(OH)_3(H_2O)_2\}_3(\gamma\text{-}SiW_{10}O_{36})_3]^{15-}$ is a good example with out-of-pocket coordination mode.[66] In the crystal structure, the iron centers displaced from the body of the POM, are corner-sharing and are no longer connected to the internal Si heteroatom oxygens. $[\gamma\text{-}SiW_{10}O_{36}\{Al(OH_2)\}_2(\mu\text{-}OH)_2]^{4-}$ is the typical structure with the in-pocket coordination mode.[67] In this polyanion, two vicinal edge-sharing aluminum centers reside in the polytungstate building pocket, with the axial positions occupied by two aquo ligands, and the opposite axial positions occupied by the oxygen atoms of the central $\{SiO_4\}$ unit. Under certain preparation conditions, $[\gamma\text{-}SiW_{10}O_{36}]^{8-}$ ($[\gamma\text{-}GeW_{10}O_{36}]^{8-}$) can be isomerized to form tri-vacant $[\beta\text{-}SiW_9O_{34}]^{10-}$ ($[\beta\text{-}GeW_9O_{34}]^{10-}$) and tetra-vacant $\{SiW_8O_{31}\}$($\{GeW_8O_{31}\}$) fragments by losing a $\{W_2O_5\}$ unit. This type of process has been well demonstrated in the published compounds $[Co_3(H_2O)(B\text{-}\beta\text{-}SiW_9O_{33}(OH))(B\text{-}\beta\text{-}SiW_8O_{29}(OH)_2)]^{11-}$ and $[Cu_3(H_2O)(B\text{-}\beta\text{-}GeW_9O_{33}(OH))(B\text{-}\beta\text{-}GeW_8O_{30}(OH))]^{12-}$.[68-72]

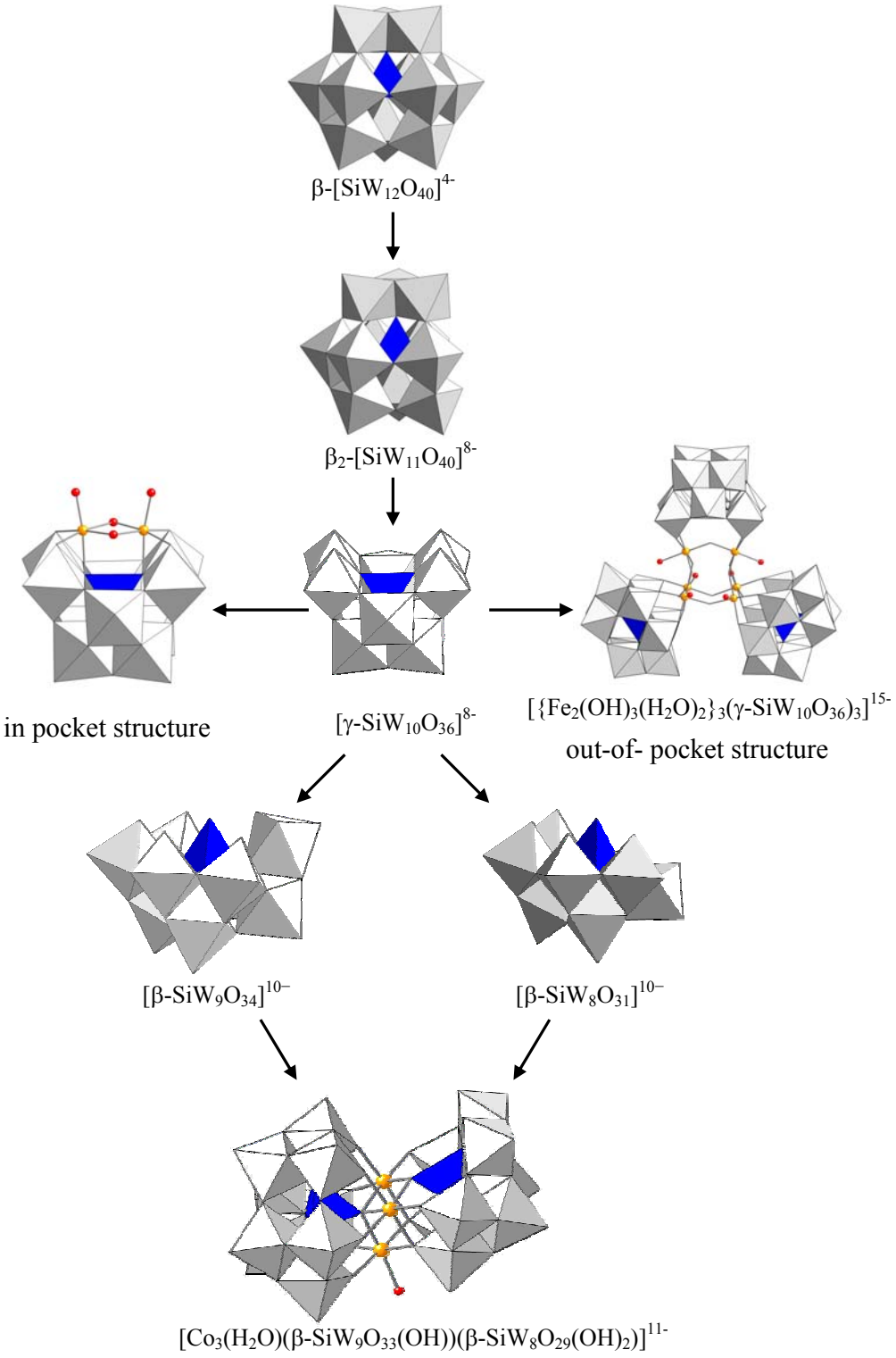

Figure 1.4. Divacant Keggin polytungstates and their coordination chemistry.

1.3 Plenary and Lacunary Wells-Dawson POMs

Another well known family of polytungstate is called the "Wells-Dawson" structure with general formula $[X_2M_{18}O_{62}]^{n-}$. It is formed by two XO_4 tetrahedra each coordinating to one M_3O_{13} triad cap and one M_6O_{14} belt which links to the other M_6O_{14} belt by sharing corner oxygen atoms. The first structurally characterized Wells-Dawson anion was reported in 1953.[73] Like the Keggin family, six Baker and Figgis isomers of the Dawson structure were proposed.[74] The β, γ-isomers of the Wells–Dawson anion derive from the α-isomer by 60° rotation of one or both 3-fold W_3O_{13} groups. Then α*, β*, γ*-isomers can be derived from α, β and γ by 60° rotation of an $\{XW_9\}$ half unit. Among the six isomers of the Dawson structures, only four of them (α, β, γ and γ*) have been observed to date and α and β isomers are the most common.

Lacunary species derived from the plenary Wells–Dawson anion, for example, $[P_2W_{18}O_{62}]^{6-}$, is similar to the Keggin series, but more diverse due to its lower symmetry and more complex composition. Mono-, tri- and hexa-lacunary Wells–Dawson ligands have been documented in the literatures (shown in **Figure 1.6**). There are two monovacant lacunary Wells–Dawson anions, namely, α_1- and α_2-$[P_2W_{17}O_{61}]^{10-}$. The α_2 isomer, $[\alpha_2\text{-}P_2W_{17}O_{61}]^{10-}$, is obtained by removing a WO_x octahedra from one of the cap W_3O_{13} triads of the $[\alpha\text{-}P_2W_{18}O_{62}]^{6-}$. The α_1 isomer has the lacunary site in the belt position and can only be prepared by adding WO_x octahedra to a hexavacant Well-Dawson structure $[P_2W_{12}O_{48}]^{14-}$. Compared to α_2-$[P_2W_{17}O_{61}]^{10-}$, α_1-$[P_2W_{17}O_{61}]^{10-}$ is less stable in solution: it will slowly convert to α_2-$[P_2W_{17}O_{61}]^{10-}$ (see below) from hydrolysis and isomerization. However, the presence of Li^+ cations can increase the solution stability of the α_1-$[P_2W_{17}O_{61}]^{10-}$ since Li^+ occupies the vacant site.

Reaction of $[\alpha_2\text{-}P_2W_{17}O_{61}]^{10-}$ with transition metals yield transition-metal-substituted complexes, $[\alpha_2\text{-}P_2W_{17}O_{61}(M{\cdot}L)]^{n-}$ (M = Mn^{III}, Fe^{III}, Co^{II}, Ni^{II} and Cu^{II}; L = H_2O or Br), the TBA salts of which are highly effective oxidation catalysts in comparison to some of the best metalloporphyrin catalysts.[75-77] When $\alpha_2\text{-}[P_2W_{17}O_{61}]^{10-}$ reacts with Ln or An ions, 1:2 sandwich and 1:1 dimeric complexes can be formed (Figure 1.5).[31,78-81] For $\alpha_1\text{-}[P_2W_{17}O_{61}]^{10-}$ ligand, addition of transition metal ions, such as Zn^{II}, forms 1:1 monomeric complexes, $\{M[\alpha_1\text{-}P_2W_{17}O_{61}]\}^{8-}$.[82] 1:2 sandwich-type, 1:1 mono-substituted and 1:1 dimeric complexes can also be obtained.[83-87]

The trivacant anion, $\alpha\text{-}[P_2W_{15}O_{56}]^{12-}$, as one of the widely used lacunary POM ligands, is formed by the removal of one W_3 "cap" unit from $\alpha\text{-}\{P_2W_{18}\}$. Its coordination modes are similar to the B-type trivacant Keggin species. Seven nucleophilic oxygen atoms can serve as electron donors to form various complexes with a wide range of metal ions. It is well known that $\alpha\text{-}[P_2W_{15}O_{56}]^{12-}$ reacts with low valent transition metal cations to afford the tetranuclear sandwich complexes, $\{M_4(H_2O)_2[\alpha\text{-}P_2W_{15}O_{56}]\}^{16-/12-}$ (M = Co^{II}, Cu^{II}, Zn^{II}, Mn^{II} and Fe^{III}),[38,88-99] and with high valent transition metal ions to give $P_2W_{15}M_3O_{62}^{9-/6-}$ (M = W^{VI}, Mo^{VI}, V^{V}, Nb^{V})[45,100] Sandwich-type POMs with two or three transition metals in the central belt based on $\alpha\text{-}[P_2W_{15}O_{56}]^{12-}$ have also been obtained. Recently, Anderson et al. reported a di-iron^{III}-substituted analogue of the tetranuclear sandwich complex, $[Fe_2(NaOH_2)_2(P_2W_{15}O_{56})_2]^{16-}$,where the two iron(III) atoms reside at the internal positions, and the two sodium cations at the external sites.[41,97,98] After that, the cobalt and copper analogues are reported. $[NaCo_3(H_2O)_2(P_2W_{15}O_{56})_2]^{17-}$ was reported by

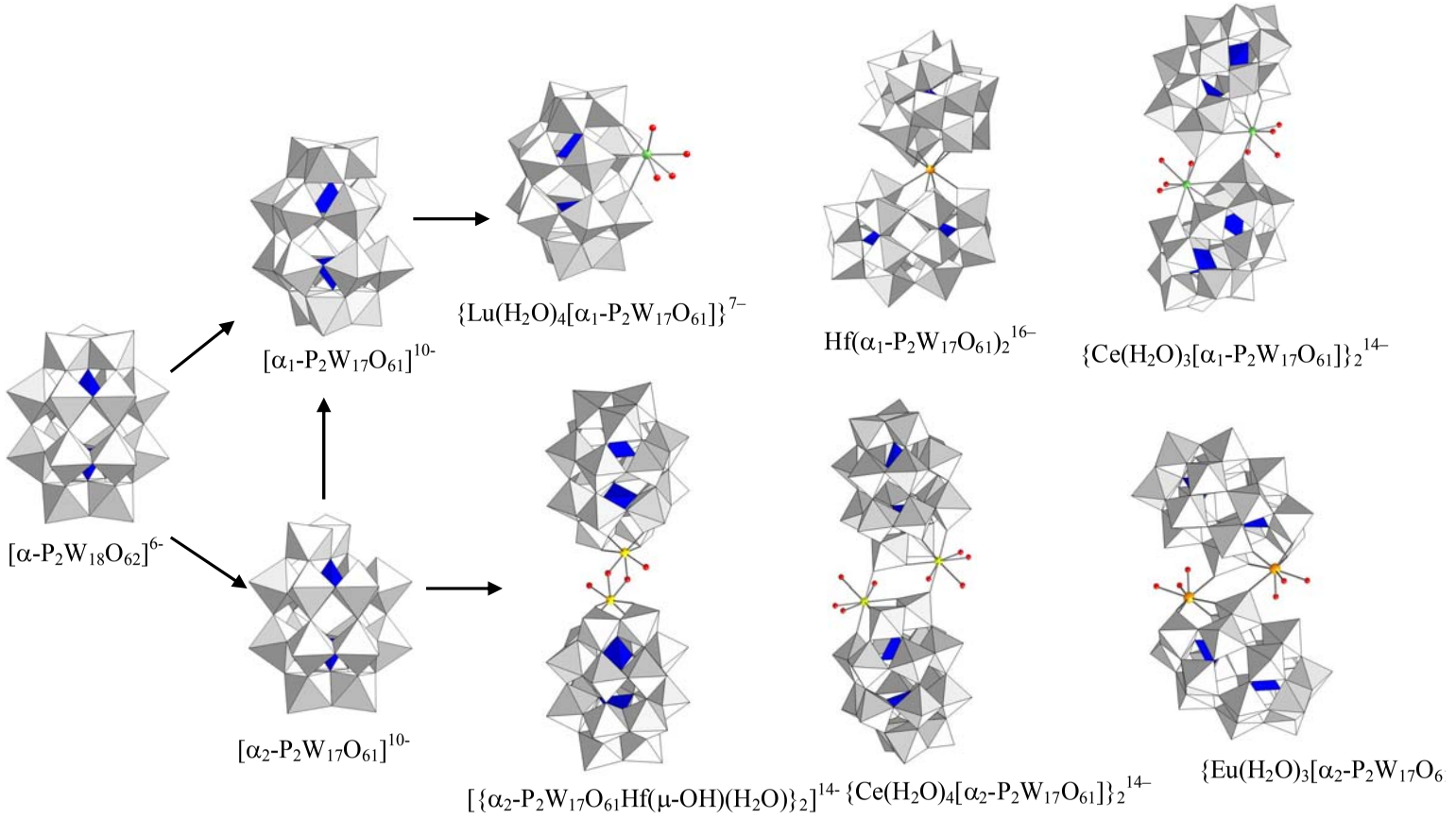

Figure 1.5. Monovacant Wells-Dawson polytungstates and their coordination chemistry.

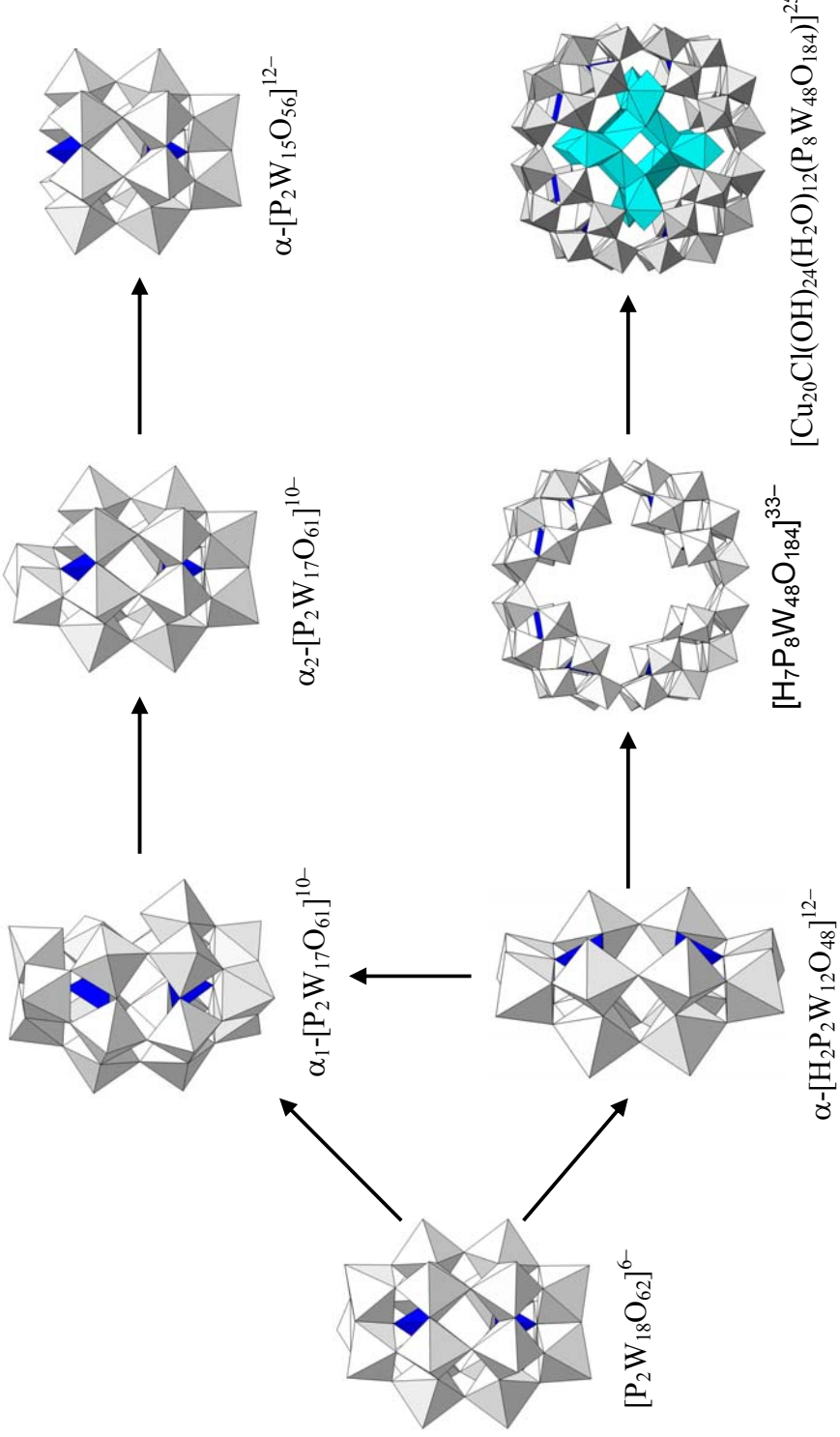

Figure 1.6. Lacunary Wells-Dawson polytungstates species.

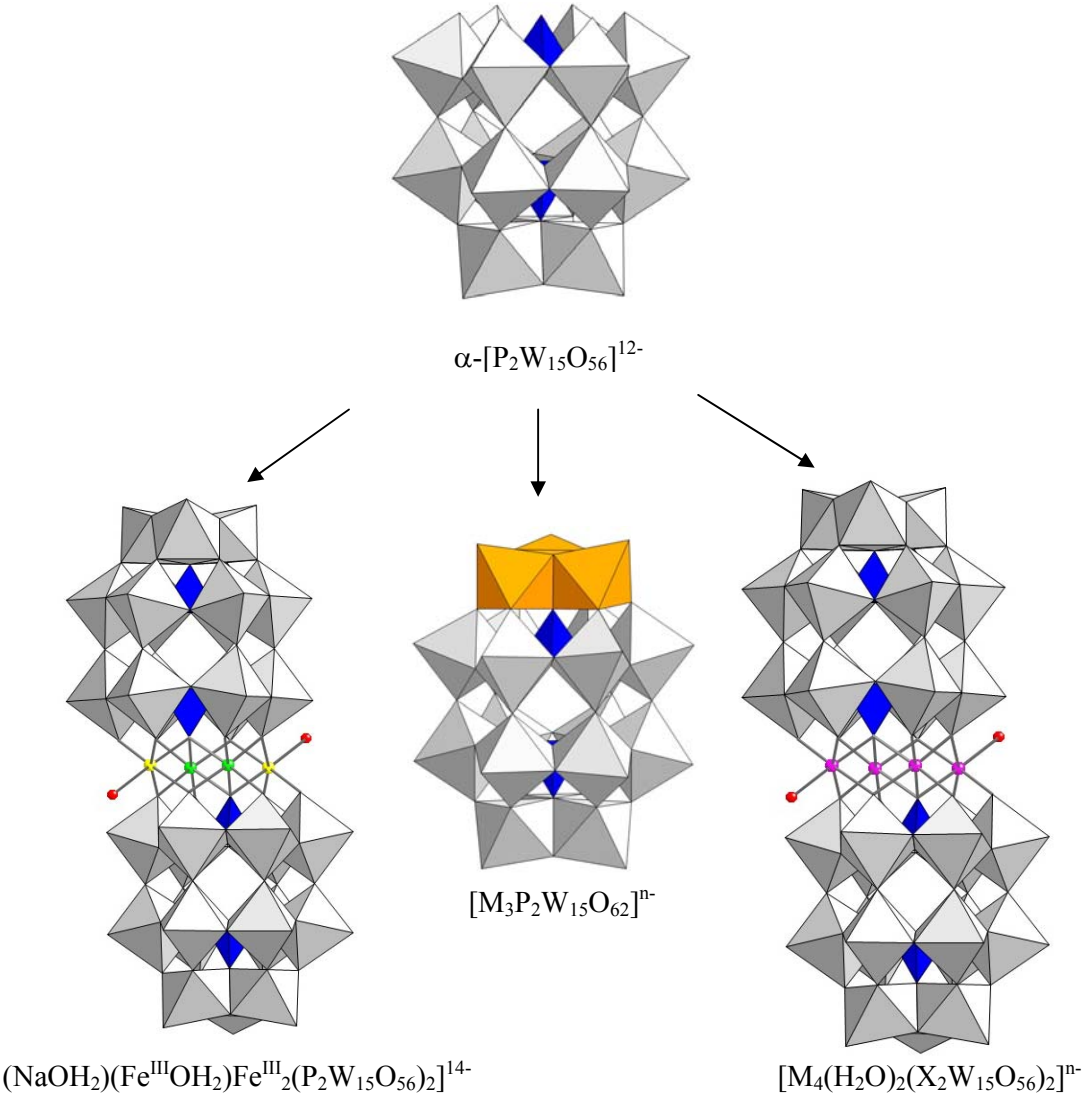

Figure 1.7. Trivacant Wells-Dawson polytungstates and their coordination chemistry.

Ruhlmann with three metals in the belt and one sodium ion in the external position.[101] The di-iron(III) and tri-cobalt(II) sandwich-type complexes can be used as an important starting material for the preparation of many heteronuclear transition metal substituted derivatives by replacing labile sodium cations with other low valent transition metals to

form $[Fe_2(MOH_2)_2(P_2W_{15}O_{56})_2]^{14-}$ (M = Ni^{II}, Cu^{II} and Zn^{II}) [102] or $[MCo_3(H_2O)_2(P_2W_{15}O_{56})_2]^{16-}$ (M = Mn^{II}, Ni^{II}, Co^{II} Zn^{II} and Cd^{II}).[103]

The hexavacant anion α-$[H_2P_2W_{12}O_{48}]^{12-}$ is derived from elimination of six tungsten atoms on one side of the Wells–Dawson structure. The crystalline solids of this hexavacant anion are not available, but its structure can be directly deduced from X-ray diffraction studies on a polyperoxo anion $[P_2W_{12}O_{56}(NbO_2)_6]^{12-}$.[104] The polyanion $[H_2P_2W_{12}O_{48}]^{12-}$ is stable in aqueous solution at its natural pH and ionic strength. Only one single peak is observed in ^{31}P NMR spectrum, which is consistent with the two symmetrically equivalent phosphorus atoms. Acidification in presence of tungstate leads back to α_2-$\{P_2W_{17}\}$ but, without tungstate, it gives two $\{P_2W_{24}\}$ dimers. Attempts to obtain crystals of the dimer $\{P_4W_{24}\}$ have been unsuccessful: only the tetramer $[P_8W_{48}O_{184}]^{40-}$ forms in a subsequent crystallization step.[105,106] It was believed that $\{P_2W_{12}\}$ and $\{P_8W_{48}\}$ do not form complexes with divalent or trivalent transition metal ions.[107] It was not until recently that this conjucture was proven to be incorrect.[108,109]

1.4 Catalytic applications of POMs

In recent years, POMs and their transition metal-substituted derivatives, have received great attention as both acid and oxidation catalysts, including several large scale industrial processes conducted in either heterogeneous and homogeneous modes. Transition metal substituted POMs have exhibited excellent catalytic activity in selective oxidation of organic substrates. In the catalytic process, POMs act as either stoichiometric oxidants or as catalysts in conjunction with environmentally friendly oxidants as O_2 and H_2O_2.[110] Transition metal substituted POMs are efficient catalysts to catalyze alkane oxidation to produce alcohols and ketones under a wide variety of

conditions.[111,112] In addition, they have also been shown to catalyze alkene oxidation to produce epoxides, allylic alcohols, allylic ketones and oxidative cleavage products.[113-115] Transition metal substituted POMs are also alternatives for decontamination of toxic agents due to their abilities to catalyze sulfoxidation under ambient conditions.[30,116,117] Very recently, particular transition metal-substituted POMs have been discovered to be efficient catalysts for water oxidation, which could play an important role in providing alternative energy.

POMs as Water oxidation catalysts (WOCs)

Water oxidation has become a very hot research area because of the recent discoveries of the structure of oxygen evolution center in *PSII* and its functioning at a molecular level and also because of its implications for new solar-energy conversion schemes. However, developing a viable WOC has proven particularly challenging. Shannon's group first reported that the POM, $Ru_2Zn_2(H_2O)_2(ZnW_9O_{34})_2]^{14-}$,[118] can catalyze water oxidation electrochemically. However, the synthesis of that compound has been controversial based on the work of several other research groups. Recently, polyanion $[Ru^{IV}_4O_4(OH)_2(H_2O)_4(\gamma\text{-}SiW_{10}O_{36})_2]^{10-}$ was reported by our group and another group simultaneously to oxidize water to dioxygen chemically (see **Figure 1.8**).[119] After that, our group proved that this compound can catalyze water oxidation photochemically in the presence of persulfate as a sacrificial electron acceptor (**Scheme 1-2**).[120]

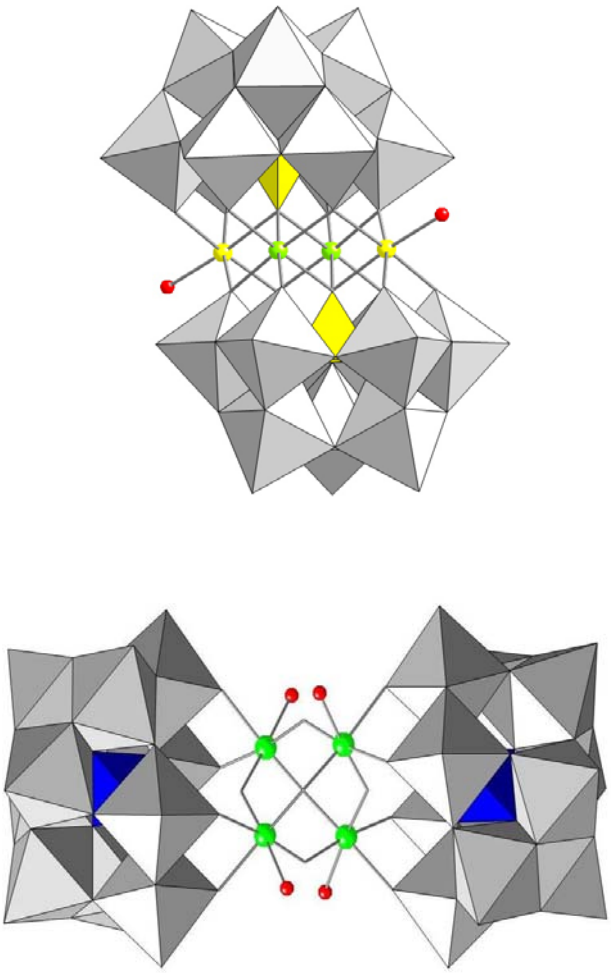

Figure 1.8. X-Ray structure of $WRuZn_2(H_2O)_2(ZnW_9O_{34})_2]^{11-}$ (top) and $[Ru^{IV}_4O_4(OH)_2(H_2O)_4(\gamma\text{-}SiW_{10}O_{36})_2]^{10-}$ (bottom) in combined polyhedral (polytungstate ligands) and ball-and-stick notation. Ru: green, O: red; WO_6 octahedra: gray, SiO_4 tetrahedra: blue. ZnO_4 tetrahedra: blue.

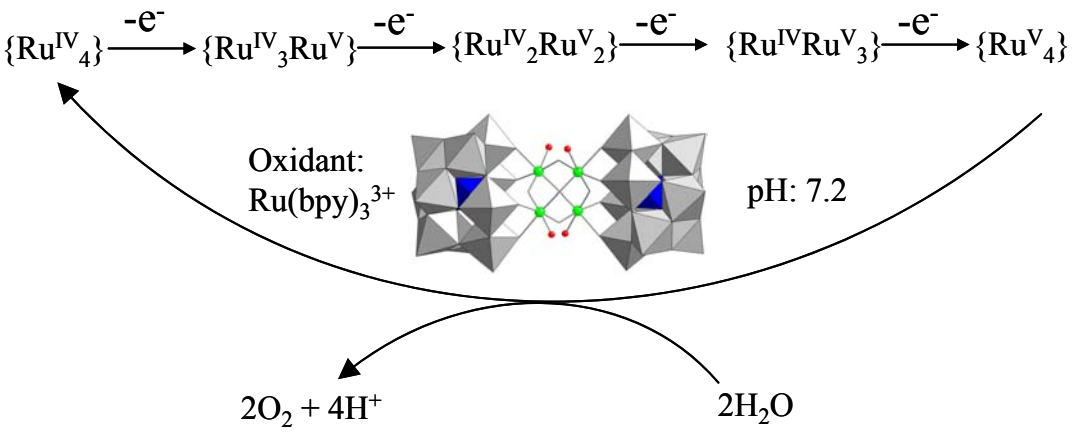

Scheme 1.1. Water oxidation catalyzed by $[Ru^{IV}_4O_4(OH)_2(H_2O)_4(\gamma\text{-}SiW_{10}O_{36})_2]^{10-}$ using $[Ru(bpy)_3]^{3+}$ as oxidant

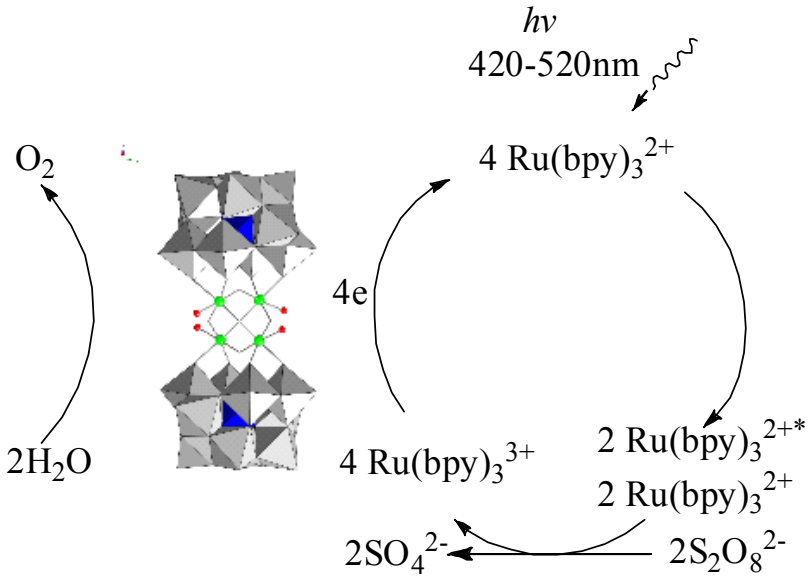

Scheme 1.2. Light-induced catalytic water oxidation by $[Ru^{IV}_4O_4(OH)_2(H_2O)_4(\gamma\text{-}SiW_{10}O_{36})_2]^{10-}$ using $[Ru(bpy)_3]^{2+}$ as a photosensitizer and persulfate as a sacrificial electron acceptor.

This is a breakthrough for water oxidation since the catalyst is free of organic structure and oxidatively resistant. No reported homogeneous water oxidation catalyst containing organic ligands (of the ca. 44 reported thus far) is faster. However, Ru is expensive and not earth abundant rendering it unsuitable for use on a realistic scale. Considering this, our group kept pursuing a stable and fast homogenous WOC, without organic ligands, based on earth abundant elements. Consequently, our group discovered that $[Co_4(H_2O)_2(\alpha\text{-}PW_9O_{34})_2]^{10-}$ (**Figure 1.9**) another carbon-free POM, is a hydrolytically and oxidatively stable homogeneous water oxidation catalyst, and the fastest homogeneous catalyst for the oxidation of water to date with turnover frequencies for O_2 production $\geq 5\ s^{-1}$ at pH 8.

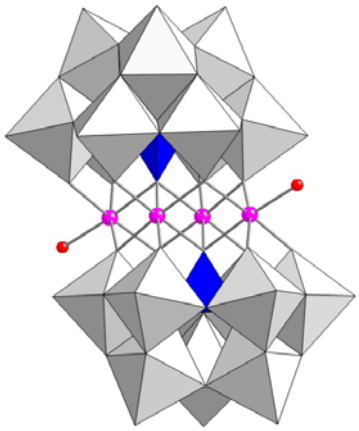

Figure 1.9. X-Ray structure of $[Co_4(H_2O)_2(\alpha\text{-}PW_9O_{34})_2]^{10-}$ in combined polyhedral (polytungstate ligands) and ball-and-stick notation. Co: pink, O: red; WO_6 octahedra: gray, PO_4 tetrahedra: blue.

1.5 **Goals of this thesis and outline**

The first of two objectives of this thesis is to extend the previous synthetic work of enantiopure POM complexes by changing the polyoxometalate framework from the lacunary Wells-Dawson to the lacunary Keggin unit. As a result, we obtained an enentiopure POM by spontaneous resolution in the absence of an organic ligand. Chapter 2 describes the synthesis, characterization and chirality of a sandwich-type POM which was obtained by spontaneous resolution upon crystallization in the absence of any chiral source.

The second objective of this thesis is to design and synthesize POMs that are expected to have novel structures, interesting properties and potential applications in homogeneous and heterogeneous catalysis, especially water oxidation. POMs can become attractive candidates as potential catalysts for water oxidation because they can be soluble, robust with respect to oxidation, and structurally tunable. They are also structurally similar to known water oxidation catalysts. In this thesis, we hope to isolate and characterize intermediates in the catalytic cycle of $[Ru^{IV}_4O_4(OH)_2(H_2O)_4(\gamma\text{-}SiW_{10}O_{36})_2]^{10-}$-catalyze water oxidation. Chapter 3 reports the one-electron-oxidized form of $[Ru^{IV}_4O_4(OH)_2(H_2O)_4(\gamma\text{-}SiW_{10}O_{36})_2]^{10-}$ and a diruthenium containing POM. The effort also focuses on exploring the possibility of using new POMs containing less expensive and more abundant transition metals as water oxidation catalysts. In chapters 4 and 5, a new family of sandwich-type POMs with two transition metals in the framework and a new sandwich POM formed from heptatungstate have been obtained. The instability of these POMs in aqueous solution precludes their use as water oxidation catalysts.

References

(1) Pope, M. T. *Heteropoly and Isopoly Oxometalates*; Springer-Verlag: Berlin, 1983.

(2) Berzelius, J. J. *Poggendorfs Ann. Phys. Chem.* **1826**, *6*, 369.

(3) Hill, C. L. *Chem. Rev.* **1998**, *98*, 1.

(4) Katsoulis, D. E. *Chem. Rev.* **1998**, *98*, 359.

(5) Maekawa, S.; Tohyama, T.; Barnes, S. E.; Ishihara, S.; Koshibae, W.; Khaliullin, G.; Springer, Berlin: 2004, p 1.

(6) Hill, C. L. *Chem. Rev.* **1998**, *98*, 1.

(7) Pope, M. T. In *Comprehensive Coordination Chemistry*; Wilkinson, G., Gillard, R. D., McCleverty, J. A., Eds.; Pergamon Press: New York, 1987; Vol. 3, p Chapter 38.

(8) Pope, M. T.; Müller, A. *Angew. Chem. Int. Ed. Engl.* **1991**, *30*, 34.

(9) Pope, M. T. In *Progress in Inorganic Chemistry*; Lippard, S. J., Ed.; John Wiley & Sons, Inc.: New York, 1991; Vol. 39, p 181.

(10) Dickman, M. H.; Pope, M. T. *Chem. Rev.* **1994**, *94*, 569.

(11) Pope, M. T. p. In *Encyclopedia of Inorganic Chemistry*; B., K. R., Ed.; Wiley: Chichester: 1994, p 3361.

(12) Hill, C. L.; Prosser-McCartha, C. M. *Coord. Chem. Rev.* **1995**, *143*, 407.

(13) Okuhara, T.; Mizuno, N.; Misono, M. *Advances in Catalysis* **1996**, *41*, 113.

(14) Neumann, R. *Prog. Inorg. Chem.* **1998**, *47*, 317.

(15) Misono, M. *Chem. Commun.* **2001**, *13*, 1141.

(16) Contant, R.; Hervé, G. *Reviews in Inorganic Chemistry* **2002**, *22*, 63.

(17) Pope, M. T. In *Comprehensive Coordination Chemistry II: From Biology to Nanotechnology*; Wedd, A. G., Ed.; Elsevier Ltd.: Oxford, UK, 2004; Vol. 4, p 635.

(18) Hill, C. L. In *Comprehensive Coordination Chemistry-II: From Biology to Nanotechnology*; Wedd, A. G., Ed.; Elsevier Ltd.: Oxford, UK, 2004; Vol. 4, p 679.

(19) Cronin, L. In *Comprehensive Coordination Chemistry II: From the Molecular to the Nanoscale: Synthesis, Structure, and Properties*; McCleverty, J. A., Meyer, T. J., Eds.; Elsevier: Amsterdam, 2004; Vol. 7, p 1.

(20) *Zeolite, Clay and. Heteropoly Acid in Organic Reactions*; Izhumi, Y.; Urabe, K.; Onake, M., Eds.; Kodansha/VCH: Tokyo, 1992.

(21) *Polyoxometalate Chemistry From Topology via Self-Assembly to Applications*; Pope, M. T.; Müller, A., Eds.; Kluwer Academic Publishers: Dordrecht, 2001.

(22) *Polyoxometalates: From Platonic Solids to Anti-retroviral Activity*; Pope, M. T.; Müller, A., Eds.; Kluwer Academic Publishers: Dordrecht, Netherlands, 1993.

(23) Moffat, J. B. *Metal-Oxygen Clusters: The Surface and Catalytic Properties of Heteropoly Oxometalates.*; Kluwer Academic/Plenum Publishers: New York, 2001; Vol. 9.

(24) *Polyoxometalate Chemistry for Nano-Composite Design*; Yamase, T.; Pope, M. T., Eds.; Kluwer Academic/Plenum Publishers: New York, 2002; Vol. 2.

(25) Keggin, J. F. *Nature* **1933**, *131*, 908.

(26) Illingworth, J. W.; Keggin, J. F. *J. Chem. Soc.* **1935**, 575.

(27) Brown, G. M.; Noe-Spirlet, M. R.; Busing, W. R.; Levy, H. A. *Acta Cryst. B* **1977**, *B33*, 1038.

(28) Baker, L. C. W.; Figgis, J. S. *J. Am. Chem. Soc.* **1970**, *92*, 3794.

(29) Hill, C. L.; Brown, R. B., Jr. *J. Am. Chem. Soc.* **1986**, *108*, 536.

(30) Okun, N. M.; Tarr, J. C.; Hilleshiem, D. A.; Zhang, L.; Hardcastle, K. I.; Hill, C. L. *J. Mol. Catal. A. Chem.* **2006**, *246*, 11.

(31) Peacock, R. D.; Weakley, T. J. R. *J. Chem. Soc. A* **1971**, 1937.

(32) Haraguchi, N.; Okaue, Y.; Isobe, T.; Matsuda, Y. *Inorg. Chem.* **1994**, *33*, 1015.

(33) Kato, C. N.; Shinohara, A.; Hayashi, K.; Nomiya, K. *Inorg. Chem.* **2006**, *45*, 8108.

(34) Nomiya, K.; Saku, Y.; Yamada, S.; Takahashi, W.; Sekiya, H.; Shinohara, A.; Ishimaru, M.; Sakai, Y. *Dalton Trans* **2009**, 5504.

(35) Sadakane, M.; Dickman, M. H.; Pope, M. T. *Angew. Chem., Int. Ed. Engl.* **2000**, *39*, 2914.

(36) Robert, F.; Tézé, A. *Acta Cryst.* **1981**, *B37*, 318.

(37) Cao, X.; Naruke, H.; Yamase, T. *Acta Cryst.* **2003**, *E59*, i116±i118.

(38) Finke, R. G.; Droege, M. W.; Domaille, P. J. *Inorg. Chem.* **1987**, *26*, 3886.

(39) Katsoulis, D. E.; Pope, M. T. *Casreact 104:168282; Cjacs* **1984**, *106*, 2737.

(40) Liu, J. G.; Ortega, F.; Sethuraman, P.; Katsoulis, D. E.; Costello, C. E.; Pope, M. T. *J. Chem. Soc., Dalton Trans.* **1992**, 1901.

(41) Anderson, T. M.; Zhang, X.; Hardcastle, K. I.; Hill, C. L. *Inorg. Chem.* **2002**, *41*, 2477.

(42) Liu, J. F.; Zhao, B. L.; Rong, C. Y.; Pope, M. T. *Acta Chimica Sinica* **1993**, *51*, 368.

(43) Qu, L.; Sun, Y.; Chen, Y.; Yu, M.; Peng, J. *Synth. React. Inorg. Met.-Org. Chem.* **1994**, *24*, 1339.

(44) Mizuno, N.; Hirose, T.; Tateishi, M.; Iwamoto, M. *J. Mol. Catal.* **1994**, *88*, L125.

(45) Meng, L.; Liu, J. F. *Chin. Chem. Lett.* **1995**, *6*, 453.

(46) Mizuno, N.; Nozaki, C.; Hirose, T.-o.; Tateishi, M.; Iwamoto, M. *J. Mol. Catal. A: Chem.* **1997**, *117*, 159.

(47) Liu, J. F.; Zhen, Y. G.; So, H. S. *Synth. React. Inorg. Met.-Org. Chem.* **1998**, *28*.

(48) Meng, L.; Zhan, X. P.; Wang, M.; Liu, J. F. *Polyhedron* **2001**, *20*.

(49) Jana, S. K.; Kubota, Y.; Tatsumi, T. *J. Catal.* **2008**, *255(1)*.

(50) Knoth, W. H.; Domaille, P. J.; Farlee, R. D. *Organometallics* **1985**, *4*, 62.

(51) Knoth, W. H.; Domaille, P. J.; Harlow, R. L. *Inorg. Chem.* **1986**, *25*, 1577.

(52) Finke, R. G.; Rapko, B.; Weakley, T. J. R. *Inorg. Chem.* **1989**, *28*, 1573.

(53) Xin, F.; Pope, M. T. *Casreact 104:168282; Cjacs* **1996**, *118*, 7731.

(54) Laronze, N.; Marrot, J.; Hervé, G. *Inorg. Chem.* **2003**, *42*, 5857.

(55) Lin, Y.; Weakley, T. J. R.; Rapko, B.; Finke, R. G. *Inorg. Chem.* **1993**, *32*, 5095.

(56) Wassermann, K.; Palm, R.; Lunk, H.-J.; Fuchs, J.; Steinfeldt, N.; Stoesser, R. *Inorg. Chem.* **1995**, *34*, 5029.

(57) Nomiya, K.; Takahashi, M.; Ohsawa, K.; Widegren, J. A. *J. Chem. Soc., Dalton Trans.* **2001**, 2872.

(58) Fang, X.; Anderson, T. M.; Neiwert, W. A.; Hill, C. L. *Inorg. Chem.* **2003**, *42*, 8600.

(59) Kortz, U.; Mbomekalle, I. M.; Keita, B.; Nadjo, L.; Berthet, P. *Inorg. Chem.* **2002**, *41*, 6412.

(60) Kortz, U.; Tézé, A.; Hervé, G. *Inorg. Chem.* **1999**, *38*, 2038.

(61) Mizuno, N.; Nozaki, C.; Kiyoto, I.; Misono, M. *J. Am. Chem. Soc.* **1998**, *120*, 9267.

(62) Mizuno, N.; Yamaguchi, K.; Kamata, K. *Coord. Chem. Rev.* **2005**, *249*, 1944.

(63) Kamata, K.; Yonehara, K.; Sumida, Y.; Yamaguchi, K.; Hikichi, S.; Mizuno, N. *Science* **2003**, *300*, 964.

(64) Canny, J.; Tézé, A.; Thouvenot, R.; Hervé, G. *Inorg. Chem.* **1986**, *25*, 2114.

(65) Nsouli, N. H.; Bassil, B. S.; Dickman, M. H.; Kortz, U.; Keita, B.; Nadjo, L. *Inorg. Chem.* **2006**, *45(10)*, 3858.

(66) Botar, B.; Geletii, Y. V.; Kögerler, P.; Musaev, D. G.; Morokuma, K.; Weinstock, I. A.; Hill, C. L. *J. Am. Chem. Soc.* **2006**, *128*, 11268.

(67) Kikukawa, Y.; Yamaguchi, S.; Nakagawa, Y.; Kazuhiro Uehara; Uchida, S.; Yamaguchi, K.; Mizuno, N. *J. Am. Chem. Soc.* **2008**, *130*, 15872.

(68) Bassil, B. S.; Kortz, U.; Tigan, A. S.; Clemente-Juan, J. M.; Keita, B.; Oliveira, P. D.; Nadjo, L. *Inorg. Chem.* **2005**, *44*, 9360.

(69) Bassil, B. S.; S.Nellutla; U.Kortz; Stowe, A. C.; Tol, J. V.; Dalal, N. S.; Keita, B.; Nadjo, L. *Inorg. Chem.* **2005**, *44*, 2659.

(70) Lisnard, L.; Mialane, P.; Dolbecq, A.; Marrot, J.; Clemente-Juan, J. M.; Coronado, E.; Keita, B.; Oliveira, P. D.; Nadjo, L.; S´echeresse, F. *Chem.–Eur. J.* **2007**, *13*, 3525.

(71) Mialane, P.; Dolbecq, A.; Marrot, J.; E.Rivière; Sécheresse, F. *Chem.–Eur. J.* **2005**, *11*, 1771.

(72) Nsouli, N. H.; Ismail, A. H.; Helgadottir, I. S.; Dickman, M. H.; Clemente-Juan, J. M.; Kortz, U. *Inorg. Chem.* **2009**, *48 (13)*, 5884.

(73) Dawson, B. *Acta Cryst. B* **1953**, *6*, 113.

(74) Baker, L. C. W.; Figgis, J. S. *J. Am. Chem. Soc.* **1970**, *92*, 3794.

(75) Lyon, D. K.; Miller, W. K.; Novet, T.; Domaille, P. J.; Evitt, E.; Johnson, D. C.; Finke, R. G. *J. Am. Chem. Soc.* **1991**, *113*, 7209.

(76) Mansuy, D.; Bartoli, J. F.; Lyon, D. K.; Finke, R. G. *J. Am. Chem. Soc.* **1991**, *113*, 7222.

(77) Randall, W. J.; Lyon, D. K.; Domaille, P. J.; Finke, R. G. In *Inorganic Syntheses*; Darensbourg, M. Y., Ed.; John Wiley & Sons, Inc.: New York, 1998; Vol. 32, p 242.

(78) Molchanov, V. N.; Kazanskii, L. P.; Torchenkova, E. A.; Simonov, V. I. *Sov. Phys. Crystallogr. (Engl. Transl.)* **1979**, *24*, 96.

(79) Sadakane, M.; Ostuni, A.; Pope, M. T. *J. Chem. Soc. Dalton Trans.* **2002**, 63.

(80) Luo, Q.; Howell, R. C.; Bartis, J.; Dankova, M.; DeW. Horrocks, J., William; Rheingold, A. L.; Francesconi, L. C. *J. Inorg. Biochem.* **2002**, *41*, 6112.

(81) Saku, Y.; Sakai, Y.; Nomiya, K. *Inorg. Chim. Acta* **2010**, *363(5)*, 967.

(82) Bartis, J.; Kunina, Y.; Blumenstein, M.; Francesconi, L. C. *Inorg. Chem.* **1996**, *35*, 1497.

(83) Zhang, C.; Howell, R. C.; Luo, Q.-H.; Fieselmann, H. L.; Todaro, L. J.; Francesconi, L. C. *Inorg. Chem.* **2005**, *44*, 3569.

(84) Boglio, C.; Lenoble, G.; Duhayon, C.; Hasenknopf, B.; Thouvenot, R.; Zhang, C.; Howell, R. C.; Burton-Pye, B. P.; Francesconi, L. C.; Lacôte, E.; Thorimbert, S.; Malacria, M.; Afonso, C.; Tabet, J.-C. *Inorg. Chem.* **2006**, *45*, 1389.

(85) Bartis, J.; Dankova, M.; Lessmann, J. J.; Luo, Q.-H.; Horrocks, W.; DeW., J.; Francesconi, L. C. *Inorg. Chem.* **1999**, *38*, 1042.

(86) Sadakane, M.; Dickman, M. H.; Pope, M. T. *Inorg. Chem.* **2001**, *40*, 2715.

(87) Luo, Q.-H.; Howell, R. C.; Dankova, M.; Bartis, J.; Williams, C. W.; William DeW. Horrocks, J.; Victor G. Young, J.; Rheingold, A. L.; Francesconi, L. C.; Antonio, M. R. *Inorg. Chem.* **2001**, *40*, 1894.

(88) Finke, R. G.; Droege, M. W. *Inorg. Chem.* **1983**, *22*, 1006.

(89) Finke, R. G.; Lyon, D. K.; Nomiya, K.; Sur, S.; Mizuno, N. *Inorg. Chem.* **1990**, *29*, 1784.

(90) Gómez-García, C. J.; Borrás-Almenar, J. J.; Coronado, E.; Ouahab, L. *Inorg. Chem.* **1994**, *33*, 4016.

(91) Finke, R. G.; Weakley, T. J. R. *Journal of Chemical Crystallography* **1994**, *24*, 123.

(92) Kirby, J. F.; Baker, L. C. W. *Casreact 104:168282; Cjacs* **1995**, *117*, 10010.

(93) Crano, N. J.; Chambers, R. C.; Lynch, V. M.; Fox, M. A. *J. Mol. Catal. A: Chem.* **1996**, *114*, 65.

(94) Zhang, X.; Chen, Q.; Duncan, D. C.; Campana, C.; Hill, C. L. *Inorg. Chem.* **1997**, *36*, 4208.

(95) Müller, A.; Peters, F.; Pope, M. T.; Gatteschi, D. *Chem. Rev.* **1998**, *98*, 239.

(96) Song, W.; Wang, X.; Liu, Y.; Liu, J.; Xu, H. *J. Electroanal. Chem.* **1999**, *476*, 85.

(97) Zhang, X.; Anderson, T. M.; Chen, Q.; Hill, C. L. *Inorg. Chem.* **2001**, *40*, 418.

(98) Anderson, T. M.; Hardcastle, K. I.; Okun, N.; Hill, C. L. *Inorg. Chem.* **2001**, *40*, 6418.

(99) Gaunt, A. J.; May, I.; Collison, D.; Holman, K. T.; Pope, M. T. *J. Mol. Struct.* **2003**, *656*, 101.

(100) Finke, R. G.; Rapko, B.; Saxton, R. J.; Domaille, P. J. *Casreact 104:168282; Cjacs* **1986**, *108*, 2947.

(101) Ruhlmann, L.; Canny, J.; Contant, R.; Thouvenot, R. *Inorg. Chem.* **2002**, *41*, 3811.

(102) Mbomekalle, I. M.; Cao, R.; Hardcastle, K. I.; Hill, C. L.; Ammam, M.; Keita, B.; Nadjo, L.; Anderson, T. M. *C. R. Chimie* **2005**, *8*, 1077.

(103) Ruhlmann, L.; Costa-Coquelard, C.; Canny, J.; Thouvenot, R. *Eur. J. Inorg. Chem.* **2007**, 1493.

(104) Judd, D. A.; Chen, Q.; Campana, C. F.; Hill, C. L. *J. Am. Chem. Soc.* **1997**, *119*, 5461.

(105) Kintzinger, J. *NMR. Basic Principles & Progress* **1981**, *17*, 1.

(106) *^{17}O NMR Spectroscopy in Organic Chemistry*; Boykin, D. W., Ed.; CRC Press, Inc.: Boca Raton, 1991.

(107) Contant, R.; Tézé, A. *Inorg. Chem.* **1985**, *24*, 4610.

(108) Godin, B.; Chen, Y.; Vaissermann, J.; Ruhlmann, L.; Verdaguer, M.; Gouzerh, P. *Angew. Chem. Int. Ed.* **2005**, *44*, 3072.

(109) Mal, S. S.; Kortz, U. *Angew. Chem. Int. Ed.* **2005**, *44*, 2.

(110) Kozhevnikov, I. V. *Chem. Rev.* **1998**, *98*, 171.

(111) Faraj, M.; Hill, C. L. *J. Chem. Soc. Chem. Comm.* **1987**, 1487.

(112) Lyons, J. E.; Ellis, P. E., Jr.; Durante, V. A. In *Studies in Surface Science and Catalysis*; Grasselli, R. A., Sleight, A. W., Eds.; Elsevier Scientific: Amsterdam, 1991; Vol. 67, p 99.

(113) Neumann, R.; Abu-Gnim, C. J. *J. Am. Chem. Soc.* **1990**, *112*, 6025.

(114) Rong, C.; Pope, M. T. *J. Am. Chem. Soc.* **1992**, *114*, 2932.

(115) Khenkin, A. M.; Hill, C. L. *Mendeleev Commun.* **1993**, *3*, 140.

(116) Okun, N. M.; Anderson, T. M.; Hardcastle, K. I.; Hill, C. L. *Inorg. Chem.* **2003**, *42*, 6610.

(117) Rossi, L. I.; Martín, S. E. *Appl. Catal. A* **2003**, *250*, 271.

(118) Howells, A. R.; Sankarraj, A.; Shannon, C. *J. Am. Chem. Soc.* **2004**, *126*, 12258.

(119) Geletii, Y. V.; Botar, B.; Kögerler, P.; Hillesheim, D. A.; Musaev, D. G.; Hill, C. L. *Angew. Chem. Int. Ed.* **2008**, *47*, 3896.

(120) Geletii, Y. V.; Huang, Z.; Hou, Y.; Musaev, D. G.; Lian, T.; Hill, C. L. *J. Am. Chem. Soc.* **2009**, *131*, 7522.

CHAPTER 2

Breaking Symmetry: Spontaneous Resolution of a Polyoxometalate

(published partially in *Chem.-Eur. J.* **2007**, *13(34)*, 9442-9447)
with Xikui Fang, and Craig L. Hill

Abstract: A chiral polyoxotungstate $[Hf(PW_{11}O_{39})_2]^{10-}$ (**2.1**) has been isolated and structurally characterized. It crystallizes in a chiral space group $P2_12_12$ as a conglomerate of two enantiomerically pure crystals without any chiral source. The absolute configuration of **2.1** was determined from the Flack parameter by X-ray crystallography. The structure of **2.1** is composed two lacunary $[PW_{11}O_{39}]^{7-}$ units each functioning as a tetra-dentate ligand sandwiching an 8-coordinate Hf^{IV} center in a distorted square antiprismatic geometry. Optically active crystals of both enantiomers were spectroscopically distinguishable via solid state circular dichroism (CD) spectroscopy. This hafnium-substituted compound, **2.1**, shows that spontaneous chiral resolution, a rare phenomenon, can be operable in POM systems.

2.1 Introduction

Spontaneous resolution which is the segregation of enantiomers upon crystallization, was originally reported by Louis Pasteur in 1848 when he manually separated left-handed from right-handed crystals of sodium ammonium tartrate.[1] When mixtures of mirror-image configurations of a compound aggregate or crystallize, they can form a racemic compound, a racemic solid solution, or a conglomerate (racemic mixture of chiral crystallites). Only the latter category, the conglomerate, involves spontaneous resolution.[2-4] Spontaneous chiral resolution upon crystallization in the absence of any chiral source is of great interest since it is closely related to homochirality in life[5-8] and absolute asymmetric synthesis in the solid state.[9-12] Statistically, between 5 and 10% of all racemated conglomerate crystals can be resolved spontaneously upon crystallization,[13] which indicate that heterochiral interations are prevalent and more facile than homochiral interactions in the formation of crystalline racemates.[14]

Although the resolution of chiral POMs is highly sought given the potential applications of these compounds in asymmetric catalysis, sensing and medicine,[15-22] the term of spontaneous resolution has not been reported in polyoxometalate (POM)[23,24] systems to the best of our knowledge. Enantiomerically pure chiral POM crystals have been prepared in the presence of chiral organic ligands,[25,26] chiral metal-organic moieties[27-29] and other chiral cluster-based building blocks.[30,31] but it is still a major challenge to achieve even partial resolution of the two enantiomers of racemic POMs in the absence of chiral influence (solute, solvent or counterion). Since the multiple metal domains in POMs can undergo facile racemization via water exchange, partial hydrolysis, or fluxional behavior, it is even more challenging to realize spontaneous resolution in some cluster systems including POMs than in most other classes of compounds. These collective processes frequently produce crystals with both enantiomers in a same unit cell. For example, sandwich-type compounds, the most popular class of POMs as homogeneous catalysts based on rates, selectivities, and tunabability (synthetic alterability)[32-39] occasionally crystallize as chiral structures but in racemic (most frequently centrosymmetric) space groups. Such chiral POMs constructed from both monovacant Keggin[40] or Wells-Dawson POM ligands[21] are known.

There are a few examples of enantiopure crystallites of POMs and other cluster molecules with a large number of metal centers, although the vast majority of POM crystals in the Cambridge Crystallographic (CCDC) and Fachinformationszentrum (FIZ) databases involve crystallization in achiral space groups. In other words, there are several examples of POMs that crystallize in chiral space groups without chiral influence. Examination of these cases, however, discloses that enantiomeric purity derives from one

of two phenomena, neither of which involves significant chirality manifested in the cluster structure itself as quantified by circular dichroism spectra. One manifestation of chirality in POMs is bond length alteration,[41-48] a general feature not only of large metal oxide clusters but also metal oxides themselves dating back to early work of Pauling.[49-51] The other manifestation of chirality in POMs and related large clusters derives from the asymmetry inherent in the association of an organic[52-54] or organometallic[55-57] group with the POM. Some of these composite compounds can potentially provide significant opportunity for chirality transfer from the POM derivative to other molecules in stoichiometric or catalytic reactions. However, these compounds don't really involve enantiopure POM units themselves; rather chirality derives from the spacial arrangement and association between the two units.

We report here the spontaneous resolution of a POM, the chirality of which is not due to bound groups, bond length alteration or other subtle packing effects. Thus this compound shows major circular dichroism because the chirality derives from significant spacial structural asymmetry. This compound is an Hf-containing cluster that affords large isolable enantiopure crystals. Before our work, there is only one other report of a crystallographically characterized POM consisting of the element Hf,[58] despite the fact that Hf centers should exhibit a rich landscape of stereochemical possibilities with cluster ligands. We chose Hf for this exploratory study because the charge (4+) and large ionic radius (0.85 Å) of Hf should facilitate strong and multidentate binding of POM ligands but with each POM occupying only one coordination hemisphere of the Hf ion. The other structurally characterized Hf-containing POM which appeared a few months before our work is a conventional achiral structure.

2.2 Experimental

2.2.1 General Methods and Materials

All common laboratory chemicals were reagent grade, purchased from commercial sources and used without further purification. $Na_9[A\text{-}\alpha\text{-}PW_9O_{34}]\bullet 16H_2O$ was obtained by the published procedure (Inorganic Syntheses, **1990**, *27*, 96-104) and its purity was confirmed by infrared spectroscopy. Elemental analyses for C, H, and N were performed by Atlantic Microlabs, Atlanta, Georgia; those for P, Hf and W were performed by Desert Analytics (Tucson, Arizona). Infrared spectra (2% sample in KBr) were recorded on a Nicolet 510 instrument. Solid-state CD spectra for the two enantiomers of **2.1** were recorded on a Jasco J-810 spectropolarimeter. Thermogravimetric data were collected on a TGA 1000 instrument. Solution ^{31}P NMR spectra were obtained on a Varian INOVA 400 MHz spectrometer, referenced to 85% H_3PO_4 as an internal standard. Solid-state ^{31}P NMR spectra were obtained on Bruker DSX400 solid state NMR spectrometer (Bruker- Biospin, Rheinstetten/Germany).

2.2.2 Synthesis

$HfCl_2O\bullet 8H_2O$ (0.143g, 0.35mmol) was dissolved in H_2O (20 mL), and the pH was adjusted to ca. 1.5 with 1M HCl solution. Solid $Na_9[A\text{-}\alpha\text{-}PW_9O_{34}]\bullet 16H_2O$ (1.00g, 0.39mmol) was added to the mixture all at once with vigorous stirring. The solution was heated at 50°C for 30 min and cooled to room temperature. Dimethylamine hydrochloride (0.25g, 3.125 mmol) was added to the solution, and then the solution was heated at 50°C for 5 min. The final pH of the reaction solution is about 5.0. Slow evaporation of the solution produced rod-like crystals after three days (yield, 0.48g, 49.5% based on W). The numbers of counter-cations and crystal water molecules were

determined by both elemental analysis and thermogravimetric analysis (TGA). FT/IR data (cm^{-1}): 3452 (m), 3149(m), 2923(w), 2852(w), 1600(W), 1464(s), 1122(s), 1056(s), 1018(w), 957(s), 886(s), 816(s), 746(s), 514(s). Elemental analysis calcd (%) for $[(CH_3)_2NH_2]_{10}[Hf(PW_{11}O_{39})_2]\bullet 8H_2O$: C, 3.9; H, 1.6; N, 2.3; Hf, 2.9; P, 1.0; W, 65.9. Found (%): C, 4.0; H, 1.7; N, 2.4; Hf, 2.8; P, 1.1; W, 65.2.

2.2.3 Solid-state CD spectroscopy

Solid-state CD spectra for the two enantiomers of **DMA2.1** were recorded on a Jasco J-810 spectropolarimeter, using KBr disks of thickness of ca. 0.25 mm and diameter of 13 mm. The disc was prepared by mixing about 100 mg of KBr (Aldrich, 98%, heated at 100°C) and about 150 μg of **DMA2.1** single crystal with a Perkin-Elmer vibrating mill for 5 min. The mixture then was pressed at 10 tons with a Perkin-Elmer press to obtain a transparent disc which was placed between two quartz slides in the sample compartment in a fixed position. An initial CD spectrum was run, the sample rotated 60-80˚ and another spectrum recorded; about five rotations were performed for each sample and the corresponding spectra recorded. The final CD spectrum is an average of several individual CD spectra recorded for the compound. In order to verify that the crystals were high-quality and single, they were carefully inspected under a microscope before use. Spectra were collected between 200 and 400 nm, with a step size of 1.0 nm and at a speed of 100 nm/min.

2.2.4 Single X-ray Crystallography

X-ray analysis and crystal data for **DMA2.1** at 173K, $[(CH_3)_2NH_2]_{10}[Hf(PW_{11}O_{39})_2]\cdot 8H_2O$: colorless rods, crystal size 0.25 x 0.08 x 0.05 mm^3, $C_{20}H_{96}HfN_{10}O_{86}P_2W_{22}$, orthorhombic, space group $P2_12_12$, a = 12.1687(13), b =

19.764(2), c = 20.598(2) Å, V = 4953.9(9) Å^3, Z = 2, M_r = 6138.20, ρ_{calcd} = 4.115 g·cm^{-3}; $\mu(Mo_{K\alpha})$ = 26.609 mm^{-1}; 1.43≤ θ ≤ 28.30º. The Flack parameter = 0.015(13) indicates the correct absolute configuration of **DMA2.1**. The refinement converged to $R(F_0)$ = 0.0325, $wR(F_0^2)$ = 0.0804, and GOF = 1.173, for 12290 reflections with I>2σ(I). Data were collected with a Bruker SMART-APEX CCD sealed tube diffractometer with graphite monochromated MoKα (0.71073 Å) radiation. Data were measured using a series of combinations of ϕ and ω scans with 30 s frame exposures and 0.3º frame widths. The structure was solved by direct methods and refined by full-matrix least-squares against F^2 of all data using SHELXTL software. Hydrogen atoms, except for the water hydrogen atoms, were included in calculated positions and assigned isotropic thermal parameters. The refinement converged with R_1 = 0.0325 and wR_2 = 0.0804 for 12290 reflections with $I > 2\sigma(I)$. Max/min residual electron density is 3.099/-1.245 e Å^3. The highest residual peaks are all associated with W atoms. CCDC-653386 contain(s) the supplementary crystallographic data for this compound. These data can be obtained free of charge from The Cambridge Crystallographic Data Centre via www.ccdc.cam.ac.uk/data_request/cif.

Table 2.1 Crystal data and structure refinement for **DMA2.1**.

Empirical formula	$C_{20}H_{96}HfN_{10}O_{86}P_2W_{22}$
Formula weight	6138.20
Temperature	173(2) K
Wavelength	0.71073 Å
Crystal system	Orthorhombic
Space group	$P2_12_12$
Unit cell dimensions	a = 12.1687(13) Å α = 90°
	b = 19.764(2) Å β = 90°
	c = 20.598(2) Å γ = 90°
Volume	4953.9(9) $Å^3$
Z	2
Density	4.115 Mg/m^3
Absorption coefficient	26.609 mm^{-1}
F(000)	5408
Crystal size	0.25 x 0.08 x 0.05 mm^3
θ range for data collection	1.43 to 28.30°
Limiting indices	-16≤h≤16, -26≤k≤26, -27≤l≤27
Reflections collected	69267
Independent Reflections	12290 [R(int) = 0.0579]
Completeness to θ = 27.47°	99.8 %
Absorption correction	Semi-empirical from equivalents
Max. and min. transmission	0.3496 and 0.0576
Refinement method	Full-matrix least-squares on F^2
Data / restraints / parameters	12290 / 0 / 344
Goodness-of-fit on F^2	1.173
Final R indices [I>2sigma(I)]	R1 = 0.0325, wR2 = 0.0804 [a]
R indices (all data)	R1 = 0.0333, wR2 = 0.0807
Flack parameter	0.015(13)
Largest diff. peak and hole	3.099 and -1.245 $e.Å^{-3}$

[a] $R_1 = \Sigma||F_0| - |F_c|| / \Sigma|F_0|$; $wR_2 = \Sigma[w(F_0^2 - F_c^2)^2]/ \Sigma[w(F_0^2)^2]^{1/2}$

2.3 Results and Discussion

2.3.1 Synthesis

Addition of powdered $Na_9[A\text{-}\alpha\text{-}PW_9O_{34}]\cdot 16H_2O$ to an aqueous solution of $HfCl_2O\cdot 8H_2O$ adjusted to pH ca. 1.5 with 1M HCl followed by addition of the hydrogen bonding counterion, dimethylammonium (DMA^+) yields $[(CH_3)_2NH_2]_{10}[Hf(PW_{11}O_{39})_2]\cdot 8H_2O$, the DMA^+ salt of $[Hf(PW_{11}O_{39})_2]^{10-}$ (**1**) (henceforth **DMA2.1**). No crystal was obtained when DMA^+ was replaced with other counter cation (K^+ or Na^+). Maintanance of the acidic pH is necessary for production of **2.1**; this keeps the polytungstates in solution while converting $[A\text{-}\alpha\text{-}PW_9O_{34}]^{9-}$ to $[PW_{11}O_{39}]^{7-}$ in situ.

2.3.2 Structure

Single crystal X-ray diffraction shows that **2.1** is a sandwich-type POM with no crystallographically imposed symmetry. The absolute configuration of **DMA2.1** is determined from the Flack parameter, which is 0.015(13).[59] The R1 and wR2 values at the statistics on **DMA2.1** are unusually good for a polytungstate. This polyoxoanion contains an 8-coordinate hafnium cation sandwiched between two lacunary anions, $[PW_{11}O_{39}]^{7-}$, in a distorted square antiprismatic geometry (**Figure 2.1**). The Hf^{IV} center is coordinated by four unsaturated oxygen atoms of each lacunary anion. Compound **DMA2.1** crystallizes in the chiral orthorhombic space group $P2_12_12$, with only one enantiomer present in the unit cell (Z = 2; **Figure 2.2**). There are extensive hydrogen-bonding interactions between **2.1**, dimethylammonium cations and H_2O molecules in the unit cell; donor-acceptor distances in key hydrogen bonds are 2.933 Å (N3S···O32), 2.941 Å (N2S···O39) and 2.838 Å (N4S···O4W).

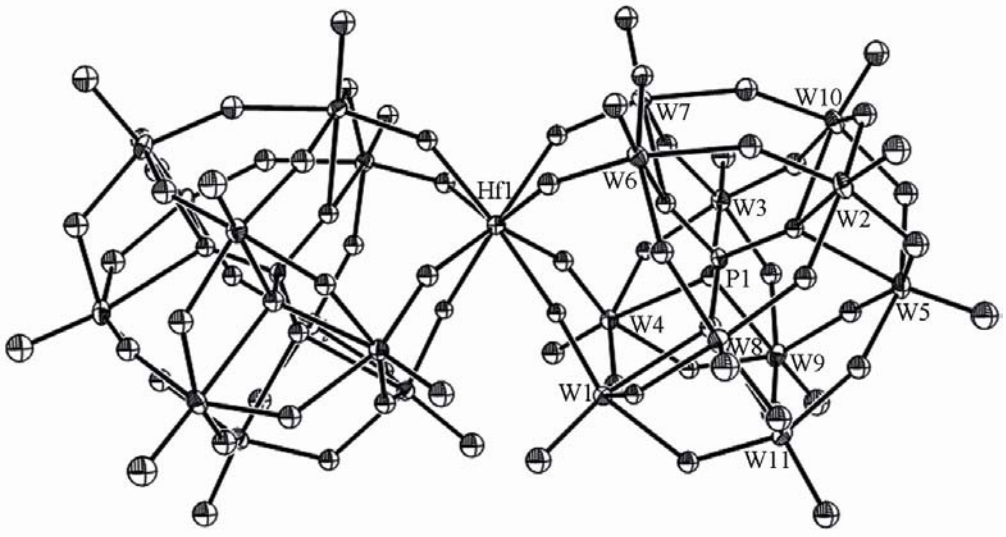

Figure 2.1 Structure (50% probability ellipsoids) of $[Hf(PW_{11}O_{39})_2]^{10-}$, **2.1**, in **DMA2.1**

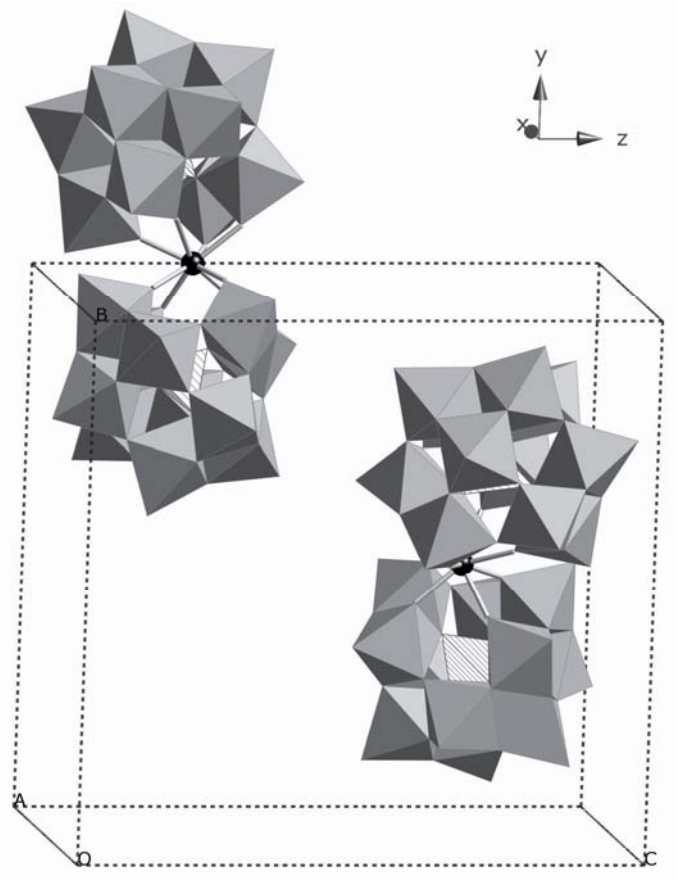

Figure 2.2 Packing of enantiopure $[Hf(PW_{11}O_{39})_2]^{10-}$, **2.1**, in the unit cell. Space group, $P2_12_12$, Z = 2. The $PW_{11}O_{39}^{7-}$ units are in polyhedral notation (WO_6 octahedra, gray; central PO_4 tetrahedra, striped). The coordination of Hf^{IV} is in ball-and-stick notation (Hf, black)

Although a series of lanthanide-substituted compounds, $[Ln(PW_{11}O_{39})_2]^{11-}$, were characterized by ^{31}P and ^{183}W NMR 35 years ago,[60] crystallographically well characterized sandwich-type polyoxometalates based on $PW_{11}O_{39}^{7-}$ are rare. The complex $Cs_{11}Eu(PW_{11}O_{39})_2 \cdot 28H_2O$ is typical: it crystallizes in a centrosymmetric space group in which the two enantiomers are related by an inversion center.[61] Thus, each independent polyoxoanion unit is chiral, but the unit cell is racemic. Usually, chiral sandwich-type POMs are racemic compounds both in the solid state or in solution. In contrast, **DMA2.1** is chiral and was obtained by spontaneous resolution on crystallization in the absence of any outside chiral influence. The chirality of the two enantiomers derives from the two configurations of **2.1** in which the two PW_{11} units are staggered relative to one another around a rotational axis through the center of the two ligating O_4 approximate planes of each PW_{11} group and the Hf atom. The antiprismatic orientation of the two O_4 ligand sets from each PW_{11} unit is neither eclipsing nor perfectly staggered as would define local idealized D_{4h} or D_{4d} $Hf(O_4)_2$ coordination polyhedra, respectively, but at an intermediate stagger (dihedral) angle of ca. 38 degrees (**Scheme 2.1**). Such chiral POMs have not been noted to crystallize as a conglomerate, i.e. one containing enantiopure crystallites.

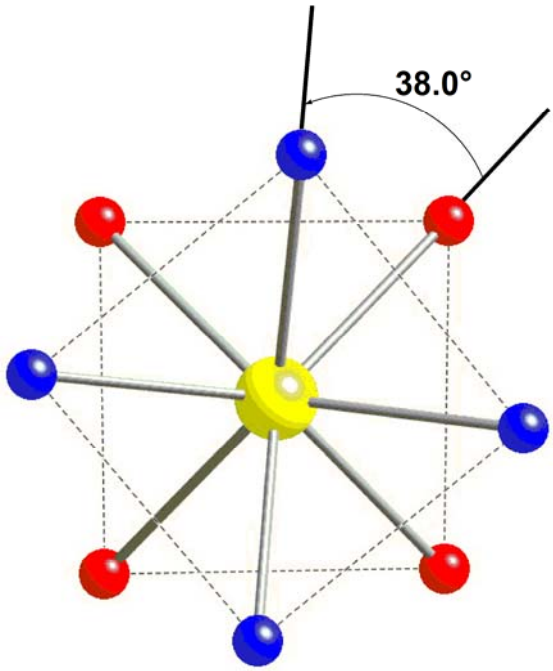

Scheme 2.1 The side view of the coordination mode of hafnium atom in one enantiomer. The red balls represent the oxygens from one $PW_{11}O_{39}^{7-}$ unit and the blue balls represent the oxygens from the other $PW_{11}O_{39}^{7-}$ unit. The yellow ball represents the hafnium atom.

2.3.3 Solid state circular dichroism

Since solid state circular dichroism has emerged as a very useful technique in stereochemistry in recent years, the formation of a conglomerate of **DMA2.1** was examined using solid state circular dichroism spectroscopy by incorporating individual crystals into KBr matrices. The two enantiomers show considerable optical activity in the solid state and afford approximately mirror-image CD spectra of each other (**Figure 2.3**). The crystals are designated as (+) and (-) based on the sign of the ellipticity at ca. 242 nm. Significantly, the circular dichroism is large, and it extends throughout the chromophore (adsorption) range of d^0 polytungstates. These two findings are consistent with those from the X-ray crystal structure that the chirality in **2.1** is largely manifested in

asymmetry of the entire cluster polyanion and not in the $Hf(O_4)_2$ coordination polyhedron. To the best of our knowledge, this is the first time that solid state circular dichroism has been used to characterize a chiral polyoxometalate.

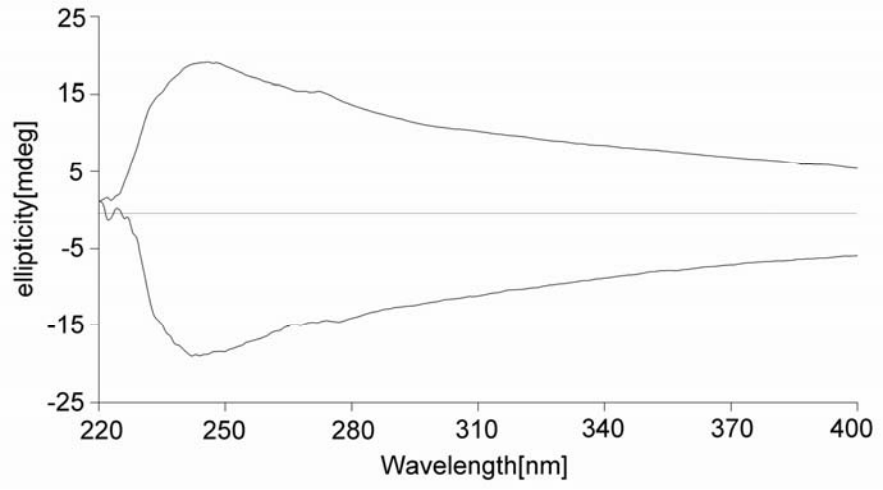

Figure 2.3 Solid state CD spectra of two enantiomeric crystals of $[Hf(PW_{11}O_{39})_2]^{10-}$, **2.1**, in KBr. A mixture of ca. 150 μg of each crystal and 100 mg of KBr was ground well and compacted into a transparent disk with a radius of 13 mm.

2.3.4 Characterizations in solid state and solution

The solid state CP-MAS ^{31}P NMR of **DMA2.1** (**Figure 2.4**) shows a single peak at -15.6 ppm indicating a pure compound with a single phosphorus center by symmetry. This is consistent with the asymmetric unit in **Figure 2.1** and the C_2 symmetry of polyanion **2.1**.

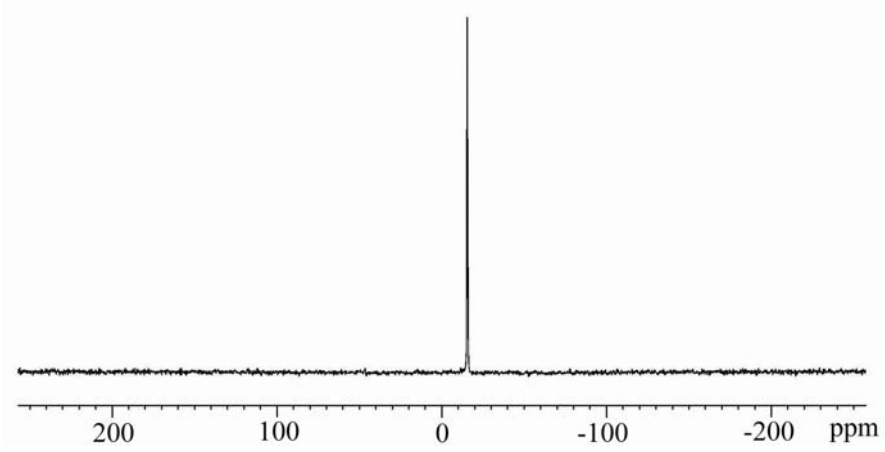

Figure 2.4 The solid state ^{31}P NMR of **DMA2.1**.

The tetraheptylammonium salt of **2.1** (THA**2.1**) was obtained via cation exchange from DMA**2.1** in chloroform solvent. The ^{31}P NMR spectrum of THA**2.1** in $CDCl_3$ solution also shows one peak at -16.7 ppm (**Figure 2.5**). In addition, the IR spectrum of **THA2.1** (**Figure 2.7**) is very similar to that of DMA**2.1 (Figure 2.6)**, which indicates that cation exchange does not change the polyoxoanion structure.

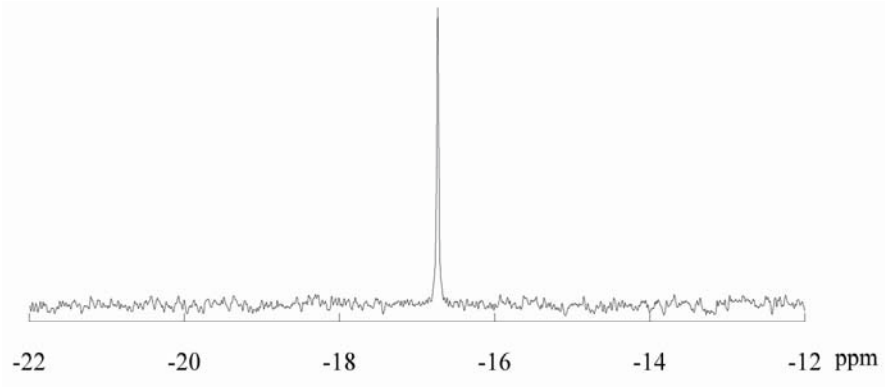

Figure 2.5 ^{31}P NMR of **THA2.1** in $CDCl_3$ solution.

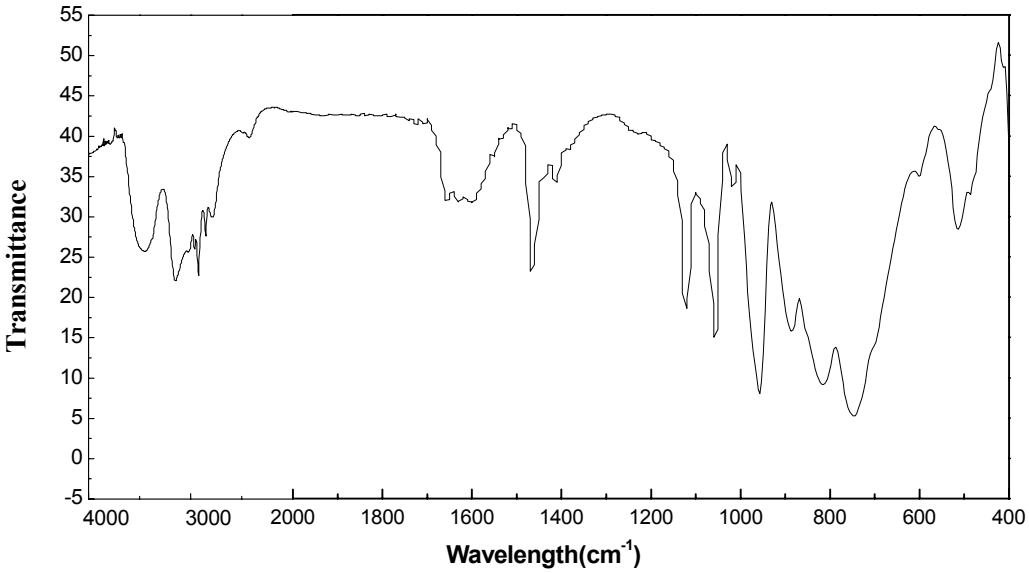

Figure. 2.6 The IR spectrum of **DMA2.1.**

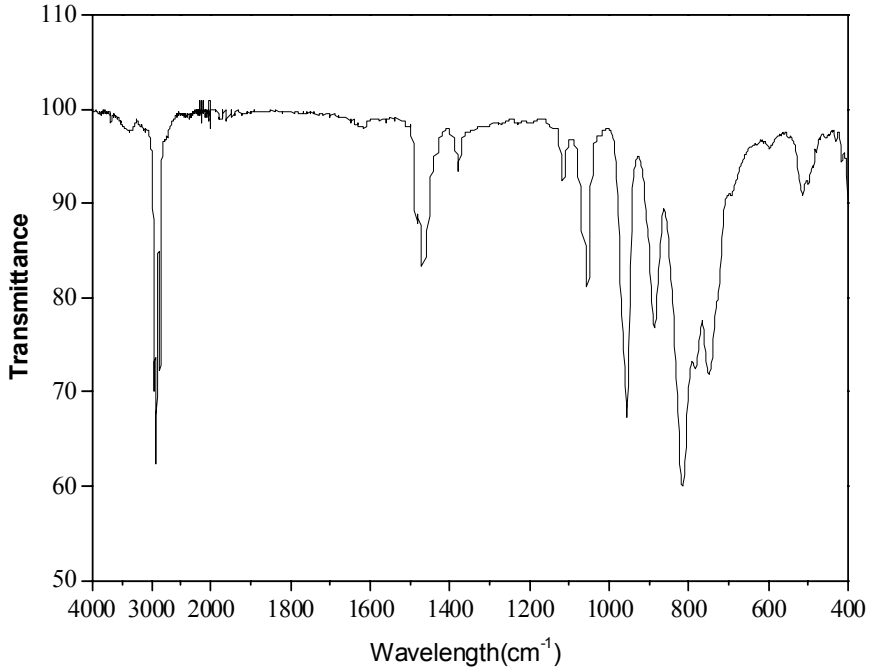

Figure. 2.7 The IR spectrum of **THA2.1.**

In contrast, dissolution of **DMA2.1** in D_2O followed by immediate (< 15 min) analysis by ^{31}P NMR shows two peaks at -14.3 and -14.2 ppm (**Figure 2.8**). To assess this spectrum, it is necessary to examine the results recently reported by Nomiya and co-workers on very similar but conventional racemic complexes $(Et_2NH_2)_{10}[M(\alpha\text{-}PW_{11}O_{39}]_2]$, M = Zr^{IV} and Hf^{IV} and the corresponding racemic Wells-Dawson Zr^{IV} and Hf^{IV} analogues, $K_{15}H[Zr(\alpha_2\text{-}P_2W_{17}O_{61})_2]$ and $K_{16}[Hf(\alpha_2\text{-}P_2W_{17}O_{61})_2]$.[58] The Keggin derivatives, $(Et_2NH_2)_{10}[M(\alpha\text{-}PW_{11}O_{39}]_2]$, M = Zr^{IV} and Hf^{IV}, crystallize with two enantiomeric pairs of C_2-symmetry diastereomers in the unit cell. The diastereomers have slightly different orientations of the two O4 tetradentate ligands on the Zr and Hf centers. The Wells-Dawson derivatives crystallize with only one pair of C_2-symmetry enantiomers in the unit cell. The ^{31}P NMR spectra of the former complexes show 2 peaks with nearly identical chemical shifts ($\alpha\text{-}PW_{11}O_{39}^{7-}$ alone, a control spectrum, shows one peak). The ^{31}P NMR spectra of the latter complexes show 2 peaks (as did the $\alpha_2\text{-}P_2W_{17}O_{61}$ alone). The authors, inferred, without discussion, that all four racemic sandwich complexes were maintaining their structures in solution.

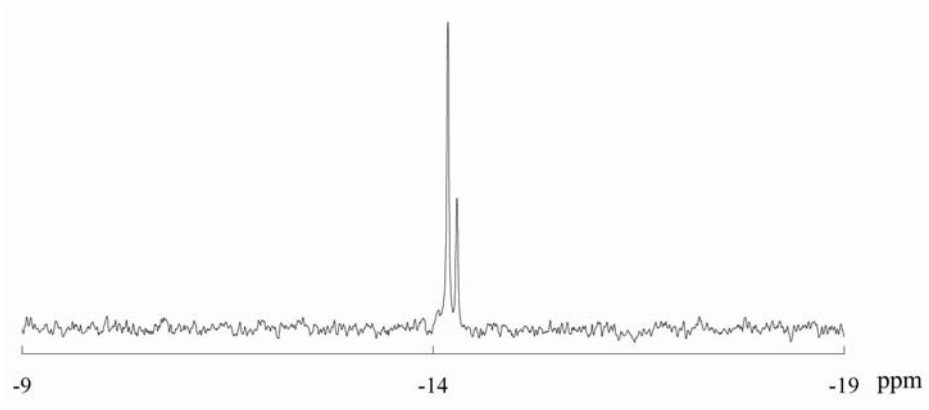

Figure 2.8 ^{31}P NMR of **DMA2.1** in D_2O solution**.**

This inference is reasonable based on two arguments: first, the rates of aqua ligand exchange on metal centers with formal 4+ oxidation states and commensurately high local positive charges such as Hf(IV), in aqueous solution is very slow; and second, that chelation as in the case of the tetradentate ligand $[A\text{-}\alpha\text{-}PW_9O_{34}]^{9-}$ further stabilizes the complex thermodynamically and kinetically. Thus the two peaks in the ^{31}P NMR spectrum of **DMA2.1** (**Figure 2.8**) most likely arise from protonation isomers (different protonation states). To evaluate this possibility, addition of ca. 2 equivalents of HCl (0.05M) to the solution in **Figure 2.8** produces a single broadened peak at -14.2 ppm. The chemical shift difference between -14.3 and -14.2 ppm is quite small, so it is reasonable that both species have nearly the same POM framework. In addition, the product recrystallized from the solution of **DMA2.1** in H_2O is also pure **DMA2.1** as confirmed by FT-IR. The results are consistent with a structurally nondisruptive reversible deprotonation of **DMA2.1** when it is dissolved in H/D_2O and that the two peaks in **Figure 2.8** arise from two different protonation states of the same complex, **DMA2.1**.

2.4 Conclusions

In summary, a chiral cluster compound, a POM, $[Hf(PW_{11}O_{39})_2]^{10-}$, **2.1**, has been obtained by spontaneous resolution upon crystallization in the absence of any chiral source. Optically active crystals of both enantiomers were isolable and spectroscopically distinguishable. The solid state CD spectrum and X-ray crystal structure of enantiopure crystals indicate significant chirality manifested throughout the entire polyanion structure.

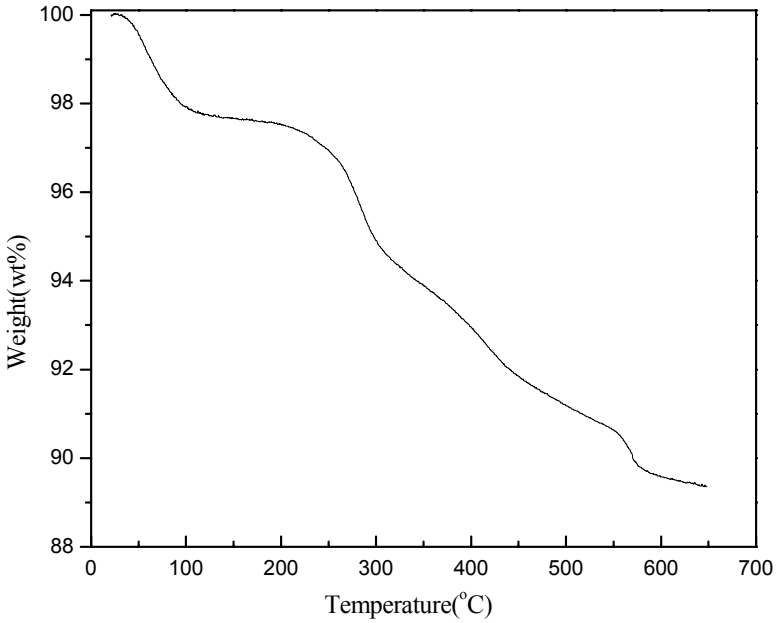

Figure 2.9 The thermogravimetric analysis (TGA) curve of **DMA2.1**.

Table 2.2. Selected bond lengths [Å] and angles [deg] for **DMA2.1**

Bond lengths			
W(1)-O(31)	1.965(7)	W(1)-O(32)	2.041(8)
W(1)-O(36)	1.782(8)	W(1)-O(4)	2.445(8)
W(1)-O(37)	1.891(7)	W(1)-O(39)	1.710(8)
W(2)-O(7)	1.719(9)	W(2)-O(9)	1.915(8)
W(2)-O(16)	1.828(8)	W(2)-O(10)	1.943(8)
W(2)-O(14)	1.917(8)	W(2)-O(1)	2.412(7)
W(3)-O(19)	1.726(9)	W(3)-O(13)	1.907(8)
W(3)-O(31)	1.888(7)	W(3)-O(20)	1.920(8)
W(3)-O(18)	1.895(8)	W(3)-O(4)	2.443(8)
W(4)-O(38)	1.720(8)	W(4)-O(29)	1.937(7)
W(4)-O(35)	1.787(7)	W(4)-O(30)	2.048(8)
W(4)-O(37)	1.933(8)	W(4)-O(3)	2.408(8)
W(5)-O(5)	1.724(9)	W(5)-O(8)	1.912(8)
W(5)-O(10)	1.906(8)	W(5)-O(11)	1.916(8)
W(5)-O(12)	1.909(8)	W(5)-O(1)	2.361(7)
W(6)-O(23)	1.711(8)	W(6)-O(22)	1.952(7)
W(6)-O(34)	1.815(8)	W(6)-O(16)	2.035(8)
W(6)-O(24)	1.916(8)	W(6)-O(2)	2.328(7)
W(7)-O(21)	1.731(8)	W(7)-O(22)	1.921(7)
W(7)-O(33)	1.787(7)	W(7)-O(15)	2.032(8)
W(7)-O(20)	1.914(8)	W(7)-O(2)	2.315(7)
W(8)-O(25)	1.695(9)	W(8)-O(14)	1.913(8)
W(8)-O(24)	1.881(8)	W(8)-O(26)	1.930(8)
W(8)-O(29)	1.905(7)	W(8)-O(3)	2.469(8)
W(9)-O(17)	1.715(10)	W(9)-O(12)	1.938(8)
W(9)-O(32)	1.855(8)	W(9)-O(18)	1.966(8)
W(9)-O(28)	1.878(8)	W(9)-O(4)	2.451(8)
W(10)-O(6)	1.715(9)	W(10)-O(13)	1.928(8)
W(10)-O(15)	1.842(8)	W(10)-O(8)	1.975(8)
W(10)-O(9)	1.913(8)	W(10)-O(1)	2.441(7)
W(11)-O(27)	1.703(9)	W(11)-O(11)	1.924(8)
W(11)-O(30)	1.843(8)	W(11)-O(28)	1.929(8)

W(11)-O(26)	1.903(8)	W(11)-O(3)	2.439(8)
Hf(1)-O(35)	2.164(7)	Hf(1)-O(33)	2.198(7)
Hf(1)-O(36)	2.180(7)	Hf(1)-O(34)	2.200(8)
P(1)-O(4)	1.519(8)	P(1)-O(3)	1.530(8)
P(1)-O(2)	1.519(8)	P(1)-O(1)	1.546(8)

Bond Angles

O(39)-W(1)-O(36)	104.7(4)	O(37)-W(1)-O(32)	83.6(3)
O(39)-W(1)-O(37)	102.7(4)	O(31)-W(1)-O(32)	81.5(3)
O(36)-W(1)-O(37)	93.1(3)	O(39)-W(1)-O(4)	167.0(3)
O(39)-W(1)-O(31)	101.6(3)	O(36)-W(1)-O(4)	86.9(3)
O(36)-W(1)-O(31)	92.2(3)	O(37)-W(1)-O(4)	82.2(3)
O(37)-W(1)-O(31)	152.9(3)	O(31)-W(1)-O(4)	71.6(3)
O(39)-W(1)-O(32)	97.6(4)	O(32)-W(1)-O(4)	70.8(3)
O(36)-W(1)-O(32)	157.7(3)		
O(7)-W(2)-O(16)	103.9(4)	O(14)-W(2)-O(10)	86.4(3)
O(7)-W(2)-O(14)	101.4(4)	O(9)-W(2)-O(10)	85.0(3)
O(16)-W(2)-O(14)	87.7(3)	O(7)-W(2)-O(1)	169.6(3)
O(7)-W(2)-O(9)	100.5(4)	O(16)-W(2)-O(1)	84.7(3)
O(16)-W(2)-O(9)	91.4(3)	O(14)-W(2)-O(1)	84.6(3)
O(14)-W(2)-O(9)	157.6(3)	O(9)-W(2)-O(1)	73.1(3)
O(7)-W(2)-O(10)	100.9(4)	O(10)-W(2)-O(1)	70.7(3)
O(16)-W(2)-O(10)	155.1(4)		
O(19)-W(3)-O(31)	102.1(4)	O(18)-W(3)-O(20)	156.3(3)
O(19)-W(3)-O(18)	102.1(4)	O(13)-W(3)-O(20)	85.8(3)
O(31)-W(3)-O(18)	88.9(3)	O(19)-W(3)-O(4)	174.0(3)
O(19)-W(3)-O(13)	100.9(4)	O(31)-W(3)-O(4)	72.8(3)
O(31)-W(3)-O(13)	156.7(3)	O(18)-W(3)-O(4)	75.1(3)
O(18)-W(3)-O(13)	90.1(3)	O(13)-W(3)-O(4)	84.4(3)
O(19)-W(3)-O(20)	101.6(4)	O(20)-W(3)-O(4)	81.3(3)
O(31)-W(3)-O(20)	85.7(3)		
O(38)-W(4)-O(35)	106.0(4)	O(37)-W(4)-O(30)	82.8(3)
O(38)-W(4)-O(37)	104.0(4)	O(29)-W(4)-O(30)	82.8(3)
O(35)-W(4)-O(37)	89.9(3)	O(38)-W(4)-O(3)	165.7(3)
O(38)-W(4)-O(29)	98.0(4)	O(35)-W(4)-O(3)	86.5(3)
O(35)-W(4)-O(29)	95.4(3)	O(37)-W(4)-O(3)	82.5(3)
O(37)-W(4)-O(29)	155.0(3)	O(29)-W(4)-O(3)	73.4(3)
O(38)-W(4)-O(30)	97.1(3)	O(30)-W(4)-O(3)	70.8(3)
O(35)-W(4)-O(30)	156.8(3)		

O(5)-W(5)-O(10)	102.0(4)	O(12)-W(5)-O(11)	85.9(3)
O(5)-W(5)-O(12)	101.9(4)	O(8)-W(5)-O(11)	157.2(3)
O(10)-W(5)-O(12)	156.1(3)	O(5)-W(5)-O(1)	171.6(4)
O(5)-W(5)-O(8)	100.5(4)	O(10)-W(5)-O(1)	72.4(3)
O(10)-W(5)-O(8)	87.6(4)	O(12)-W(5)-O(1)	83.8(3)
O(12)-W(5)-O(8)	88.2(3)	O(8)-W(5)-O(1)	73.4(3)
O(5)-W(5)-O(11)	102.3(4)	O(11)-W(5)-O(1)	84.1(3)
O(10)-W(5)-O(11)	88.9(3)		
O(23)-W(6)-O(34)	101.7(4)	O(24)-W(6)-O(16)	80.4(3)
O(23)-W(6)-O(24)	100.6(3)	O(22)-W(6)-O(16)	85.2(3)
O(34)-W(6)-O(24)	95.3(3)	O(23)-W(6)-O(2)	171.5(3)
O(23)-W(6)-O(22)	98.6(3)	O(34)-W(6)-O(2)	78.9(3)
O(34)-W(6)-O(22)	92.2(3)	O(24)-W(6)-O(2)	87.7(3)
O(24)-W(6)-O(22)	157.6(3)	O(22)-W(6)-O(2)	73.0(3)
O(23)-W(6)-O(16)	98.9(3)	O(16)-W(6)-O(2)	80.7(3)
O(34)-W(6)-O(16)	159.3(3)		
O(21)-W(7)-O(33)	102.7(4)	O(20)-W(7)-O(15)	81.0(3)
O(21)-W(7)-O(20)	100.1(4)	O(22)-W(7)-O(15)	84.5(3)
O(33)-W(7)-O(20)	95.9(3)	O(21)-W(7)-O(2)	173.3(3)
O(21)-W(7)-O(22)	99.6(4)	O(33)-W(7)-O(2)	79.3(3)
O(33)-W(7)-O(22)	91.6(3)	O(20)-W(7)-O(2)	86.0(3)
O(20)-W(7)-O(22)	156.8(3)	O(22)-W(7)-O(2)	73.8(3)
O(21)-W(7)-O(15)	97.0(3)	O(15)-W(7)-O(2)	81.1(3)
O(33)-W(7)-O(15)	160.3(3)		
O(25)-W(8)-O(24)	103.8(4)	O(29)-W(8)-O(26)	87.3(3)
O(25)-W(8)-O(29)	102.3(4)	O(14)-W(8)-O(26)	86.5(3)
O(24)-W(8)-O(29)	89.8(3)	O(25)-W(8)-O(3)	171.7(3)
O(25)-W(8)-O(14)	102.2(4)	O(24)-W(8)-O(3)	82.9(3)
O(24)-W(8)-O(14)	86.1(3)	O(29)-W(8)-O(3)	72.5(3)
O(29)-W(8)-O(14)	155.4(3)	O(14)-W(8)-O(3)	82.9(3)
O(25)-W(8)-O(26)	100.7(4)	O(26)-W(8)-O(3)	72.9(3)
O(24)-W(8)-O(26)	155.3(3)		
O(17)-W(9)-O(32)	103.5(4)	O(28)-W(9)-O(18)	157.2(3)
O(17)-W(9)-O(28)	102.2(4)	O(12)-W(9)-O(18)	84.3(3)
O(32)-W(9)-O(28)	92.9(3)	O(17)-W(9)-O(4)	172.7(4)
O(17)-W(9)-O(12)	102.3(4)	O(32)-W(9)-O(4)	73.4(3)
O(32)-W(9)-O(12)	153.9(3)	O(28)-W(9)-O(4)	84.6(3)
O(28)-W(9)-O(12)	85.3(3)	O(12)-W(9)-O(4)	80.5(3)
O(17)-W(9)-O(18)	99.8(4)	O(18)-W(9)-O(4)	73.7(3)
O(32)-W(9)-O(18)	87.8(3)		
O(6)-W(10)-O(15)	104.4(4)	O(9)-W(10)-O(8)	85.8(3)

O(6)-W(10)-O(9)	101.2(4)	O(13)-W(10)-O(8)	84.6(3)
O(15)-W(10)-O(9)	93.3(3)	O(6)-W(10)-O(1)	169.1(3)
O(6)-W(10)-O(13)	102.0(4)	O(15)-W(10)-O(1)	85.0(3)
O(15)-W(10)-O(13)	86.2(3)	O(9)-W(10)-O(1)	72.5(3)
O(9)-W(10)-O(13)	156.2(3)	O(13)-W(10)-O(1)	83.8(3)
O(6)-W(10)-O(8)	100.6(4)	O(8)-W(10)-O(1)	70.5(3)
O(15)-W(10)-O(8)	154.6(3)		
O(27)-W(11)-O(30)	102.5(4)	O(26)-W(11)-O(28)	157.0(3)
O(27)-W(11)-O(26)	101.3(4)	O(11)-W(11)-O(28)	83.5(3)
O(30)-W(11)-O(26)	90.0(3)	O(27)-W(11)-O(3)	173.4(3)
O(27)-W(11)-O(11)	102.5(4)	O(30)-W(11)-O(3)	73.2(3)
O(30)-W(11)-O(11)	154.9(3)	O(26)-W(11)-O(3)	74.0(3)
O(26)-W(11)-O(11)	87.3(3)	O(11)-W(11)-O(3)	82.1(3)
O(27)-W(11)-O(28)	101.2(4)	O(28)-W(11)-O(3)	83.9(3)
O(30)-W(11)-O(28)	89.6(3)		
O(35)-Hf(1)-O(35)#1	80.0(4)	O(33)#1-Hf(1)-O(33)	80.4(4)
O(35)-Hf(1)-O(36)	72.1(3)	O(35)-Hf(1)-O(34)	74.2(3)
O(35)#1-Hf(1)-O(36)	74.1(3)	O(35)#1-Hf(1)-O(34)	146.7(3)
O(35)-Hf(1)-O(36)#1	74.1(3)	O(36)-Hf(1)-O(34)	116.1(3)
O(35)#1-Hf(1)-O(36)#1	72.1(3)	O(36)#1-Hf(1)-O(34)	80.7(3)
O(36)-Hf(1)-O(36)#1	135.4(4)	O(33)#1-Hf(1)-O(34)	74.4(3)
O(35)-Hf(1)-O(33)#1	138.4(3)	O(33)-Hf(1)-O(34)	73.0(3)
O(35)#1-Hf(1)-O(33)#1	115.0(3)	O(35)-Hf(1)-O(34)#1	146.7(3)
O(36)-Hf(1)-O(33)#1	147.7(3)	O(35)#1-Hf(1)-O(34)#1	74.2(3)
O(36)#1-Hf(1)-O(33)#1	74.6(3)	O(36)-Hf(1)-O(34)#1	80.7(3)
O(35)-Hf(1)-O(33)	115.0(3)	O(36)#1-Hf(1)-O(34)#1	116.1(3)
O(35)#1-Hf(1)-O(33)	138.4(3)	O(33)#1-Hf(1)-O(34)#1	73.0(3)
O(36)-Hf(1)-O(33)	74.6(3)	O(33)-Hf(1)-O(34)#1	74.4(3)
O(36)#1-Hf(1)-O(33)	147.7(3)	O(34)-Hf(1)-O(34)#1	136.9(4)
O(4)-P(1)-O(2)	110.7(4)	O(4)-P(1)-O(1)	108.8(4)
O(4)-P(1)-O(3)	108.3(4)	O(2)-P(1)-O(1)	108.8(4)
O(2)-P(1)-O(3)	111.2(4)	O(3)-P(1)-O(1)	109.0(4)

Symmetry transformations used to generate equivalent atoms: #1 -x+1,-y+1,z #2 -x+1,-y+2,z

References

(1) Pasteur, L. *Ann. Chim. Phys.* **1848**, *24*, 442.

(2) Jacques, J.; Collet, A.; Wilen, S. H.; Krieger Publishing Company, Malabar, Florida: 1994.

(3) Wen, R.; Bernal, I. In *217th ACS National Meeting* Anaheim, CA, 1999.

(4) Perez-Garcia, L.; Amabilino, D. B. *Chem. Soc. Rev.* **2002**, *31*, 342.

(5) Cohen, M. D.; Schmidt, G. M. J. *J. Chem. Soc.* **1964**, 1996.

(6) Green, B. S.; Lahav, M.; Rabinovich, D. *Acc. Chem. Res.* **1979**, *12*, 191.

(7) Mason, S. F. *Nature (London)* **1984**, *311*, 19.

(8) Kaupp, G.; Haak, M. *Angew. Chem., Int. Ed. Engl.* **1993**, *32*, 694.

(9) Toda, F.; Yagi, M.; Soda, S. *J. Chem. Soc., Chem. Commun.* **1987**, 1413.

(10) Takahashi, M.; Sekine, N.; Fujita, T.; Watanabe, S.; Yamaguchi, K.; Sakamoto, M. *J. Am. Chem. Soc.* **1998**, *120*, 12770.

(11) Kohmoto, S.; Masu, H.; Tatsuno, C.; Kishikawa, K.; Yamamoto, M.; Yamaguchi, K. *J. Chem. Soc., Perkin Trans.* **2000**, 4464.

(12) Sakamoto, M.; Iwamoto, T.; Nono, N.; Ando, M.; Arai, W.; Mino, T.; Fujita, T. *J. Org. Chem.* **2003**, *68*, 942.

(13) Katsuki, I.; Motoda, Y.; Sunatsuki, Y.; Matsumoto, N.; Nakashima, T.; Kojima, M. *J. Am. Chem. Soc.* **2002**, *124*, 629.

(14) Brock, C. P.; Schweizer, W. B.; Dunitz, J. D. *J. Am. Chem. Soc.* **1991**, *113*, 9811.

(15) Okuhara, T.; Mizuno, N.; Misono, M. *Advances in Catalysis* **1996**, *41*, 113.

(16) Rhule, J. T.; Hill, C. L.; Judd, D. A.; Schinazi, R. F. *Chem. Rev.* **1998**, *98*, 327.

(17) Neumann, R. *Prog. Inorg. Chem.* **1998**, *47*, 317.

(18) Judd, D. A.; Nettles, J. H.; Nevins, N.; Snyder, J. P.; Liotta, D. C.; Tang, J.; Ermolieff, J.; Schinazi, R. F.; Hill, C. L. *J. Am. Chem. Soc.* **2001**, *123*, 886.

(19) Neumann, R. *Mod. Oxidation Methods.* **2004**, 223.

(20) Kortz, U.; Matta, S. *Inorg. Chem.* **2001**, *40*, 815.

(21) Sadakane, M.; Dickman, M. H.; Pope, M. T. *Inorg. Chem.* **2001**, *40*, 2715.

(22) Shigeta, S.; Mori, S.; Kodama, E.; Kodama, J.; Takahashi, K.; Yamase, T. *Antiviral Res.* **2003**, *58*, 265.

(23) Hill, C. L.; Prosser-McCartha, C. M. *Coord. Chem. Rev.* **1995**, *143*, 407.

(24) Hill, C. L. In *Comprehensive Coordination Chemistry-II: From Biology to Nanotechnology* 2004; Vol. 4, p 679.

(25) Inoue, M.; Yamase, T. *Bull. Chem. Soc. Jpn.* **1995**, *68*, 3055.

(26) Kortz, U.; Savelieff, M. G.; Ghali, F. Y. A.; Khalil, L. M.; Maalouf, S. A.; Sinno, D. I. *Angew. Chem., Int. Ed. Engl.* **2002**, *41*, 4070.

(27) Fang, X.; Anderson, T. M.; Hou, Y.; Hill, C. L. *Chem. Commun.* **2005**, 5044.

(28) Fang, X.; Anderson, T. M.; Hill, C. L. *Angew. Chem. Int. Ed.* **2005**, *44*, 3540.

(29) An, H. Y.; Wang, E. B.; Xiao, D. R.; Li, Y. G.; Su, Z. M.; Xu, L. *Angew. Chem., Int. Ed. Engl.* **2006**, *45*, 904.

(30) Long, D.; Kögerler, P.; Farrugia, L. J.; L. Cronin, C. *Asi. J.* **2006**, *1*, 352.

(31) Tan, H.; Li, Y.; Zhang, Z.; Qin, C.; Wang, X.; Wang, E.; Su, Z. *J. Am. Chem. Soc.* **2007**, 10066.

(32) Zhang, X.; Sasaki, K.; Hill, C. L. *J. Am. Chem. Soc.* **1996**, *118*, 4809.

(33) Neumann, R.; Khenkin, A. M. *J. Mol. Catal. A: Chem.* **1996**, *114*, 169.

(34) Neumann, R.; Khenkin, A. M.; Juwiler, D.; Miller, H.; Gara, M. *J. Mol. Catal. A: Chem.* **1997**, *117*, 169.

(35) Neumann, R.; Dahan, M. *J. Am. Chem. Soc.* **1998**, *120*, 11969.

(36) Boesing, M.; Noeh, A.; Loose, I.; Krebs, B. *J. Am. Chem. Soc.* **1998**, *120*, 7252.

(37) Okun, N. M.; Anderson, T. M.; Hill, C. L. *J. Mol. Catal. A: Chem.* **2003**, *197*, 283.

(38) Nardello, V.; Aubry, J.-M.; Vos, D. E. D.; Neumann, R.; Adam, W.; Zhang, R.; Elshof, J. E. T.; Witte, P. T.; Alsters, P. L. *J. Mol. Catal. A Chem.* **2006**, *251(1-2)*, 185.

(39) Bonchio, M.; Carraro, M.; Farinazzo, A.; Sartorel, A.; Scorrano, G.; Kortz, U. *J. Mol. Catal. A: Chem. Special Issue* **2007**, *262*, 36.

(40) Copping, R.; Gaunt, A. J.; May, I.; Sarsfield, M. J.; Collison, D.; Helliwell, M.; Denniss, I. S.; Apperley, D. C. *Dalton Trans.* **2005**, 1256.

(41) Knoth, W. H.; Harlow, R. L. *J. Am. Chem. Soc.* **1981**, *103*, 1865.

(42) Niu, J.-Y.; You, X.-Z.; Duan, C.-Y.; Fun, H.-K.; Zhou, Z.-Y. *Inorg. Chem.* **1996**, *35*, 4211.

(43) Chen, Q.; Hill, C. L. *Inorg. Chem.* **1996**, *35*, 2403.

(44) Tézé, A.; Cadot, E.; Bereau, V.; Hervé, G. *Inorg. Chem.* **2001**, *40*, 2000.

(45) Wu, C.-D.; Lu, C.-Z.; Chen, S.-M.; Zhuang, H.-H.; Huang, J.-S. *Polyhedron* **2003**, *22*, 3091.

(46) Manos, M. J.; Miras, H. N.; Tangoulis, V.; Woollins, J. D.; Slawin, A. M. Z.; Kabanos, T. A. *Angew. Chem., Int. Ed. Engl.* **2003**, *42*, 425.

(47) Sartorel, A.; Carraro, M.; Bagno, A.; Scorrano, G.; Bonchio, M. *Angew. Chem. Int. Ed.* **2007**, *46*, 3255.

(48) Fang, X.; Hill, C. L. *Angew. Chem. Int. Ed. Engl.* **2007**, *46*, 3877.

(49) Pauling, L. In *The nature of the chemical bond and the structure of molecules and crystals; an introduction to modern structural chemistry*; 3rd Ed ed.; Cornell University Press: Ithaca, 1960.

(50) Day, V. W.; Klemperer, W. G.; Maltbie, D. J. *J. Am. Chem. Soc.* **1987**, *109*, 2991.

(51) Leclerc-Laronze, N.; Haouas, M.; Marrot, J.; Taulelle, F.; Hervé, G. *Angew. Chem. Int. Ed. Engl.* **2006**, *45*, 139.

(52) Mayer, C. R.; Herson, P.; Thouvenot, R. *Inorg. Chem.* **1999**, *38*, 6152.

(53) Proust, A.; Thouvenot, R.; Herson, P. *J. Chem. Soc , Dalton Trans.* **1999**, 51.

(54) Peng, Z. H. *Angew. Chem. Int. Ed. Engl.* **2004**, *43*, 930.

(55) You, W. S.; Wang, E. B.; Xu, Y.; Li, Y. G.; Xu, L.; Hu, C. W. *Inorg. Chem.* **2001**, *40*, 5468.

(56) Bi, L. H.; Hussain, F.; Kortz, U.; Sadakane, M.; Dickman, M. H. *Chem. Commun.* **2004**, 1420.

(57) Felices, L. S.; Vitoria, P.; Gutirrez-Zorrilla, J. M.; Reinoso, S.; Etxebarria, J.; Lezama, L. *Chem. Eur. J.* **2004**, *10*, 5138.

(58) Kato, C. N.; Shinohara, A.; Hayashi, K.; Nomiya, K. *Inorg. Chem.* **2006**, *45*, 8108.

(59) Flack parameter: The Flack parameter = 0.015(13) indicates the correct absolute configuration of 1. Flack parameter, x., defined from the equation, I(hkl) = (1-x) |F(hkl)|2 + x |F(-h-k-l)|2 and it is used to estimate the absolute configuration of a structural model. The physically meaningful range of x is between 0 and 1. The ideal value of 0 indicates the correctness of the absolute structure given by the structural refinement. In the experimental data, x(μ) represents the Flack parameter and its standard uncertainty. When x(μ) is within the reasonable statistical fluctuation | x | $\leqslant$ 3μ, its value will be near to 0 which helps certify the correctness of the structure.

(60) Peacock, R. D.; Weakley, T. J. R. *J. Chem. Soc. A.* **1971**, 1836.

(61) Zhang, C.; Robertha, C.; Howell, K. B.; Scotland, F. G.; Perez, L. T.; Lynn, C. F. *Inorg. Chem.* **2004**, *43*, 7691.

CHAPTER

3

Syntheses and Characterizations of Diruthenium and Tetraruthenium Containing Polytungstosilicates

(published partially in *J. Am. Chem. Soc.*, **2009**, *131 (47)*, 17360–17370)
with Yurii V. Geletii, Claire Besson, Qiushi Yin, Djamaladdin G. Musaev, David Quionero, Rui Cao, Kenneth I. Hardcastle, Anna Proust, Paul Kgerler and Craig L. Hill

Abstract: In this chapter, a diruthenium containing polyanion, $[\{Ru_2O_2(OH_2)_2\}(\gamma\text{-}SiW_{10}O_{36})]^{6-}$ (**3.1**), and a one-electron oxidized tetratuthenium containing polyanion, $[\{Ru^{V}Ru^{IV}_3O_6(OH_2)_4\}(\gamma\text{-}SiW_{10}O_{36})_2]^{11-}$ (**3.2**), have been synthesized and characterized. The structure of **3.1** was deduced from element analysis, infrared spectroscopy, UV-vis spectroscopy. Compound **3.2** was characterized thoroughly by voltammetric rest potentials, X-ray structure, extinction coefficient, elemental analysis and magnetism. All of these lines of evidence indicate that **3.2** is a one-electron oxidized form of $[\{Ru^{IV}_4O_4(OH)_2(H_2O)_4\}(\gamma\text{-}SiW_{10}O_{36})_2]^{10-}$ which is a highly efficient water oxidation catalyst. Cation effects on the cyclic voltammograms of $Rb_8K_2[\{Ru_4O_4(OH)_2(H_2O)_4\}(\gamma\text{-}SiW_{10}O_{36})_2]$ have been studied by adding alkali metal cations.

3.1 Introduction

Recently, mankind's need to replace fossil fuels with abundant, clean, and renewable energy sources has been brought to the forefront of the world's attention.[1] One long-sought solution is to develop a photoelectrochemical device which is able to split water into O_2 and H_2.[2] Thus, exploring new, efficient O_2 evolution catalysts is a key task toward this goal.[3] A suitable water oxidation catalyst (WOC) must be fast, capable of water oxidation at a potential minimally above the thermodynamic value ($H_2O \rightarrow O_2 + 4H^+ + 4e^-$; 1.229–0.059×pH at 25 °C), and importantly, stable to oxidative, hydrolytic, and thermal degradation under turnover conditions. Currently, WOCs have been developed into two classes: solid state metal-oxide catalytic surfaces [4-17]and molecular catalysts[4,18-45]. Solid state WOCs are generally inexpensive, easily to be incorporated into electrochemical devices, and critically, robust under oxidative conditions. An amorphous, non-conducting Co:P:O phase formed upon electrooxidation of Co^{2+} has shown good catalytic activity in water oxidation.[14] In addition, nanoscopic particles of

Co_3O_4 spinel [46] and colloidal $IrO_2 \cdot nH_2O$ particles[17] have also been found to exhibit considerably high catalytic water oxidation rates. The development of molecular catalysts is inspired by the discovery of the structure of oxygen evolution center (OEC) in *photosystem II* whose active site contains a $CaMn_4O_x$ core.[47-51] With this model in hand, many efforts have been devoted to develop WOCs based on ruthenium, manganese, and iridium containing complexes. The first and representative molecular WOC was the Meyer group's "blue dimer" in which two Ru^{III} atoms are bridged by oxygen.[19,41] Since its discovery, a range of oxo-bridged Ru dimer catalysts and mononuclear Ru complexes have been reported to oxidize water.[19-22,25,26,28,29,37-45,52] Several Mn complexes and a new family of iridium complexes are also described in the literatures as catalysts for water oxidation.[23,24,27,31,32,34-36,53,54] It should be noted to mention that most of these complexes have organic ligands on the structure, which results in decomposition under oxidation conditions.[19,25,28,29,35,44,55-59]

Our objective is to design water soluble WOCs which is stable under water oxidation turnover conditions. Organic-solvent-soluble tetrabutylammonium (TBA) salt of $[\{Ru_2(OH)_2(OH_2)_2\}(\gamma\text{-}SiW_{10}O_{36})]^{4-}$ has been reported earlier.[60] We expect that water soluble salt of this di-ruthenium complex could be a good candidate as water oxidation catalyst because of its structural similarity to Meyer's blue dimer. The cesium salt, $Cs_6[\{Ru_2O_2(OH_2)_2\}(\gamma\text{-}SiW_{10}O_{36})]\cdot 25H_2O$ **3.1**, was obtained by using a similar synthetic method. Compound **3.1** is not stable in aqueous solution which has been clearly revealed by following the UV-vis spectra with time. It also turns out that $[\{Ru_2O_2(OH_2)_2\}(\gamma\text{-}SiW_{10}O_{36})]^{6-}$ will dimerize to $[\{Ru_4O_4(O_H)_2(H_2O)_4\}(\gamma\text{-}SiW_{10}O_{36})_2]^{10-}$ in a more acidic condition. Compound $Rb_8K_2[\{Ru_4O_4(OH)_2(H_2O)_4\}(\gamma\text{-}SiW_{10}O_{36})_2]$, **3.3**, has been isolated

and structurally characterized.[61] In the structure of **3.3**, two polytungstate ligands, γ-$SiW_{10}O_{36}^{8-}$, sandwich a Ru_4O_6 core with four Ru atoms in IV oxidation state. This compound exhibits several reversible one-electron redox couples by cyclic voltammetry and catalyzes water oxidation electrochemically at low overpotentials. It can catalyze water oxidation chemically in the presence of $[Ru(bpy)_3]^{3+}$ as an oxidant in buffer solution at pH around 7 and also photochemically under light driven conditions in the presence of a sacrificial electron acceptor (persulfate).[62]

Attempting to explore the mechanism of water oxidation, we isolated a one-electron-oxidized form of **3.3** with a formula $H_2Ce_{2.5}K(NH_4)_{0.5}[\{Ru^{V}Ru^{IV}{}_3O_6(OH_2)_4\}(\gamma\text{-}SiW_{10}O_{36})_2]$ (**3.2**). In this chapter, the syntheses and characterization of **3.1** and **3.2**, and cation effects on electrochemistry of polyanion **3.3** are reported.

3.2 Experimental

3.2.1 General Methods and Materials

Potassium γ-decatungstosilicate, $K_8[\gamma\text{-}SiW_{10}O_{36}]\cdot 12H_2O$ and $Rb_8K_2[\{Ru^{IV}{}_4O_4(OH)_2(H_2O)_4\}(\gamma\text{-}SiW_{10}O_{36})_2]\cdot 25H_2O$ (**3.3**) were prepared by the literature methods. Elemental analyses were performed by Columbia Analytical Services (Tucson, AZ) and Atlantic Microlab Inc. (Norcross, GA). Water for the preparation of solutions was obtained from a Barnstead Nanopure® water-purification system, and all other chemicals and salts were from commercial sources. Infrared spectra (2% sample in KBr) were recorded on a Nicolet 510 FTIR spectrometer. UV-vis spectra were acquired using an Agilent 8453 spectrophotomer. Electrochemical data were obtained at room temperature using a BAS CV-50W electrochemical analyzer equipped with a glassy-carbon working electrode, a Pt-wire auxiliary electrode, and a Ag/AgCl (3 M NaCl) BAS

reference electrode. All reduction potentials are measured relative to this reference electrode (~250 mV difference between the NHE and BAS electrodes; this value may vary slightly depending on solution acidity and ionic strength). Cyclic voltammograms (CVs) were obtained under Ar using 0.5-2 mM POM concentrations in 0.1 M HCl, 0.1 M H_2SO_4, 10-200 mM sulfate buffer (pH 2.0), or 10-200 mM phosphate buffer (pH 7.2) with scan rates 25 and 100 mV s^{-1}. Sulfate buffers were prepared from H_2SO_4 and LiOH, NaOH, or KOH. Phosphate buffers were prepared from H_3PO_4 and NaOH, or KOH. The appropriate amounts of LiCl, NaCl, or KCl were added to buffer solutions to examine the effect of differing cations.

3.2.2 Synthesis of 3.1

$K_8[\gamma\text{-}SiW_{10}O_{36}]\cdot 12H_2O$ (4 g, 1.35 mmol) is added to 21.5 mL H_2O at 40 °C and the mixture vigorously stirred for 10-15 min. The slightly cloudy mixture is filtered through a fine frit to obtain a clear pH 7.8 solution to which 0.6 g (2.66 mmol) of solid $RuCl_3\cdot H_2O$ is added. The resulting clear, dark brown solution (pH 2.4) is concentrated using a rotary evaporator to yield a black metallic powder, which is redissolved in 21.5 mL H_2O and filtered. Immediately after filtration, 1.6 g (9.5 mmol) of CsCl is added resulting in a brown precipitate. This precipitate is isolated and washed with a cold 1 M CsCl solution, ethanol, then ether and dried under vacuum overnight. The yield of **Cs_6-2** is *ca.* 2.6 g (49.8% based on W). FT/IR data (cm^{-1}): 1057(m), 1004(m), 959(s), 917(s), 882(s), 807(s), 781(s), 713(w), 561(m). UV-Vis in 0.1M HCl displayed one characteristic peak at 460 nm ($\varepsilon = 3.7\times10^4$ $M^{-1}cm^{-1}$). Elemental analysis calcd (%) for $Cs_6[\{Ru_2O_2(OH_2)_2\}(\gamma\text{-}SiW_{10}O_{36})]\cdot 25H_2O$: Cs, 20.5; Ru, 5.2; Si, 0.7; W: 47.2. Found (%): Cs, 22.4; Ru, 5.3; Si, 0.9; W: 44.4.

3.2.3 Synthesis of 3.2

To a vigorously stirred solution of 2.0g (0.67mmol) of $K_8[\gamma\text{-}SiW_{10}O_{36}]\cdot 12H_2O$ in 32.5 mL of water is added 0.3 g (1.33 mmol) of solid $RuCl_3\cdot H_2O$. The pH of the dark brown solution is lowered from 3 to 1.65 by adding several drops of 4 M HCl. After 5 min of stirring, a solution of 1.6 g (2.9 mmol) of $Ce(NH_4)_2(NO_3)_6$ (CAN) dissolved in 10 mL of 0.1 M HCl is added drop-wise. The solution is then filtered and allowed to stand in a 50 mL beaker open to air. The first crystals form within a few hours. Dark crystalline **3.3** (350mg; 0.054 mmol, 8 % based on W) is collected after 4 days. FT/IR data (cm^{-1}): 483 (w), 539 (m), 573 (m), 688 (m), 780 (s), 804 (s), 864 (s), 912 (m), 945 (m), 999 (w), 1025 (w), 1411 (w), 3200 (br sh). Elemental analysis, calcd (%) for $\mathbf{H_2Ce_{2.5}K(NH_4)_{0.5}[\{Ru^{V}Ru^{IV}_3O_6(OH_2)_4\}(\gamma\text{-}SiW_{10}O_{36})_2]\cdot 33H_2O}$: Si, 0.9; Ru, 6.2; W, 56.6; K, 0.6; Ce, 5.4; N, 0.11. Found (%): Si, 1.0; Ru, 6.2; W, 54.1; K, 0.7; Ce, 5.2; N, 0.16.

3.2.4 X-Ray Crystallography

Complete datasets for **3.2** ($Ce_{2.5}H_{78}N_{0.5}KO_{118}Ru_4Si_2W_{20}$) were collected at Emory University. Single crystals of each of these compounds suitable for X-ray analysis were coated with Paratone-N oil, suspended in a small fiber loop, and placed in a cooled gas stream on a Brüker D8 SMART APEX CCD sealed tube diffractometer. Diffraction intensities were measured using graphite monochromated Mo Kα radiation (λ = 0.71073 Å) at 173(2) K and a combination of φ and ω scans with 10 s frames traversing about ω at 0.3° increments were taken. Data collection, indexing, and initial cell refinements were carried out using SMART;[63] frame integration and final cell refinements were done using SAINT.[64] The molecular structure of each complex was determined using Direct Methods and Fourier techniques and refined by full-matrix least squares. A multiple

absorption correction, including face indexed absorption correction, was applied using the program SADABS.[65] The largest residual electron density for each structure was located close to (less than 1.0 Å from) the countercation or tungsten atoms, and was most likely due to imperfect absorption corrections frequently encountered in heavy-metal atom structures. All the heavy atoms, including Ce, K, Si, Cl, Ru, and W were refined anisotropically. Scattering factors and anomalous dispersion corrections were taken from the *International Tables for X-ray Crystallography*. Structure solution, refinement, graphic and generation of publication materials were performed by using SHELXTL, V6.14 software.[66] Refinement details and structural parameters are summarized in **Table 3.1**.

3.2.5 Effect of Li^+, Na^+ and K^+ Cations on Reduction Potentials of 3.3.

The effect of different cations (LiCl, NaCl, and KCl were used) on the CV reduction/oxidation peaks was studied in 0.1 M HCl, as well as at pH 2.0 (0.2 M lithium, sodium or potassium sulfate buffer) and at pH 7.2 (0.1 M sodium or potassium phosphate buffers). In a typical experiment, 1.9 mg (2.8 μmol, 0.7 mM) of **3.3** was dissolved in 4 mL of 0.2 M lithium sulfate buffer and its CV was recorded between 1.2 and (-0.58)V (vs. Ag/AgCl) at scan rate 25 $mV \cdot s^{-1}$. Then, 0.1 mL of a 2.9 M solution of LiCl or solid LiCl was added. The CVs were recorded after each addition. The same procedure was used to determine the effect of sodium or potassium cations by adding NaCl or KCl to the solution of **3.3** in 0.2 M sodium or potassium sulfate buffer (pH 2.0), 0.1 M HCl, or 0.1 M sodium or potassium phosphate buffers (pH 7.2).

Table 3.1. Crystal data and refinement parameters for the X-ray structure of **3.3**

Molecular formula	$Ce_{2.5}H_{78}N_{0.5}KO_{118}Ru_4Si_2W_{20}$
Formula wt. (g mol^{-1})	6504.33
Temperature (K)	173(2)
Radiation (λ, Å)	0.71073
Crystal system	Triclinic
Space group	*P-1 (#2)*
a (Å)	16.083(3)
b (Å)	18.405(4)
c (Å)	20.111(4)
α (°)	102.564(10)
β (°)	99.400(10)
γ (°)	91.116(11)
Volume ($Å^3$)	5723.2(19)
Z	2
μ (mm^{-1})	21.828
F(000)	5764
Crystal size (mm^3)	0.18 x 0.11 x 0.08
Reflections collected	90904
Independent reflections	23312 [R(int) = 0.0734]
Absorption correction	semi-empirical from equivalents
Refinement method	full-matrix least-squares on F^2
Goodness-of-fit on F^2	1.028
Final R indices	$R1^a$ = 0.0529
[R > 2σ (I)]	$wR2^b$ = 0.1296
R indices (all data)	$R1^a$ = 0.0622 $wR2^b$ = 0.1347

$^a R_1 = \Sigma||F_o| - |F_c|| / |F_o|$

$^b wR_2 = \{\Sigma[w(F_o^2 - F_c^2)^2] / \Sigma[w(F_o^2)^2]\}^{0.5}$

3.3 Results and Discussion

3.3.1 Synthesis

Polyanion of **3.1** is oxidized by air (O_2) in water to polyanion of **3.3** via eq 1 (below and in the text), thus the key to isolating **3.1** is the use of CsCl which facilitates rapid kinetic precipitation of **3.1** in ca. ~50% yield before it can undergo oxidative dimerization (eq 1).

$$2[\{Ru^{III}_2O_2(OH_2)_2\}(\gamma\text{-}SiW_{10}O_{36})]^{6-} + O_2 + 2H^+ \rightarrow [\{Ru^{IV}_4O_4(OH)_2(H_2O)_4\}(\gamma\text{-}SiW_{10}O_{36})_2]^{10-} \quad (1)$$

When a 2.2-fold molar excess of Ce(IV) is present over the $RuCl_3$ reactant in the synthesis of **3.3**, the one-electron-oxidized $Ru^{IV}_3Ru^V$ form of **3.2** an be isolated.

3.3.2 X-ray Crystal Structures of 3.2

The X-ray structures of **3.3**,[61] and **3.2** show that both polyanions, **3.3** and **3.2**, are very similar (**Figure 3.1**): D_{2d} polyanions with $[Ru_4O_6]$ cores of approximately T_d local symmetry sandwiched between two symmetry equivalent tetra-dentate $[\gamma\text{-}SiW_{10}O_{36}]^{8-}$ ligands. All the Ru centers in the two structures are out of pocket, i.e. the rutheniums are not bonded to the central heteroatom oxygens. The crystal data and refinement parameters for **3.2** are summarized in **Table 3.1** (Experimental section) and the structure of polyanion **3.2** is given in **Figure 3.3**. Despite the near structural congruity of polyanions **3.3** and **3.2**, there are noteworthy differences in bond lengths and angles that reflect differing protonation of the $[Ru_4O_6]$ oxygens and different oxidation states of the Ru centers. The protonation state of the six bridging oxygens in the $[Ru_4O_6]$ core can be distinguished by bond valence sum (BVS) calculations. Both **3.3** [61] and the related Cs salt, of Sartorel *et al*[67] were reported to have two of these Ru-O-Ru oxygens protonated.

In **3.2**, none are protonated, but the higher charge on the Ru_4 core in **3.2** is compensated by Ru terminal hydroxo ligands (versus aqua ligands in **3.3**). Protonation of Ru-O-Ru oxygens is consistent with simple charge arguments along with considerable X-ray structural and reactivity work on other POMs [68-70] indicating these oxygen sites would be more basic than the W^{VI}-O-Ru^{IV} and W^{VI}-O-W^{VI} oxygen sites.

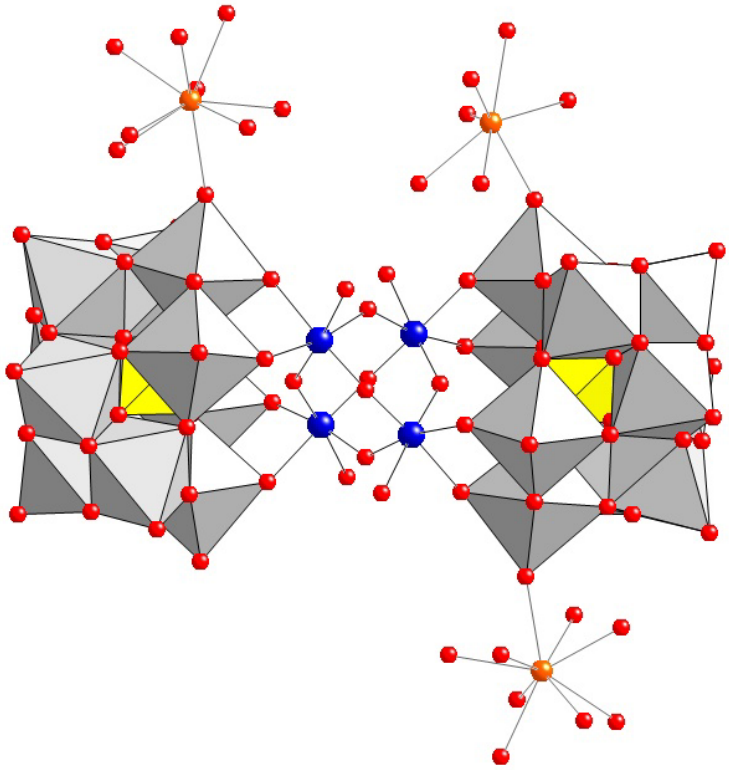

Figure 3.1. X-Ray structure of **3.2** in combined polyhedral (polytungstate ligands) and ball-and-stick notation (the Ce atoms and the central Ru_4O_6 core). Ru: blue, O: red; Ce: orange; WO_6 octahedra: gray, SiO_4 tetrahedra: yellow. Hydrogen atoms, water molecules and the potassium cations (not coordinated to the POM) are omitted for clarity.

There are five pieces of evidence that the tetra-ruthenium core in **3.2** is one-electron more oxidized than that in **3.3**, namely, $[Ru^{IV}_3Ru^{V}]$:

(1) Production of **3.2** from **3.3** requires an excess of Ce(IV);

(2) BVS calculations on all four Ru centers yield oxidation states of 4.21, 4,24, 4.26, and 4.38 (average 4.27; the sum is 17.09) consistent with one-electron oxidation of the $[Ru(IV)_4]$ core in **3.3**. This charge is delocalized over all four Ru centers on the X-ray data collection time scale. (Note there are four symmetry-distinct Ru centers because **3.2** crystallizes in the tricilinic *P*-1 space group in contrast to **3.3** which has two distinct Ru centers in the unit cell.);

(3)Related to point two, the Ru···Ru separations in **3.2** (3.42–3.44 Å) are significantly smaller than those in **3.3** (3.47–3.66 Å);

(4) The oxidation state assignment of a $[Ru^{IV}_3Ru^{V}]$ core was confirmed by back titration of **3.2** with the reductant Sn(II) to polyanion **3.3**;

(5) **Figure 3.6** clearly shows that the UV-visible spectra of two complexes are distinct from one another as discussed below.

3.3.3 Electrochemistry of 3.1 and 3.2

Cyclic voltammograms of **3.1** does not show informative peaks (**Figure 3.2**). Cyclic voltammograms of **3.2** in 0.1M HCl is similar to that of **3.3** showing six reversible peaks but at slightly more positive potentials (**Figure 3.6**). In addition, the peaks of **3.2** are more pronounced and a new anodic peak at 872 mV appears. The rest potentials of **3.2** and **3.3** are about 800 mV, and 600 mV respectively. The differences in the peak positions are due to effect of ion-pairing and the effect of electrolyte on interfacial electron transfer.

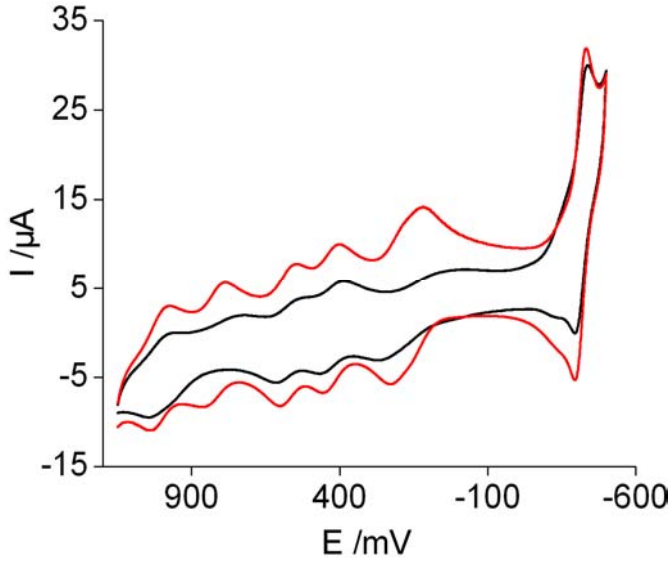

Figure 3.2. Cyclic voltammograms of 0.7 mM **3.3** (black curve) and 0.7 mM **3.2** (red curve) in 0.1 M HCl. Scan rate 25 mV/s.

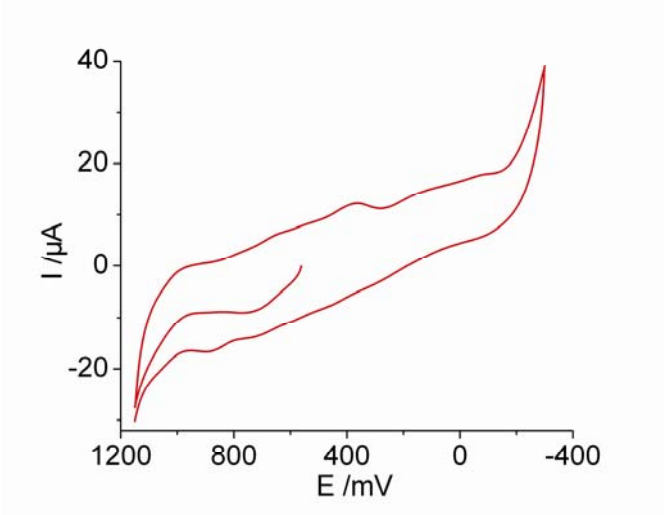

Figure 3.3 Cyclic voltammogram of 0.7 mM **3.1** in 0.1M HCl (freshly prepared solution). Scan rate, 25 mV/s.

3.3.4 Electronic spectroscopy of 3.1 and 3.2

The Uv-vis spectrum of **3.1** and **3.3** are shown in **Figure 4**, from which we can see the difference between them. The maximum absorbance peak of **3.1** is blue shifted from 445 to 460nm.

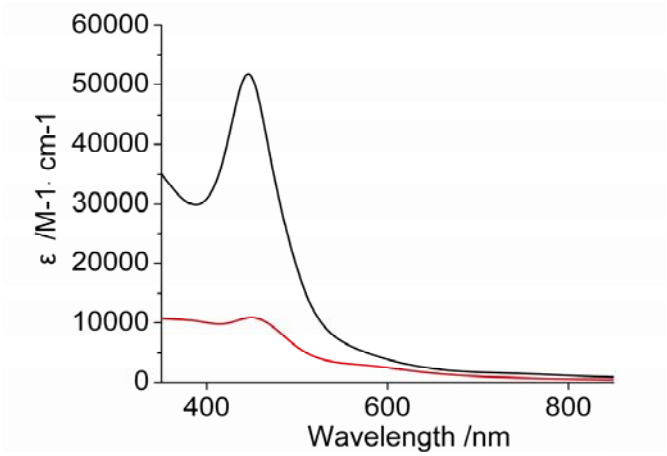

Figure 3.4. UV-Vis spectra of **3.1** and **3.3** in 0.1M HCl

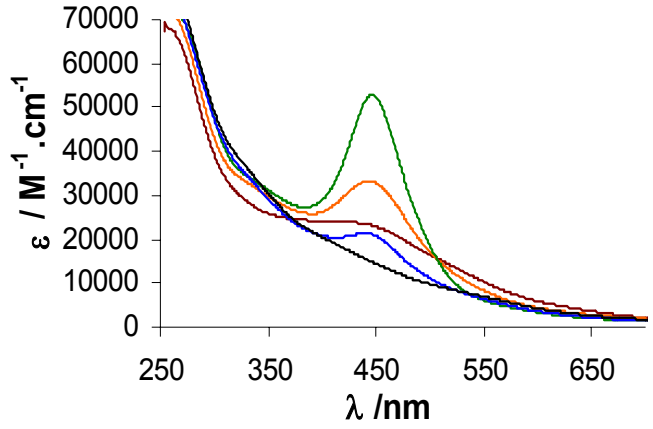

Figure 3.5. UV-vis spectra of **3.3** with different oxidation states in 0.1 M H_2SO_4: black: $[Ru^{IV}{}_2Ru^{V}{}_2]$, blue: $[Ru^{IV}{}_3Ru^{V}]$, green: $[Ru^{IV}{}_4]$, orange: $[Ru^{IV}Ru_3{}^{III}]$, brown: $[Ru_2{}^{IV}Ru_2{}^{III}]$.

The relationship of tetraruthenium POM with different oxidation states with their electronic spectroscopy (**Figure 3.5**) has been established by potentiometric and UV-vis titrations. Based on this, we assigned the oxidation state of tetraruthenium core of **3.2** to $[Ru^{IV}_3Ru^{V}]$, along with other evidences. UV-Vis spectra of **3.2** are compared with that for **3.3** in **Figures 3.6**. UV-vis spectrum in 0.1 M HNO_3 has the same characteristic peak at 445 nm but with $\varepsilon_{445} = 2x10^4$ $M^{-1}\cdot cm^{-1}$, which is ~2.3 times lower than for **3.3** (**Figure 3.6**).

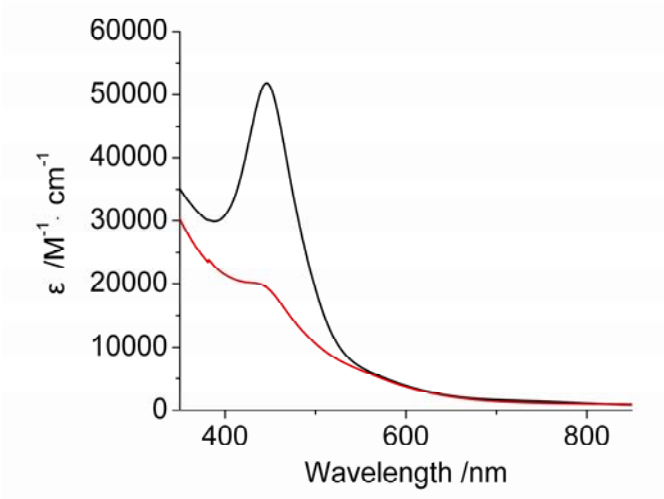

Figure 3.6. The UV-Vis spectra of **3.2** (black) and **3.3** (red) in 0.1 M HNO_3.

3.3.5 Effect of pH and alkali metal cations on the electrochemistry of 3.3

Cyclic voltammograms of aqueous solutions of **3.3** are pH and ionic strength dependent (**Figures 3.7-3.9**). At pH 2.0 in 0.2 M lithium sulfate buffer, four cathodic peaks are well separated in the positive domain, a broad peak is also seen at *ca.* -175 mV, while the peak at *ca.* -395 mV overlaps with an intense peak of W(VI/V) reduction at *ca.* -540 mV. At a lower pH in 0.1 M HCl, peaks in the positive domain are shifted to more

positive values, and the difference between cathodic and anodic potentials moves closer to 60 mV. The replacement of 0.2M lithium sulfate buffer with 0.1 M HCl results in a very large shift of the broad cathodic wave from *ca.* -175 mV to *ca.* 35 mV. Thus, at low alkali metal cation concentration at acidic pH, seven quasi-reversible waves are observed in the range from 1.05 to -0.55V. These waves are assigned to the following couples: $[Ru^{IV}{}_2Ru^{V}{}_2]/[Ru^{IV}{}_3Ru^{V}]$, $[Ru^{IV}{}_3Ru^{V}]/[Ru^{IV}{}_4]$, $[Ru^{IV}{}_4]/[Ru^{IV}Ru_3{}^{III}]$, $[Ru^{IV}Ru_3{}^{III}]/[Ru_2{}^{IV}Ru_2{}^{III}]$, $[Ru_2{}^{IV}Ru_2{}^{III}]/[Ru^{III}{}_4]$, (two broad converged 1-electron peaks) $[Ru^{III}{}_4]/[Ru_3{}^{III}Ru^{II}]$, $[Ru_3{}^{III}Ru^{II}]/ [Ru_2{}^{III}Ru_2{}^{II}]$. Reduction of W^{VI} to W^{V} takes place in the last couple. The data are summarized in **Table 3.2**.

Table 3.2. Potentials of anodic (E_a) and cathodic (E_c) peaks in cyclic voltammograms of 0.7 mM **3.2**

pH = 2 (0.2 M lithium sulfate buffer)			0.1 M HCl		
$E_{1/2}$	E_a	E_c	$E_{1/2}$	E_a	E_c
973	1010	935	1012	1045	980
749	*ca*. 830	667	809	856	762
529	580	479	581	615	547
370	428	312	424	458	390
30	235	-175	154	272	35
-365	-335	-395	-310	-255	-365
-499	-458	-540	-415	-382	-447

Addition of alkali metal cations (as chloride or other salts) also changes the shape and position of reduction and oxidation peaks of **3.2** at different pH (**Figure 3.7-3.9**). The weakest effect is seen with LiCl and the strongest with KCl. In general, the peaks become better separated and shift to more positive potentials. The shifts are more pronounced for the peaks at lower potentials. To further explain this, the effect of potassium at pH 2 is discussed here. The broad cathodic and anodic peaks (-175 mV and

235 mV, respectively) split into two separate peaks and shift to higher potentials. Two adjoining anodic peaks at the highest potential (ca. 830 and 1010 mV) become well separated. The peak at *ca.* -395 mV (overlapping with an intense peak for W(VI/V) reduction at *ca.* -540 mV) also shifts to more positive values while the last peak (corresponding to the tungsten reduction) shifts slightly to a more negative value.

The voltammetric peaks depend on the nature and concentration of cations present and this effect is more pronounced for the more reduced POMs (more negative in polyanion). While these findings are consistent with ion pairing at more negative potentials (more reduced polyanions),[71-76] the voltammetric behavior at more positive potentials cannot be explained exclusively by ion pairing.

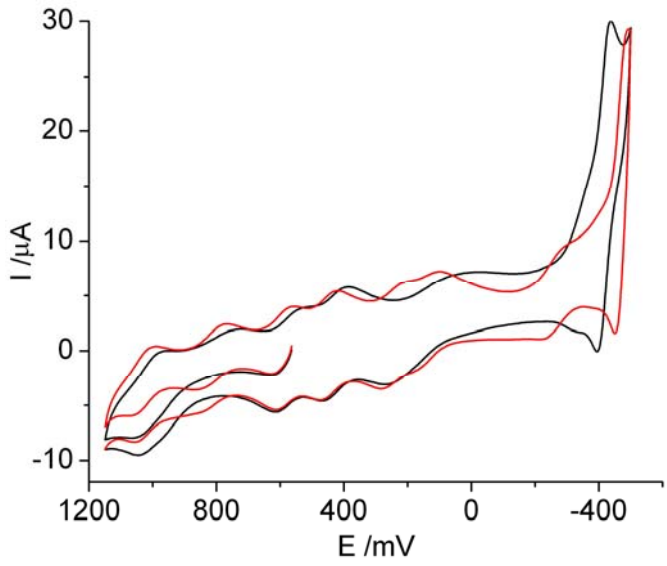

Figure 3.7. Cyclic voltammograms of 0.7 mM of **3.2** in 0.1 M HCl at pH 1.0 (black curve) and in the presence of 0.58 M KCl (red curve). Scan rate 25 mV/s.

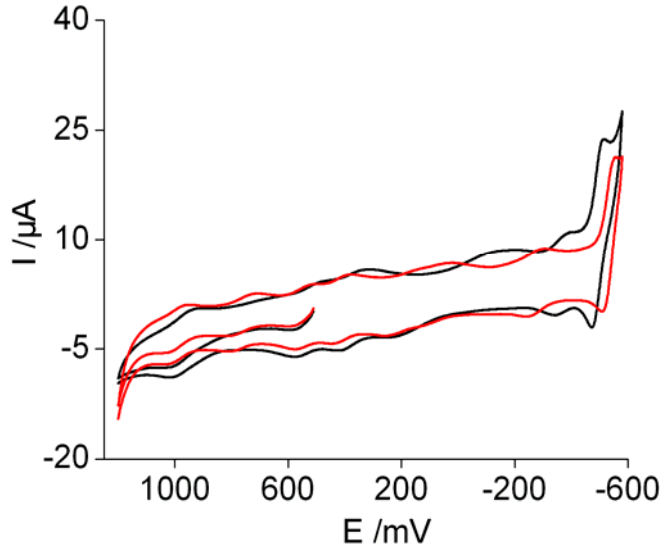

Figure 3.8. Cyclic voltammograms of 0.7 mM of **3.2** in 0.2 M lithium sulfate buffer at pH 2.0 (black curve) and in the presence of 0.58 M KCl (red curve). Scan rate 25 mV/s.

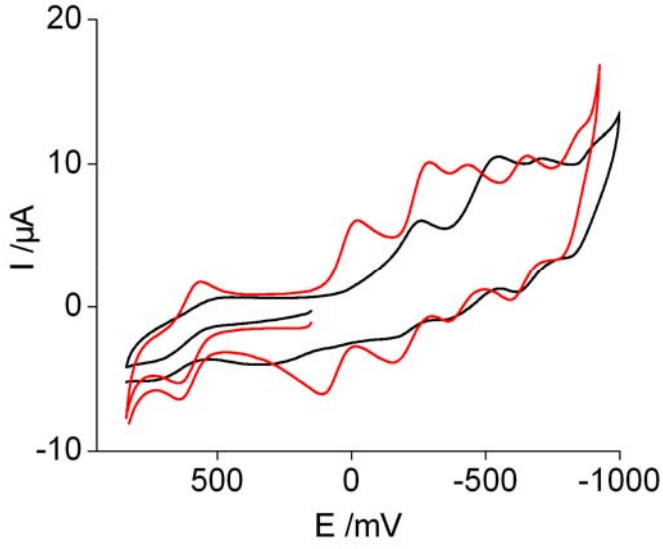

Figure 3.9. Cyclic voltammograms of 0.7 mM of **3.3** in 20 mM potassium phosphate buffer at pH 7.2 in the presence of 0.1 M (black curve) and 0.4 M KCl (red curve). Scan rate 25 mV/s.

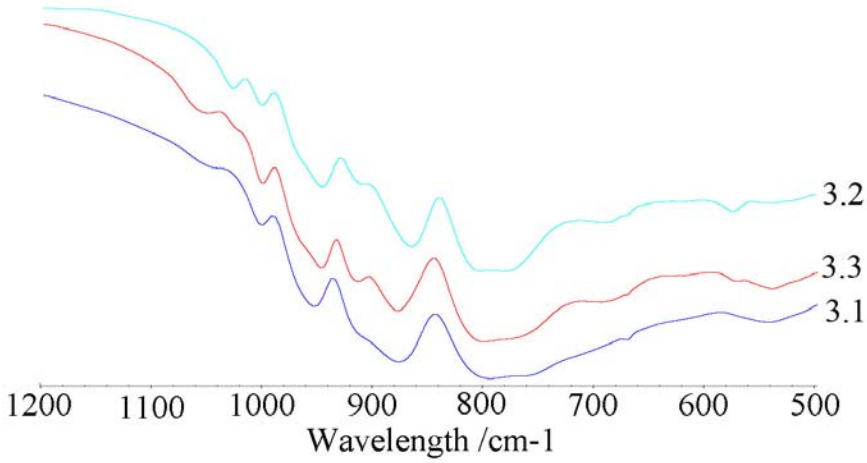

Figure 10. IR of **3.1**, **3.2** and **3.3**

3.4 Conclusions

Compound **3.2** has been prepared and characterized by X-ray crystallography and several other techniques. It is one-electron more oxidized than **3.3**. The rest potentials, X-ray structure/BVS calculations, electronic spectrum, full elemental analysis, and requirement of an oxidant (Ce^{IV}) in the synthesis are all consistent with $[Ru^{V}Ru^{IV}{}_{3}O_{6}]$ cores in **3.2.** The monomer $Cs_6[\{Ru_2O_2(OH_2)_2\}(\gamma\text{-}SiW_{10}O_{36})]\cdot 25H_2O$ has also been obtained and its structure was characterized by elemental analysis, electronic spectroscopy, and infrared spectroscopy. Addition of alkali metal cations (K^+, Na^+, Li^+) have exhibited the predictable effect on the cyclic voltammograms of **3.3.** These cation-polyanion interactions need to be studied more in the future.

References

(1) Chow, J.; Kopp, R. J.; Portney, P. R. *Science* **2003**, *302*, 1528.

(2) Turner, J. A. *Science* **2004**, *305*, 972.

(3) Eisenberg, R.; Gray, H. B. *Inorg. Chem.* **2008**, *47*, 1697.

(4) Ghosh, P. K.; Brunschwig, B. S.; Chou, M.; Creutz, C.; Sutin, N. *J. Am. Chem. Soc.* **1984**, *106*, 4772.

(5) Shafirovich, V. Y.; Khannanov, N. K.; Strelets, V. V. *Nouveau J. de Chimie* **1980**, *4*, 81.

(6) Shafirovich, V. Y.; Shilov, A. E. *Kinetika i Kataliz* **1979**, *20*, 1156.

(7) Ramaraj, R.; Kira, A.; Kaneko, M. *Angew. Chem. Int. Ed. Engl.* **1986**, *25*, 825.

(8) Ramaraj, R.; Kira, A.; Kaneko, M. *Chem. Lett.* **1987**, *16*, 261.

(9) Harriman, A.; Richoux, M.-C.; Christensen, P. A.; Mosseri, S.; Neta, P. *J. Chem. Soc., Faraday Trans. 1* **1987**, *83*, 3001.

(10) Parmon, V. N. *Catal. Today* **2000**, *58*, 55.

(11) Elizarova, G. L.; Zhidomirov, G. M.; Parmon, V. N. *Catal. Today* **2000**, *58*, 71.

(12) Hammarström, L.; Sun, L.; Åkermark, B.; Styring, S. *Catal. Today* **2000**, *58*, 57.

(13) Hoertz, P. G.; Kim, Y.-I.; Youngblood, W. J.; Mallouk, T. E. *J. Phys. Chem. B* **2007**, *111*, 6845.

(14) Kanan, M. W.; Nocera, D. G. *Science* **2008**, *321*, 1072.

(15) Kanan, M. W.; Surendranath, Y.; Nocera, D. G. *Chem. Soc. Rev.* **2009**, *38*, 109.

(16) Lutterman, D. A.; Surendranath, Y.; Nocera, D. G. *J. Am. Chem. Soc.* **2009**, *131*, 3838.

(17) Youngblood, W. J.; Lee, S.-H. A.; Kobayashi, Y.; Hernandez-Pagan, E. A.; Hoertz, P. G.; Moore, T. A.; Moore, A. L.; Gust, D.; Mallouk, T. E. *J. Am. Chem. Soc.* **2009**, *131*, 926.

(18) Lehn, J. M.; Sauvage, J. P.; Ziesel, R. *Nouveau J. de Chimie* **1979**, *3*, 423.

(19) Gersten, S. W.; Samuels, G. J.; Meyer, T. J. *J. Am. Chem. Soc.* **1982**, *104*, 4029.

(20) Gilbert, J. A.; Eggleston, D. S.; Wyatt R. Murphy, J.; Geselowitz, D. A.; Gersten, S. W.; Hodgson, D. J.; Meyer, T. J. *J. Am. Chem. Soc.* **1985**, *107*, 3855.

(21) Comte, P.; Nazeeruddin, M. K.; Rotzinger, F. P.; Frank, A. J.; Grätzel, M. *J. Mol. Catal.* **1989**, *52*, 63.

(22) Schoonover, J. R.; Ni, J.; Roecker, L.; White, P. S.; Meyer, T. J. *Inorg. Chem.* **1996**, *35*, 5885.

(23) Rüttinger, W.; Dismukes, G. C. *Chem. Rev.* **1996**, *97*, 1.

(24) Limburg, J.; Vrettos, J. S.; Liable-Sands, L. M.; Rheingold, A. L.; Crabtree, R. H.; Brudvig, G. W. *Science* **1999**, *283*, 1524.

(25) Wada, T.; Tsuge, K.; Tanaka, K. *Angew. Chem. Int. Ed.* **2000**, *39*, 1479.

(26) Sens, C.; Romero, I.; Rodríguez, M.; Llobet, A.; Parella, T.; Benet-Buchholz, J. *J. Am. Chem. Soc.* **2004**, *126*, 7798.

(27) Chen, H.; Faller, J. W.; Crabtree, R. H.; Brudvig, G. W. *J. Am. Chem. Soc.* **2004**, *126*, 7345.

(28) Hurst, J. K. *Coord. Chem. Rev.* **2005**, *249*, 313.

(29) Zong, R.; Thummel, R. *J. Am. Chem. Soc.* **2005**, *127*, 12802.

(30) Yang, X.; Baik, M.-H. *J. Am. Chem. Soc.* **2006**, *128*, 7476.

(31) Tagore, R.; Chen, H.; Zhang, H.; Crabtree, R. H.; Brudvig, G. W. In *Inorg. Chimica Acta* 2007; Vol. 360, p 2983.

(32) Tagore, R.; Crabtree, R. H.; Brudvig, G. W. *Inorg. Chem.* **2007**, *46*, 2193.

(33) McDaniel, N. D.; Coughlin, F. J.; Tinker, L. L.; Bernhard, S. *J. Am. Chem. Soc.* **2008**, *130*, 210.

(34) Tagore, R.; Crabtree, R. H.; Brudvig, G. W. *Inorg. Chem.* **2008**, *47*, 1815.

(35) Brimblecombe, R.; Swiegers, G. F.; Dismukes, G. C.; Spiccia, L. *Angew. Chem. Int. Ed.* **2008**, *47*, 7335.

(36) Siegbahn, P. E. M. *Inorg. Chem.* **2008**, *47*, 1779.

(37) Liu, F.; Concepcion, J. J.; Jurss, J. W.; Cardolaccia, T.; Templeton, J. L.; Meyer, T. J. *Inorg. Chem.* **2008**, *47*, 1727.

(38) Hurst, J. K.; Cape, J. L.; Clark, A. E.; Das, S.; Qin, C. *Inorg. Chem.* **2008**, *47*, 1753.

(39) Deng, Z.; Tseng, H.-W.; Zong, R.; Wang, D.; Thummel, R. *Inorg. Chem.* **2008**, *47*, 1835.

(40) Romero, I.; Rodríguez, M.; Sens, C.; Mola, J.; Kollipara, M. R.; Francàs, L.; Mas-Marza, E.; Escriche, L.; Llobet, A. *Inorg. Chem.* **2008**, *47*, 1824.

(41) Concepcion, J. J.; Jurss, J. W.; Templeton, J. L.; Meyer, T. J. *Proc. Nat. Acad. Sci.* **2008**, *105*, 17632.

(42) Concepcion, J. J.; Jurss, J. W.; Templeton, J. L.; Meyer, T. J. *J. Am. Chem. Soc.* **2008**, *130*, 16462.

(43) Sala, X.; Romero, I.; Rodr┐ íguez, M.; Escriche, L. í.; Llobet, A. *Angew. Chem. Int. Ed.* **2009**, *48*, 2842.

(44) Romain, S.; Bozoglian, F.; Sala, X.; Llobet, A. *J. Am. Chem. Soc.* **2009**, *131*, 2768.

(45) Xu, Y.; Åkermark, T.; Gyollai, V.; Zou, D.; Eriksson, L.; Duan, L.; Zhang, R.; Åkermark, B.; Sun, L. *Inorg. Chem.* **2009**, *48*, 2717.

(46) Jiao, F.; Frei, H. *Angew. Chem. Int. Ed.* **2009**, *48*, 1841.

(47) Ferreira, K. N.; Iverson, T. M.; Maghlaoui, K.; Barber, J.; Iwata, S. *Science* **2004**, *303*, 1831.

(48) Barber, J. *Inorg. Chem.* **2008**, *47*, 1700.

(49) Yano, J.; Kern, J.; Sauer, K.; Latimer, M. J.; Pushkar, Y.; Biesiadka, J.; Loll, B.; Saenger, W.; Messinger, J.; Zouni, A.; Yachandra, V. K. *Science* **2006**, *314*, 821.

(50) Yano, J.; Yachandra, V. K. *Inorg. Chem.* **2008**, *47*, 1711.

(51) Yeagle, G. J.; Gilchrist, M. L.; McCarrick, R. M.; Britt, R. D. *Inorg. Chem.* **2008**, *47*, 1803.

(52) Rotzinger, F. P.; Munavalli, S.; Comte, P.; Hurst, J. K.; Gratzel, M.; Pern, F.-J.; Frank, A. J. *J. Am. Chem. Soc.* **1987**, *109*, 6619.

(53) Yagi, M.; Kaneko, M. *Chem. Rev.* **2001**, *101*, 21.

(54) McDaniel, N. D.; Coughlin, F. J.; Tinker, L. L.; Bernhard, S. *J. Am. Chem. Soc.* **2008**, *130*, 210.

(55) Limburg, J.; Vrettos, J. S.; Chen, H.; Paula, J. C. d.; Crabtree, R. H.; Brudvig, G. W. *J. Am. Chem. Soc.* **2001**, *123*, 423.

(56) Muckerman, J. T.; Polyansky, D. E.; Wada, T.; Tanaka, K.; Fujita, E. *Inorg. Chem.* **2008**, *47*, 1787.

(57) Kohl, S. W.; Weiner, L.; Schwartsburd, L.; Konstantinovski, L.; Shimon, L. J. W.; Ben-David, Y.; Iron, M. A.; Milstein, D. *Science* **2009**, *324*, 74.

(58) Hull, J. F.; Balcells, D.; Blakemore, J. D.; Incarvito, C. D.; Eisenstein, O.; Brudvig, G. W.; Crabtree, R. H. *J. Am. Chem. Soc.* **2009**, *131*, 8730.

(59) Kunkely, H.; Vogler, A. *Angew. Chem. Int. Ed.* **2009**, *48*, 1685.

(60) Quiñonero, D.; Wang, Y.; Morokuma, K.; Khavrutskii, L. A.; Botar, B.; Geletii, Y. V.; Hill, C. L.; Musaev, D. G. *J. Phys. Chem.* **2006**, *110*, 170.

(61) Geletii, Y. V.; Botar, B.; Kögerler, P.; Hillesheim, D. A.; Musaev, D. G.; Hill, C. L. *Angew. Chem. Int. Ed.* **2008**, *47*, 3896.

(62) Geletii, Y. V.; Huang, Z.; Hou, Y.; Musaev, D. G.; Lian, T.; Hill, C. L. *J. Am. Chem. Soc.* **2009**, *131*, 7522.

(63) Bruker AXS, I.; Analytical X-ray Sysems: Madison, WI, 2003.

(64) Bruker AXS, I.; Analytical X-Ray Sytems: Madison, WI, 2003.

(65) SADABS, S., G.; 2.10 ed. **2003**.

(66) Bruker AXS, I. Madison, WI, 2003.

(67) Sartorel, A.; Carraro, M.; Scorrano, G.; Zorzi, R. D.; Geremia, S.; McDaniel, N. D.; Bernhard, S.; Bonchio, M. *J. Am. Chem. Soc* **2008**, *130*, 5006.

(68) Day, V. W.; Klemperer, W. G.; Schwartz, C. *J. Am. Chem. Soc.* **1987**, *109*, 6030.

(69) Hill, C. L. In *Comprehensive Coordination Chemistry-II: From Biology to Nanotechnology*; Wedd, A. G., Ed.; Elsevier Ltd.: Oxford, UK, 2004; Vol. 4, p 679.

(70) Villa, E. M.; C. André Ohlin, D.; Edina Balogh, D.; Travis M. Anderson, D.; May D. Nyman, D.; William H. Casey, P. *Angew. Chem. Int. Ed.* **2008**, *47*, 4844.

(71) Grigoriev, V. A.; Hill, C. L.; Weinstock, I. A. *J. Am. Chem. Soc.* **2000**, *122*, 3544.

(72) Grigoriev, V. A.; Cheng, D.; Hill, C. L.; Weinstock, I. A. *J. Am. Chem. Soc.* **2001**, *123*, 5292.

(73) Keita, B.; Mbomekalle, I. M.; Lu, Y. W.; Nadjo, L.; Berthet, P.; Anderson, T. M.; Hill, C. L. *Eur. J. Inorg. Chem.* **2004**, 3462.

(74) Casey, W. H. *Chem. Rev.* **2006**, *106*, 1.

(75) Anderson, T. M.; Thoma, S. G.; Bonhomme, F.; Rodriguez, M. A.; Park, H.; Parise, J. B.; Alam, T. M.; Larentzos, J. P.; Nyman, M. *Crystal Growth & Design* **2007**, *7*, 719.

(76) Antonio, M. R.; Nyman, M.; Anderson, T. M. *Angew. Chem. Int. Ed.* **2009**, *48*, 6136.

CHAPTER

4

A New Family of Sandwich-Type Polytungstophosphates Containing Two Types of Metals in the Central Belt

(published partially in *Inorg. Chem.* **2010***, 49(9),* 4125-4132)
with Lin Xu, Morgan J. Cichon, Sheri Lense, Kenneth I. Hardcastle and Craig L. Hill

Abstract: A new family of sandwich-type polytungstophosphates containing two types of metals in the central belt, $M'_2M_2(PW_9O_{34})_2^{12-}$ (M' = Na or Li, M = Mn^{2+}, Co^{2+}, Ni^{2+}, Zn^{2+}), have been synthesized and characterized by infrared spectroscopy, ^{31}P solution NMR spectroscopy, and elemental analysis. Compounds $Na_2Co_2(PW_9O_{34})_2^{12-}$ (**4.1**), $Na_2Ni_2(PW_9O_{34})_2^{12-}$ (**4.2**), $Li_2Ni_2(PW_9O_{34})_2^{12-}$ (**4.2a**) $Na_2Mn_2(PW_9O_{34})_2^{12-}$ (**4.3**), and $Li_2Zn_2(PW_9O_{34})_2^{12-}$ (**4.4a**), were characterized by single X-ray crystallography. All these compounds have similar structures, in which two transition metal ions and two alkali metal ions (sodium or lithium) are sandwiched between two [B-α-PW_9O_{34}]$^{9-}$ units; the transition metals and alkali metals reside in the internal and external (solvent exposed) positions of the central belt, respectively. By adding LiCl to aqueous solutions of compounds **4.1, 4.2, 4.3, or 4.4**, lithium-sodium exchanges in the external belt positions are observed by ^{31}P solution NMR spectroscopy and X-ray crystallography. Magnetic measurements indicate ferromagnetic exchange interactions between the two Ni^{2+} ions in **4.2** at 10-300K and the two Co^{2+} ions in **4.1** at 6-30K. In contrast, **4.3** exhibits an antiferromagnetic interaction between the Mn^{2+} ions at 2-50K.

4.1 Introduction

Polyoxometalates (POMs) and transition-metal-containing POMs (d^0 POMs binding one or more d-electron metals) are a large class of highly modifiable discrete metal-oxygen anionic clusters[1-9] with substantial structural diversity and widely ranging properties facilitating applications in medicine,[10-19] catalysis,[20-30] and magnetism.[31-36] Within the family of transition-metal-containing POMs, sandwich-type compounds (one or more transition metals bonded between two POM lacunary fragments) represent the largest subclass.[37] They have been referred to as oxidatively stable inorganic analogues of metalloporphyrins and used as catalysts for a range of organic oxidations.[38-41]

Trivacant Keggin and Wells-Dawson lacunary POMs have been extensively used as precursors to prepare sandwich-type POMs because replacement of several adjacent high-valent tungsten centers with low-valent metals modifies the surface properties of metal-oxide-like structural units.[42-44] As mentioned in the chapter 1, trivacant POMs are classified as A type (removal of one corner-sharing MO_6 octahedron from each of three adjacent M_3O_{13} triads) and B type (removal of one entire M_3O_{13} triad).[44]

Reactions of A-type tricavant POMs and transition or main group metals commonly form structures with a single substituted POM unit such as those with the formula $[A\text{-}M_3(H_2O)_3XW_9O_{37}]^{n-}$ ($X = Si^{IV}$, Ge^{IV}; $M = Al^{3+}$, Ga^{3+}, In^{3+}, Cr^{3+}, V^{3+}, Fe^{3+}, Mn^{2+}, Co^{2+}, Ni^{2+}, Cu^{2+};[42,43,45-52] $X = P^{V}$; $M_3 = Fe_{3-x}Ni_x$[47,49]) or those with a sandwich type structure, such as $[M_3(H_2O)_3(A\text{-}XW_9O_{34})_2]^{n-}$ ($X = P^{V}$, Si^{IV}; $M = Sn^{2+}$, Co^{2+}, Mn^{2+}, Ni^{2+}, Cu^{2+}, Zn^{2+}, Fe^{3+} Pd^{2+}), $[(CeO)_3(H_2O)_2(A\text{-}PW_9O_{34})_2]^{12-}$ and $[(ZrOH)_3(A\text{-}SiW_9O_{34})_2]^{11-}$.[53-57]

Among the POMs based on $[B\text{-}\alpha\text{-}XW_9O_{34}]^{n-}$ and $[B\text{-}\alpha\text{-}X_2W_{15}O_{56}]^{n-}$ polyanions, those with three or four transition metals in the structures are widely documented, including the following: $[M_3(H_2O)_3(\alpha\text{-}XW_9O_{33})_2]^{n-}$ ($X = As^{III}$, Sb^{III}, Se^{IV}, Te^{IV}; $M = Mn^{2+}$, Co^{2+}, Ni^{2+}, Cu^{2+}, Zn^{2+}); $[(VO)_3(\alpha\text{-}XW_9O_{33})_2]^{n-}$ ($X = As^{III}$, Sb^{III}, Bi^{III});[58-64] $[M_3P_2W_{15}O_{62}]^{n-}$ ($M = Ti^{4+}$, Zr^{4+}, Hf^{4+}, V^{5+}, Nb^{5+}, Ta^{5+}, Mo^{6+});[1,65,66] $[As_2W_{15}Mg_3O_{62}]^{18-}$[67] $[(NaOH_2)Co_3(H_2O)(P_2W_{15}O_{56})_2]^{17-}$ [41] $[\alpha\alpha\beta\alpha\text{-}(NaOH_2)(Fe^{III}OH_2)Fe^{III}_2(P_2W_{15}O_{56})_2]^{14-}$;[44] $[Ni_3Na(H_2O)_2(XW_9O_{34})_2]^{11-}$ ($X = P^{V}$, As^{V});[68,69] $[M_4(H_2O)_2(XW_9O_{34})_2]^{n-}$ ($X = P^{V}$, Si^{IV}, Ge^{IV}; $M = Mn^{2+}$, Co^{2+}, Zn^{2+}, Co^{2+}, Ni^{2+});[70-75] and $[M_4(H_2O)_2(X_2W_{15}O_{56})_2]^{n-}$ ($X = P^{V}$, As^{V}; $M = Mn^{2+}$, Co^{2+}, Ni^{2+}, Cu^{2+}, Zn^{2+}, Cd^{2+}, Fe^{3+}).[76-89]

While many sandwich-type POMs containing three or four transition metals in the central belt based on Keggin or Wells-Dawson fragments have been documented, very

few of the corresponding derivatives with two transition metals in the belt are known. The Hill group reported X-ray crystal structures of Wells-Dawson derivatives containing two transition metals in the central belt $[(NaOH_2)_2M_2(X_2W_{15}O_{56})_2]^{n-}$ ($X = P^V$, $M = Fe^{3+}$, Cu^{2+}; $X = As^V$, $M = Fe^{3+}$),[44,86,87,90-92] and subsequently, Ruhlmann and Thouvenot's group reported the Co^{2+} analogue whose structure was confirmed by IR, elemental analysis, and ^{31}P solution NMR spectroscopy.[41] In addition, diuranium and dineptunium containing POMs have also been obtained based on A type trivacant Keggin unit, including $[M_2(UO_2)_2(A\text{-}XW_9O_{34})_2]^{n-}$ ($X = P^V$, $M = K$, Na, NH_4; $X = Ge^{IV}$, Si^{IV}; $M = Na$), $[(UO_2)_2(H_2O)_2(XW_9O_{33})_2]^{n-}$ ($X = Sb^{III}$, Te^{IV})[93-97], and $[Na_2(NpO_2)_2(A\text{-}PW_9O_{34})_2]^{14-}$.[98] However, sandwich-type polyoxoanions with two transition metals in the central belt based on the $[B\text{-}\alpha\text{-}PW_9O_{34}]^{9-}$ Keggin fragment are, to our knowledge, unknown.

We report here the syntheses, structures and magnetic properties of a new family of sandwich-type polyoxoanions, $[M'_2M_2(PW_9O_{34})_2]^{12-}$, (M' = Na or Li, $M = Mn^{2+}$, Co^{2+}, Ni^{2+}, Zn^{2+}) in which two $[B\text{-}\alpha\text{-}PW_9O_{34}]^{9-}$ units sandwich two metal ions in the internal positions of the central belt and two sodium or lithium ions reside in the exterior positions of this belt.

4.2 Experimental

4.2.1 General Methods and Materials

All common laboratory chemicals were reagent grade, purchased from commercial sources and used without further purification. Elemental analyses for Li, Na, K, P, Co, Ni, Mn, Zn and W were performed by Desert Analytics, now Columbia (Tucson, Arizona) and Galbraith Laboratories, Inc. (Knoxville, Tennessee). Elemental analyses for H were performed by Atlantic microlab (Norcross, GA). Infrared spectra (2% sample in KBr)

were recorded on a Nicolet 510 instrument. The kinetics was studied using an Agilent 8453 spectrophotomer. Solution ^{31}P NMR spectra were obtained on Unity Plus 600 (277K, 286K, and 296K) or Varian INOVA 400 spectrometers (296K), referenced to 85% H_3PO_4 (0.0 ppm) external standard. The numbers of counter cations were determined by elemental analysis. The magnetic susceptibility measurements were carried out on polycrystalline samples using a Quantum Design MPMS-XL5 SQUID magnetometer at 1000 Oe in the temperature range 2-300 K. Diamagnetic corrections were estimated from Pascal's constants.

4.2.2 Synthesis

$K_8Na_4[Na_2Co_2(PW_9O_{34})_2]\cdot 28H_2O$ (4.1): $Na_2WO_4\cdot 2H_2O$ (5g, 15.2 mmol) and Na_2HPO_4 (0.24, 1.7 mmol) were dissolved in 100 ml H_2O followed by addition of $Co(NO_3)_2\cdot 6H_2O$ (0.31g, 1.1mmol) resulting in a cloudy suspension. The pH was adjusted to 7.5 by dropwise addition of 6M HCl and a purple solution formed. The solution was heated at 90 °C for 1h and then was allowed to cool to room temperature. Powdered KCl (0.6g, 8.0 mmol) was added and the solution was left to slowly evaporate at room temperature. After several days, purple needle crystals suitable for X-ray diffraction were formed (yield 0.2 g, 7% based on W). Reheating and evaporation of the filtrate can increase the yield (up to 20%). FTIR data (cm^{-1}): 1057(s), 1019(s), 970(sh), 954(sh), 934(s), 904(m), 865(m), 801(s), 734(s). Elemental analysis calcd (%) for **4.1**: K, 5.6; Na, 2.5; P, 1.1; W, 59.8; Co, 2.1. Found (%): K, 5.8; Na, 2.4; P, 1.2; W, 59.6; Co, 2.0.

$K_8Na_4[Na_2Ni_2(PW_9O_{34})_2]\cdot 30H_2O$ (4.2): The synthetic procedure was similar to that for **4.1**, but using $Ni(NO_3)_2\cdot 6H_2O$ (0.31g, 1.1 mmol) in place of $Co(NO_3)_2\cdot 6H_2O$. After several days, yellow green needle crystals suitable for X-ray diffraction were formed

(yield 0.3 g, 10% based on W). Reheating and evaporation of the filtrate can increase the yield up to 23%. FTIR data (cm^{-1}): 1041(s), 1021(s), 968(sh), 955(sh), 933(m), 922(m), 908(m), 872(m), 805(s), 737(s). Elemental analysis calcd (%) for **4.2**: K, 5.6; Na, 2.5; P, 1.1; W, 59.5; Ni, 2.1. Found (%): K, 5.9; Na, 2.7; P, 1.1; W, 60.0; Ni, 2.0.

$Na_{12}[Na_2Mn_2(PW_9O_{34})_2]\cdot 36H_2O$ (4.3): The synthetic procedure was similar to that for **4.1**, but $Mn(CH_3COO)_2\cdot 4H_2O$ (0.266g, 1.1 mmol) was used instead of the cobalt(II) precursor. After several days, yellow crystals suitable for X-ray diffraction were formed (yield 0.3g, 10% based on W). FTIR data (cm^{-1}): 1057(s), 1019(s), 965(sh), 957(sh), 937(s), 893(s), 861(m), 810(s), 740(s). Elemental analysis calcd (%) for **4.3**: Na, 6.1; P, 1.2; W, 62.4; Mn, 2.1. Found (%): Na, 5.9; P, 1.1; W, 61.1; Mn, 2.1.

$K_8Na_4[Na_2Zn_2(PW_9O_{34})_2]\cdot 31H_2O$ (4.4): The synthetic procedure was similar to the preparation of **4.1**, but $Zn(NO_3)_2\cdot 6H_2O$ (0.31g, 1.1 mmol) was used. After heating the reaction solution at 90 °C for 1h, a very small quantity of precipitate formed which was removed by filtration and 0.5g KCl was then added. The solution was left to slowly evaporate at room temperature until colorless crystals were obtained (yield 0.5 g, 15% based on W). FTIR data (cm^{-1}): 1051(s), 1016(s), 968(sh), 956(sh), 935(s), 921(s), 906(m), 869(sh), 805(s), 735(s). Elemental analysis calcd (%) for **4.4**: K, 5.7; Na, 2.5; P, 1.1; W, 60.1; Zn, 2.3. Found (%): K, 5.5; Na, 2.7; P, 1.2; W, 59.2; Zn, 2.1.

$K_6Li_6[Li_2Co_2(PW_9O_{34})_2]\cdot 38H_2O$ (4.1a): **4.1** (1.3 g) was dissolved in minimal amount of 1M LiCl solution. Purple crystals were obtained after several days upon slow evaporation (yield 0.7g, 54% based on W). FTIR data (cm^{-1}): 1056(s), 1028(s), 969(sh), 958(sh), 940(s), 899(s), 866(sh), 800(s), 742(s). Elemental analysis calcd (%) for **4.1a**:

Li, 1.0; K, 4.2; P, 1.1; W, 59.6; Co, 2.1. Found (%): Li, 0.9; K, 4.2; P, 1.0; W, 58.6; Co, 2.0.

$K_6Li_6[Li_2Ni_2(PW_9O_{34})_2]\cdot 28H_2O$ (4.2a): **4.2** (1.0 g) was dissolved in a minimal amount of 1M LiCl solution. Single crystals suitable for X-ray crystallography were obtained after several days upon slow evaporation (yield 0.44g, 44% based on W). FTIR data (cm^{-1}): 1041(s), 1033(s), 974(sh), 959(sh), 943(m), 920(sh), 904(m), 872(sh), 796(sh), 743(s). Elemental analysis calcd (%) for **4.2a**: K, 4.4; Li, 1.0; P, 1.2; W, 61.7; Ni, 2.2. Found (%): K, 4.5; Li, 1.0; P, 1.1; W, 59.9; Ni, 2.0.

$K_3Na_3Li_6[Li_2Mn_2(PW_9O_{34})_2]\cdot 40H_2O$ (4.3a): **4.3** (1.5 g) was dissolved in a minimal amount of 1M LiCl solution. Yellow crystals were obtained after several days upon slow evaporation (yield 0.42 g, 27% based on W). FTIR data (cm^{-1}): 1058(s), 1024(s), 971(sh), 957(sh), 939(s), 893(s), 861(w), 797(m), 741(s). Elemental analysis calcd (%) for **4.3a**: Li, 1.0; K, 2.1; P, 1.1; W, 59.8; Mn, 2.0. Found (%): Li, 1.0; K, 1.9; P, 1.0; W, 58.2; Mn, 1.9.

$K_6Na_2Li_4[Li_2Zn_2(PW_9O_{34})_2]\cdot 25H_2O$ (4.4a): **4.4** (0.8 g) was dissolved in a minimal amount of 1M LiCl solution. Single crystals suitable for X-ray crystallography were obtained after several days upon slow evaporation (yield 0.31 g, 38% based on W). FTIR data (cm^{-1}): 1052(s), 1025(s), 971(sh), 958(sh), 939(s), 903(m), 867(sh), 793(m), 743(s). Elemental analysis calcd (%) for **4.4a**: K, 4.4; Na, 0.9; P, 1.2; W, 61.8; Zn, 2.4. Found (%): K, 4.2; Na, 0.7; P, 1.1; W, 59.0; Zn, 2.2.

4.2.3 Lithium-sodium exchange experiments

Typically, about 15 mg of **4.1** or **4.2** was added to a 700μL D_2O solution in a 5-mm i.d. NMR tube and spectrum recorded quickly. Compounds **4.1** and **4.2** did not

dissolve completely, so the exact concentration of **4.1** or **4.2** in the Lithium-sodium exchange experiments is not attainable. In the indicated cases, 10μL of 0.2M LiCl D_2O solution was added (the resulting concentration of LiCl is 2.8mM) and the NMR spectra were recorded as a function of time. These experiments were conducted at three different temperatures: 277K, 286K and 296K.

4.2.4 X-ray Crystallography

The complete datasets for **4.1**, **4.2**, **4.2a**, **4.3** and **4.4a** were collected at Emory University. Single crystals of all five of these new complexes suitable for X-ray analysis were each coated with Paratone-N oil, suspended in a small fiber loop, and placed in a cooled gas stream on a Brüker D8 SMART APEX CCD sealed tube diffractometer. Diffraction intensities were measured using graphite monochromated Mo Kα radiation (λ = 0.71073 Å) at 173(2) K with a combination of φ and ω scans with 10 s frames traversing about ω at 0.3° increments. Data collection, indexing, and initial cell refinements were carried out using SMART;[99] frame integration and final cell refinements were done using SAINT.[100] The molecular structure of each complex was determined using Direct Methods and Fourier techniques and refined by full-matrix least squares.[101] Multiple absorption corrections, including face indexed absorption correction, was applied using the program SADABS.[102] The largest residual electron density for each structure was located close to (less than 1.0 Å from) counter-cation and tungsten atoms and was most likely due to imperfect absorption corrections frequently encountered in polytungstates and other structures dominated by heavy-metal atoms. All the heavy atoms, including K, Na, Li, P, Co, Ni, Mn, Zn and W were refined anisotropically. Scattering factors and anomalous dispersion corrections are taken from

the International Tables for X-ray Crystallography. Structure solution, refinement, graphics and generation of publication materials were performed by using SHELXTL, V6.14 software. Refinement details, structural parameters, selected metal oxygen bond lengths are summarized in **Table 4.1-4.2**. The corresponding CIF files are available as supplementary material.

Table 4.1. Crystal data and structure refinement for **4.1, 4.2, 4.2a, 4.4a and 4.3**

	4.1	**4.2**	**4.2a**	**4.4a**	**4.3**
Empirical Formula	$H_{56}K_8Na_6Co_2O_{96}P_2W_{18}$	$H_{60}K_8Na_6Ni_2O_{98}P_2W_{18}$	$H_{26.8}K_3Li_4NiO_{47.40}PW_9$	$H_{50}K_6Na_2Li_6Zn_2O_{93}P_2W_{18}$	$H_{46}Na_{14}Mn2O_{91}P_2W_{18}$
Fw ($g \cdot mol^{-1}$)	5532.53	5507.40	2647.79	5360.70	5258.98
T(K)	173(2)	173(2)	173(2)	173(2)	173(2)
Radiation (λ, Å)	0.71073	0.71073	0.71073	0.71073	0.71073
Crystal system	Triclinic	Triclinic	Triclinic	Triclinic	Triclinic
Space group	$P\bar{1}$	$P\bar{1}$	$P\bar{1}$	$P\bar{1}$	$P\bar{1}$
a (Å)	11.6790(8)	11.6706(15)	11.550(5)	11.6835(12)	11.442(4)
b (Å)	13.1564(9)	13.1351(16)	13.250(6)	13.1470(13)	12.572(4)
c (Å)	16.3125(11)	16.249(2)	16.056(8)	16.1275(16)	16.438(6)
α (°)	84.7880(10)	84.778(2)	83.972(7)	84.746(2)	76.545(5)
β (°)	70.4500(10)	70.453(2)	71.200(7)	70.677(2)	70.883(5)
γ (°)	68.9890(10)	69.077(2)	67.303(6)	68.127(2)	72.475(5)
V ($Å^3$)	2203.7(3)	2191.3(5)	2145.5(18)	2168.0(4)	2106.7(12)
Z	1	1	2	1	1
d_{calcd}, $Mg \cdot m^{-3}$	4.126	4.173	4.099	4.069	4.145
μ, mm^{-1}	24.316	24.507	24.897	24.765	24.979
GOF	1.044	1.043	1.004	1.112	1.021
Final R indices [R>2σ(I)]	R_1[a] = 0.0412, wR_2[b] = 0.1012	R_1[a] = 0.0347 wR_2[b] = 0.0876	R_1[a] = 0.0432 wR_2[b] = 0.1143	R_1[a] = 0.0441, wR_2[b] = 0.1110	R_1[a] = 0.0785, wR_2[b] = 0.2454
R indices (all data)	R_1[a] = 0.0577, wR_2[b] = 0.1097	R_1[a] = 0.0439 wR_2[b] = 0.0923	R_1[a] = 0.0593 wR_2[b] = 0.1246	R_1[a] = 0.0631, wR_2[b] = 0.1195	R_1[a] = 0.1193, wR_2[b] = 0.2870

[a] $R_1 = \Sigma||F_0| - |F_c|| / \Sigma|F_0|$;

[b] $wR_2 = \Sigma[w(F_0^2 - F_c^2)^2] / \Sigma[w(F_0^2)^2]^{1/2}$

Table 4.2. Selected metal-oxygen bond lengths [Å]			
		4.4a	
Zn(1)-O(31)	2.018(7)	Zn(1)-O(34)	2.036(7)
Zn(1)-O(30)	2.039(7)	Zn(1)-O(33)	2.017(7)
Zn(1)-O(16)	2.206(7)	Zn(1)#7-O(16)	2.220(7)
		4.1	
Co(1)-O(30)	2.027(7)	Co(1)-O(31)	2.044(7)
Co(1)-O(34)#1	2.030(7)	Co(1)-O(28)	2.204(7)
Co(1)-O(29)#1	2.039(7)	Co(1)-O(28)#1	2.212(6)
		4.2	
Ni(1)-O(34)#8	2.007(5)	Ni(1)-O(33)#8	2.030(5)
Ni(1)-O(29)	2.008(5)	Ni(1)-O(28)#8	2.165(5)
Ni(1)-O(30)	2.016(5)	Ni(1)-O(28)	2.169(5)
		4.2a	
Ni(1)-O(30)	1.989(8)	Ni(1)-O(33)#4	2.019(8)
Ni(1)-O(34)#4	2.008(8)	Ni(1)-O(31)#4	2.139(7)
Ni(1)-O(32)	2.014(7)	Ni(1)-O(31)	2.159(7)
		4.3	
Mn(1)-O(24)#1	2.106(15)	Mn(1)-O(32)	2.098(14)
Mn(1)-O(30)	2.129(15)	Mn(1)-O(34)	2.135(15)
Mn(1)-O(29)	2.282(13)	Mn(1)-O(29)#1	2.293(13)

Table 4.3. ^{31}P NMR data for the $[M'_2M_2(PW_9O_{34})_2]^{12-}$ species			
Compound	277K δ(ppm)	286K δ (ppm)	296K δ (ppm)
4.1	1764	1697	1635
4.1a	1588	1532	1464
4.2	1341	1284	1231
4.2a	1222	1173	1117
4.4	-2.5	-2.4	-2.2
4.4a	-3.9	-3.7	-3.6

Experimental conditions for paramagnetic **4.1, 4.1a** and **4.2, 4.2a**: Unity 243 spectrometer, Spectral width: 100 kHz; pulse width: 4 μs (~40° flip angle); number of points: 4800; acquisition time: 24ms; line broadening factor:100 Hz for **4.1, 4.1a**, and 400 Hz for **4.2, 4.2a**.

Experimental conditions for diamagnetic **4 and 4a:** Unity 243 spectrometer, Spectral width: ~32 kHz; pulse width: 8 μs; number of points: 63898; acquisition time: 1s; line broadening factor: 3 Hz.

4.3 Results and discussion

4.3.1 Structures

Compounds **4.1-4.4** and **4.1a-4.4a** are isostructural. They consist of two lacunary B-α-$[PW_9O_{34}]^{9-}$ Keggin moieties linked *via* two M^{2+} ions and two sodium or lithium ions leading to a sandwich-type structure of C_i symmetry (see **Figure 4.1**). The central core (belt) of $[M'_2M_2(PW_9O_{34})_2]^{12-}$ complexes is a rhomb-like $M'_2M_2^{6+}$ (M = Co, Ni, Mn, Zn) tetragon consisting of two M^{2+} ions located in the two internal positions and two sodium or lithium ions in the external positions. The two transition metal centers are chemically equivalent and octahedrally coordinated. Each sodium ion or lithium ion is coordinated to six oxygen atoms which are from two B-α-$[PW_9O_{34}]^{9-}$ units. The bond distance of Li to bridging W–O–W oxygen (ca. 2.8-2.9 Å) is longer than the distance of Na to the corresponding bridging W–O–W oxygen (ca. 2.58-2.69 Å). This phenomenon very likely derives from the relative ionic radii of these two alkali metal cations. The tri-vacant B-α-$PW_9O_{34}^{9-}$ anion contains seven unsaturated oxygen atoms which is very similar to $X_2W_{15}O_{56}^{12-}$ (X = P, As). The coordination modes between metal and lacunary POM units in the $[M'_2M_2(PW_9O_{34})_2]^{12-}$ compounds are also very similar to those in the reported Wells–Dawson-derived sandwich-type complexes, $[(NaOH_2)_2(Fe^{III})_2(X_2W_{15}O_{56})_2]^{16-}$ (X=P^V and As^V).[16] The junctions between the two lacunary Keggin fragments with the central unit in the complexes reported here are analogous to the junctions between a particular M_3O_{13} group and the remainder of the POM structural framework in the parent Keggin and Wells-Dawson polyanions. Specifically, the β isomer for the Keggin derivatives has the M_9 moiety relative to the adjacent unit (the M_3 triad in the case of the parent POMs and the M'_2M_2 unit in the

complexes reported here) rotated 60° related to the α isomer. Of all previously known sandwich-type POMs with trivacant B-Keggin units and central M_4 units, most have two β junctions between these units as exemplified in the tetranuclear compounds $[M_4(H_2O)_2(XW_9O_{34})_2]^{n-}$ (X= P^V, Si^{IV}, Ge^{IV}; M = Mn^{2+}, Co^{2+}, Zn^{2+}, Co^{2+} Ni^{2+}), while a few POMs have both α and β juctions as exemplified in the tri-metal-containing POM $[Ni_3Na(H_2O)_2(XW_9O_{34})_2]^{11-}$(X=$P^V$, As^V).[13] The $[M'_2M_2(PW_9O_{34})_2]^{12-}$ complexes in this chapter have two α junctions between the trivacant POM units and the central M_2 unit. This is as same inter-unit isomerism seen in $[(NaOH_2)_2(Fe^{III})_2(X_2W_{15}O_{56})_2]^{16-16}$, namely αααα. Such inter-unit isomerism has not heretofore been seen in the Keggin-based POMs.

Relatively few sandwich-type POMs based on trivacant Keggin units contain two transition metals in the belt and all known examples are based on A type Keggin POM units (A-$PW_9O_{34}^{9-}$, A-$GeW_9O_{34}^{10-}$, A-$SiW_9O_{34}^{10-}$, $Sb^{III}W_9O_{33}^{9-}$, $Te^{IV}W_9O_{33}^{8-}$)[17], and actinyl species UO_2^{2+} and NpO_2^{2+}. In the actinyl polyoxoanions formed from A-$XW_9O_{34}^{n-}$, the UO_2^{2+} and NpO_2^{2+} moieties are in the external positions and each bear one terminally ligated aqua ligand, while two sodium ions are sit in the internal positions. In contrast, there is no sodium ion in the central belt in the diuranium POM based on $Sb^{III}W_9O_{33}^{9-}$ and $Te^{IV}W_9O_{33}^{8-}$ and the two uranium centers are seven coordinate with three terminal aqua ligands each. Xu's group reported the X-ray structure of three complexes that contain the trivacant unit, $[As^VMo_9O_{33}]^{7-}$, namely $[Mn_2(As^VMo_9O_{33})_2]^{10-}$, which is a monomeric, and $[Mn_2(As^VMo_9O_{33})_2]^{10-}$ or $[Co_2(As^VMo_9O_{33})_2]^{10-}$ which are polymeric (one-dimensional structures). The common structural component, $[As^VMo_9O_{33}]^{7-}$, is a derivative of the B-β trivacant Keggin unit. To the best of our

knowledge, sandwich POMs with two transition metals in the belt, $[M'_2M_2(PW_9O_{34})_2]^{12-}$, we report here represent a new family of POMs based on B-α Keggin trivacant polyanion.

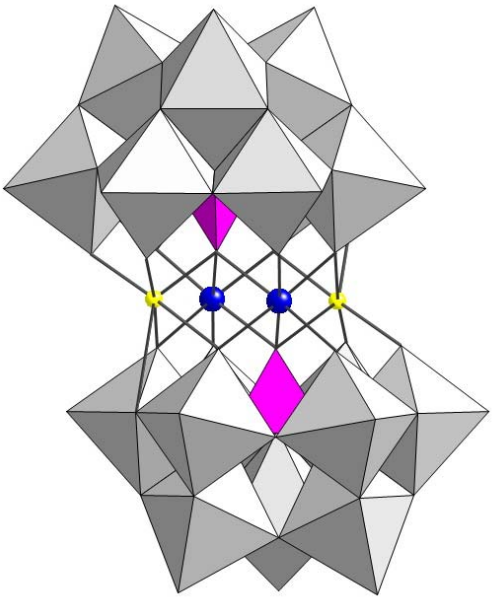

(a)

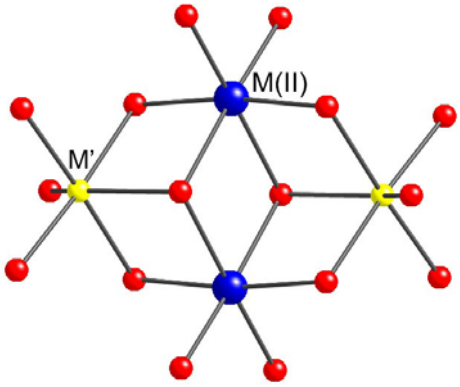

(b)

Figure 4.1. (a) X-ray structure of the polyanions in $[M'_2M_2(PW_9O_{34})_2]^{12-}$. The transition metals and sodium or lithium are in ball-and-stick notation (transition metals: blue; sodium or lithium: yellow) and the rest of the polyoxometalate framework is in polyhedral notation (WO_6 octahedra: gray, PO_4 tetrahedron: pink). Hydrogen atoms are omitted for clarity. (b) The connection motif of the metal atoms between two B-α-$PW_9O_{34}^{9-}$ units. M: transition metal; M': sodium or lithium.

4.3.2 IR characterization

The infrared spectra of these POMs in the P-O, W-O and W-O-W stretch regions are very similar to each other strongly suggesting that these complexes are isostructural to one another (**Figure 4.2** and **Figure 4.3**). The ν_3 vibrational mode of the central PO_4 unit in these compounds is split, indicating a structural distortion and consequent lowering of the symmetry around these central units. The peaks in the low energy (<1000 cm^{-1}) region are attributed to the characteristic $\nu(W–O_d)$, $\nu(W–O_b–W)$ and $\nu(W–O_c\text{-}W)$ absorptions, where O_b = double-bridging oxygen; O_c = central oxygen; O_d = terminal oxygen.

4.3.3 ^{31}P NMR Characterization

^{31}P NMR spectroscopy is a very useful technique to address the purity and stability of polytungstophosphates. ^{31}P NMR spectra of $[M'_2M_2(PW_9O_{34})_2]^{12-}$ in D_2O or 1M LiCl/D_2O solution in low frequency region at room temperature show that the $[M'_2M_2(PW_9O_{34})_2]^{12-}$ complexes dissociate to metal ions and B-α-$PW_9O_{34}^{9-}$ which further decomposes to $PW_{11}O_{39}^{7-}$ and PO_4^{3-} (**Figure 4.4**). The ^{31}P NMR spectra for **4.1, 4.1a**, **4.2, 4.2a**, **4.4** and **4.4a** in D_2O at 277K, 286K and 296K (before decomposition products can be detected) are reported in **Figures 4.14** and **4.15**, all data are given in **Table 4.3**. The chemical shifts of **4.1, 4.1a**, **4.2,** and **4.2a** increase with decreasing temperature, while those of **4.4** and **4.4a** are fairly temperature independent (**Figure 4.16**). No signal is observed for **4.3** and **4.3a** in the high frequency region because of the strong influence of the $S = 5/2$ Mn^{2+} centers on ^{31}P nuclear relaxation rates.

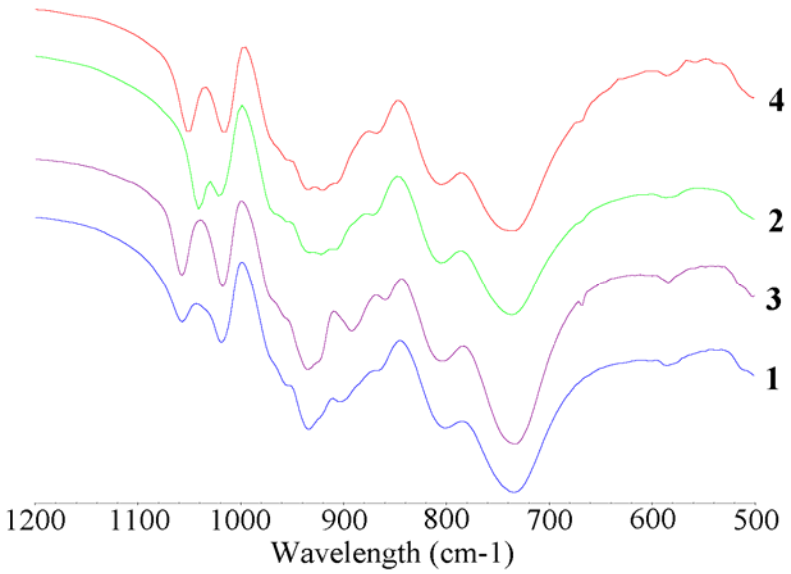

Figure 4.2. IR spectra of **4.1-4.4**.

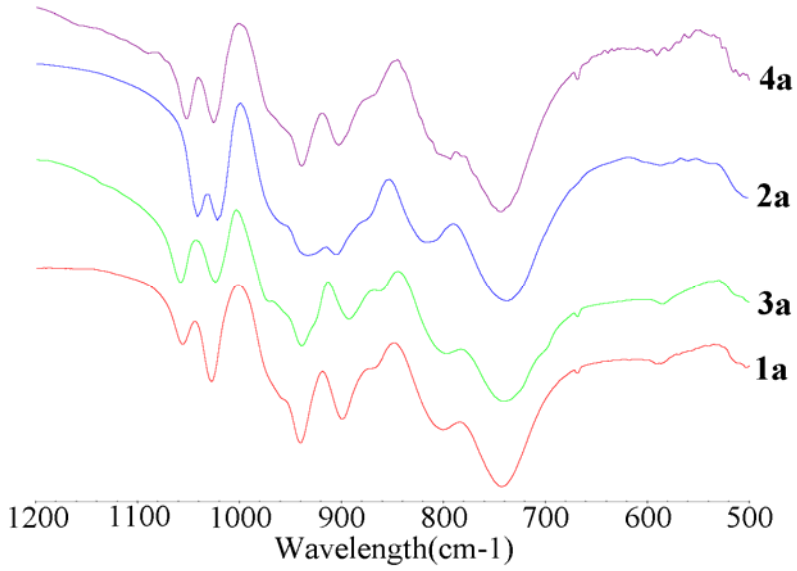

Figure 4.3. IR spectra of **4.1a-4.4a**.

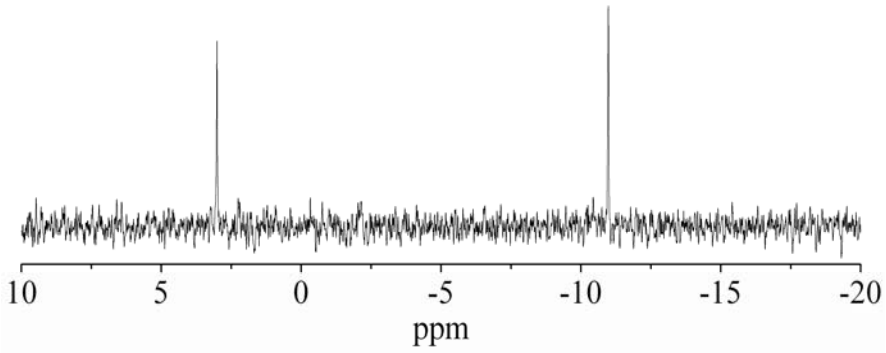

(a)

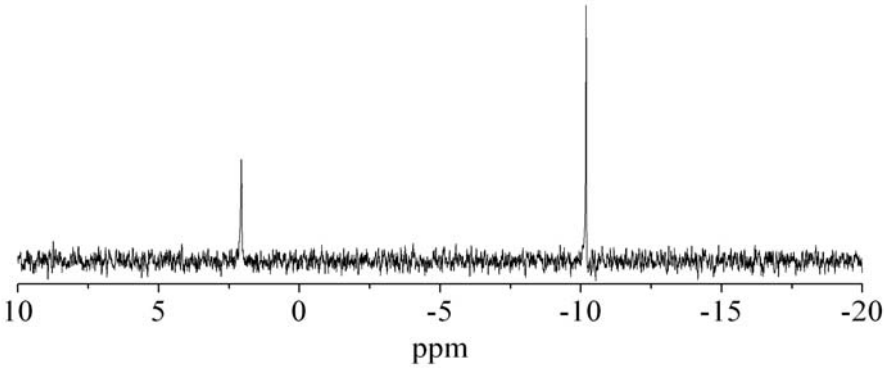

(b)

Figure 4.4. (a) Diamagnetic ^{31}P NMR spectrum of the decomposition products of **4.1a** in D_2O ($PW_{11}O_{39}^{7-}$,-11.0 ppm; PO_4^{3-}, 3.0 ppm). Compound **4.2a** and **4.3a** shows similar results. (b) Diamagnetic ^{31}P NMR spectrum of the decomposition products ($PW_{11}O_{39}^{7-}$,-10.2 ppm; PO_4^{3-}, 2.1 ppm) of **4.1** in D_2O. Compound **4.2** and **4.3** shows similar results.

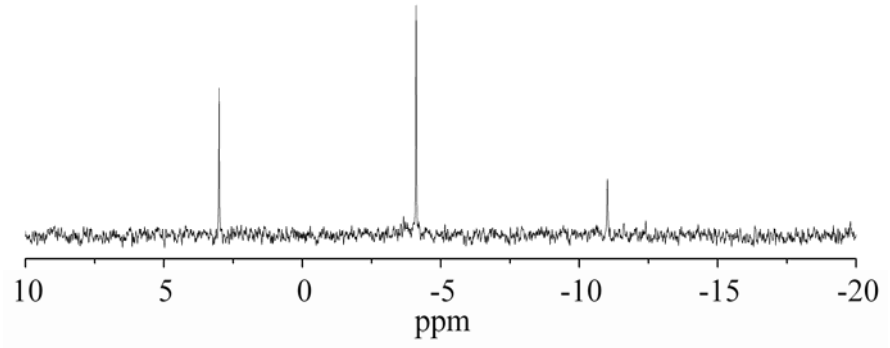

Figure 4.5. ^{31}P NMR spectrum of **4.4a** 1day after dissolving in 1M LiCl solution ($PW_{11}O_{39}^{7-}$, -11.0 ppm; PO_4^{3-}, 3.0 ppm; $[Zn_4(H_2O)(PW_9O_{34})_2]^{10-}$, -4.1ppm).

Since the solubility of $[M'_2M_2(PW_9O_{34})_2]^{12-}$ in D_2O is much lower than in 1M LiCl, we choose to study the decomposition of **4.1a-4.4a** in 1M LiCl.[23] The ^{31}P NMR spectrum of **4.4a** in 1M LiCl obtained immediately after mixing shows a single peak at -3.6 ppm. After 1 day, a new peak at -4.1±0.1 ppm attributable to the $[Zn_4(H_2O)(PW_9O_{34})_2]^{10-}$ (**Figure 4.5**) forms in addition to peaks for PO_4^{3-} and $PW_{11}O_{39}^{7-}$. The ^{31}P NMR spectra for the paramagnetic compounds, **4.1a** and **4.2a,** in 1M LiCl exhibit one line at about 1464 ppm (**Figure 4.6**) and 1117 ppm (**Figure 4.7**) respectively, consistent with two equivalent $PW_9O_{34}^{9-}$ moieties in both cases. After 6 days, no additional peaks were observed in the spectrum of **4.2a**, indicating no other species forms in the solution (**Figure 4.8**). The solution of **4.1a** shows the generation of $Co_4(H_2O)_2(PW_9O_{34})_2^{10-}$ and other species after several days (**Figure 4.9**). $[Co_3Na(H_2O)_2(XW_9O_{34})_2]^{11-}$ could well be one of these other decomposition products; the isostructural nickel analogue is known.[13] $CoPW_{11}O_{39}^{5-}$, (448 ppm) could well be an intermediate but it is not observed. When $Li_2Co_2(H_2O)_2(PW_9O_{34})_2^{12-}$ or

$Li_2Zn_2(H_2O)_2(PW_9O_{34})_2^{12-}$ dissociate, free $PW_9O_{34}^{9-}$ units prefer to bind the metals first to form sandwich type structures, then the unreacted $PW_9O_{34}^{9-}$ left in the solution subsequently decomposes to $PW_{11}O_{39}^{7-}$ and PO_4^{3-}. The relative rates of metal cation exchange reactions correlate with the ligand field stabilization energies of the central transition metals in the belt of these sandwich POMs: **4.4a** (most reactive; LFSE = 0) > **4.1a** (LFSE = $0.8\Delta_o$) > **4.2a** (least reactive; LFSE = $1.2\Delta_o$).

Addition of 10μL of 0.2M LiCl D_2O solution to aqueous solutions (final LiCl concentration ~2.8mM) of **4.1** and **4.2** at different temperature (277K, 286K and 296K) results in a new peak that corresponds to a new species (**Figure 4.14c, 4.14f, 4.14i and Figure 4.15c, 4.15f, 4.15i**). The chemical shifts of the new species are similar to those of the **4.1a** and **4.2a**, which indicates a lithium-sodium exchange has taken place in solution. In fact, lithium-sodium exchange has also been confirmed by X-ray crystallography. Lithium-sodium exchange is also seen for solutions of **4.4** but fast decomposition of this complex renders the spectral quality poor due to the short data acquisition time.

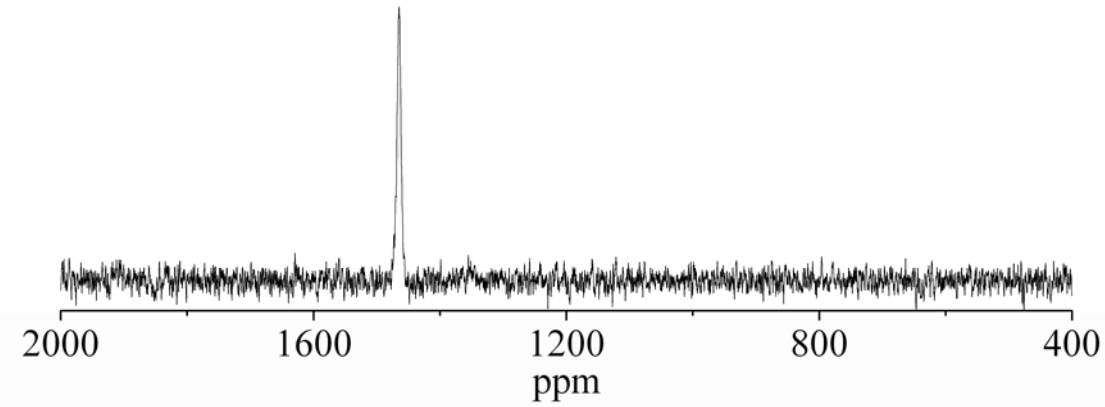

Figure 4.6. ^{31}P NMR spectrum of **4.1a** 2h after dissolving in 1M LiCl (D_2O). ($Li_2Co_2(PW_9O_{34})_2^{12-}$, 1458 ppm)

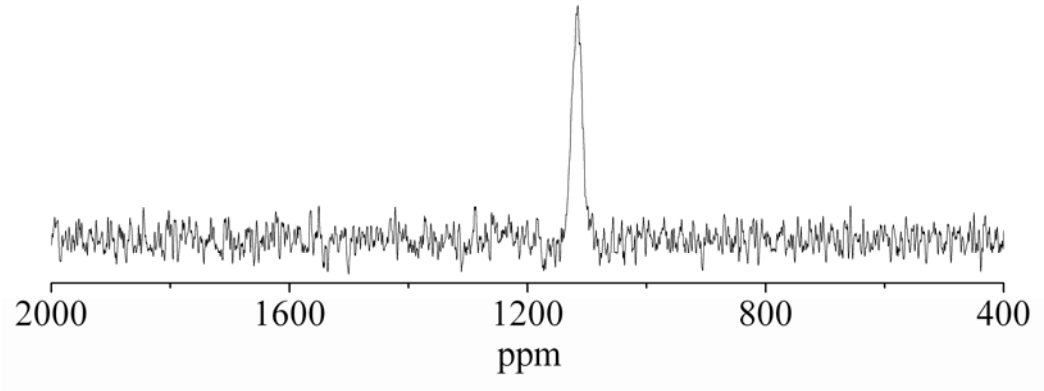

Figure 4.7. ^{31}P NMR spectrum of **4.2a** 2h after dissolving in 1M LiCl (D_2O). ($Li_2Ni_2(PW_9O_{34})_2^{12-}$, 1094 ppm)

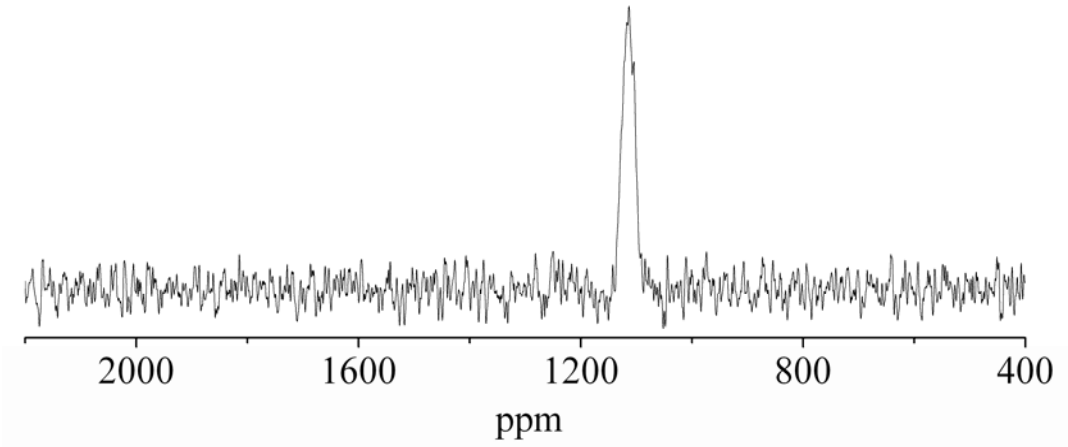

Figure 4.8. ^{31}P NMR spectrum of **4.2a** 7 days after dissolving in 1M LiCl (D_2O) ($Li_2Ni_2(PW_9O_{34})_2^{12-}$, 1094 ppm)

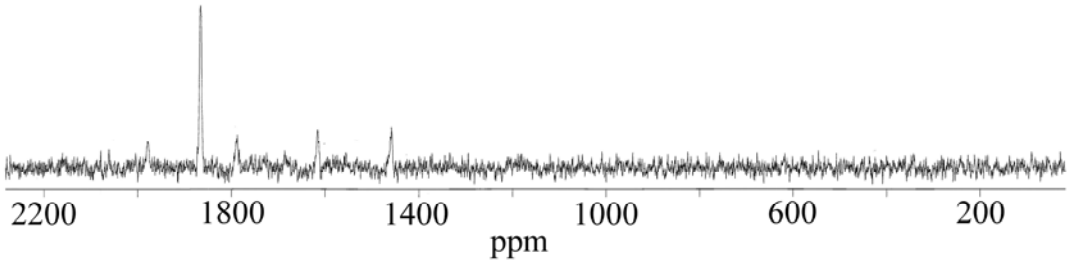

Figure 4.9. ^{31}P NMR spectrum of **4.1a** 7 days after dissolving in 1M LiCl (D_2O). ($Li_2Co_2(PW_9O_{34})_2^{12-}$, 1458 ppm; $Co_4(H_2O)_2(PW_9O_{34})_2^{10-}$, 1853 ppm; other unknown species, 1610 ppm, 1787 ppm, 1974 ppm)

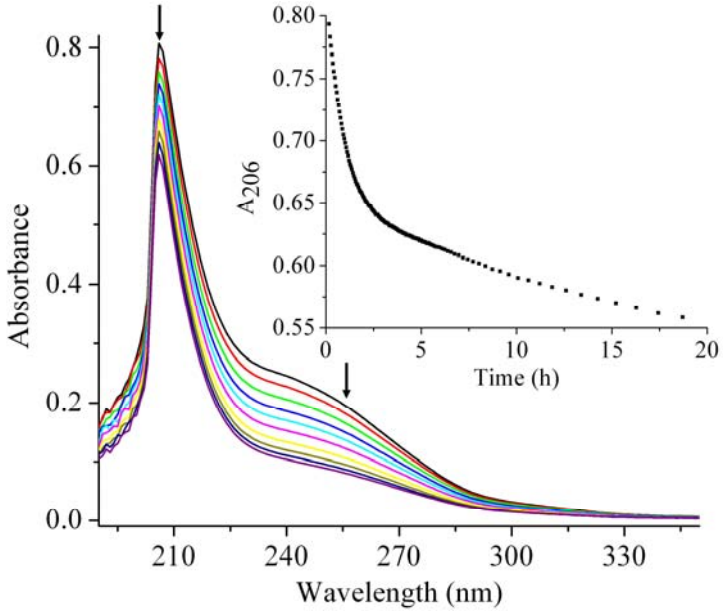

Figure 4.10. Time profile of electronic absorption spectra of 6.2×10^{-6} M **4.1a** in 1M LiCl at 25 °C. For clarity, not all spectra are shown in this figure. The kinetics at 206 nm is shown in the inset.

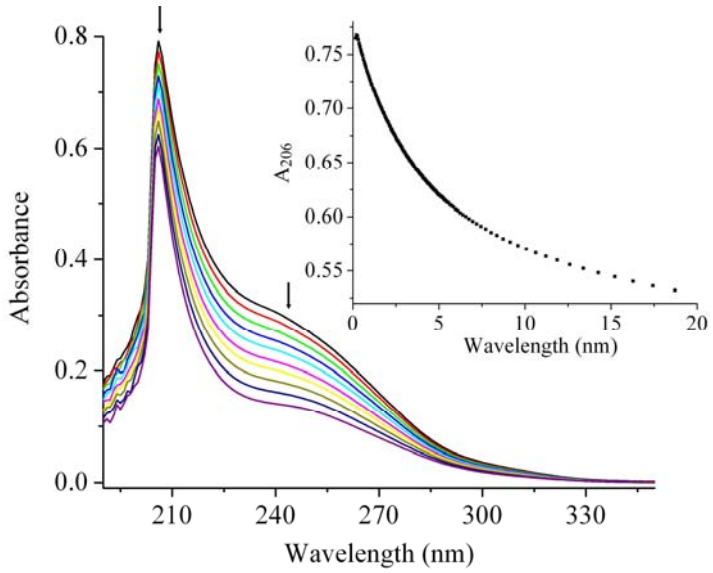

Figure 4.11. Time profile of electronic absorption spectra of ca. 5.6×10^{-6} M **4.2a** in 1M LiCl at 25 °C. For clarity, not all spectra are shown in this figure. The kinetics at 206 nm is shown in the inset.

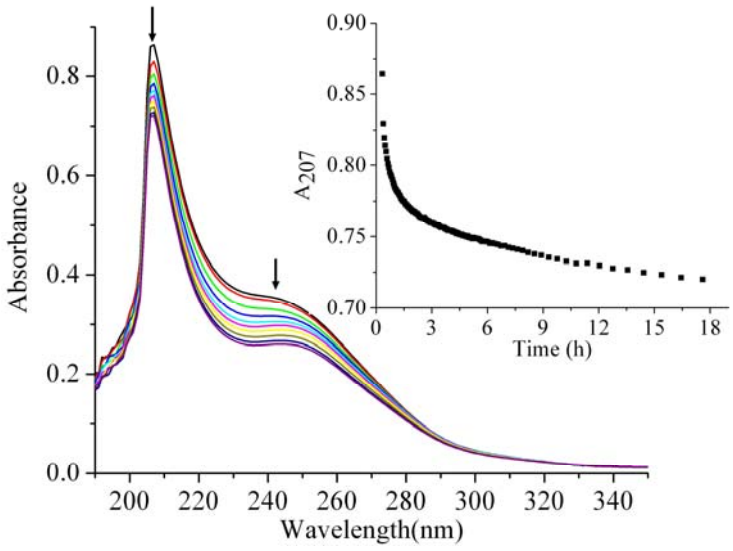

Figure 4.12. Time profile of electronic absorption spectra of ca. 6.4×10^{-6} M **4.3a** in 1M LiCl at 25 °C. For clarity, not all spectra are shown in this figure. The kinetics at 207 nm is shown in the inset.

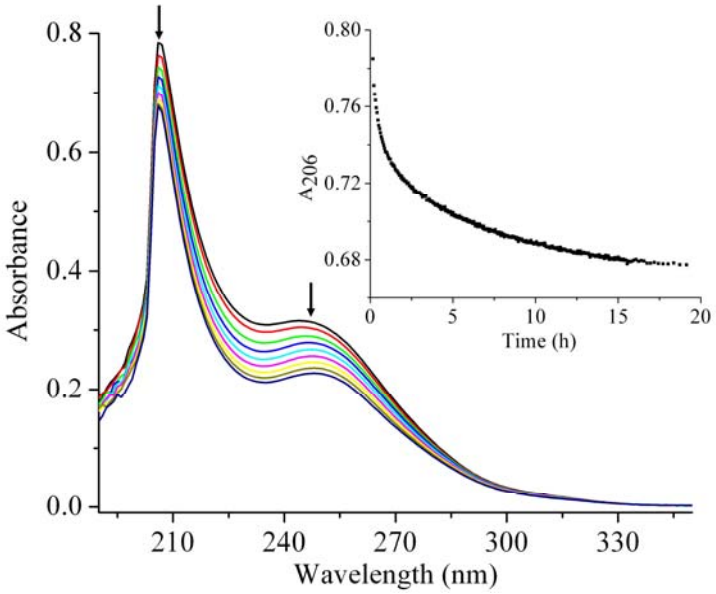

Figure 4.13. Time profile of electronic absorption spectra of ca. 7.2×10^{-6} M **4.4a** in 1M LiCl at 25 °C. For clarity, not all spectra are shown in this figure. The kinetics at 206 nm is shown in the inset.

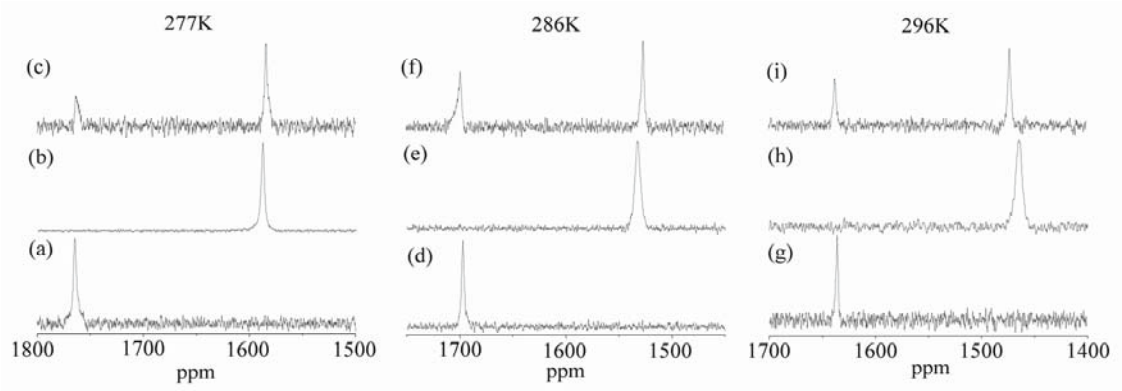

Figure 4.14. ^{31}P NMR spectra of aqueous solutions of (a) **4.1** (b) **4.1a** (c) **4.1** (in the presence of 2.8mM LiCl) at 277K; (d) **4.1** (e) **4. 1a** (f) **4.1** (in the presence of 2.8mM LiCl) at 286K; (g) **4.1** (h) **4.1a** (i) **4.1** (in the presence of 2.8mM LiCl) at 296K.

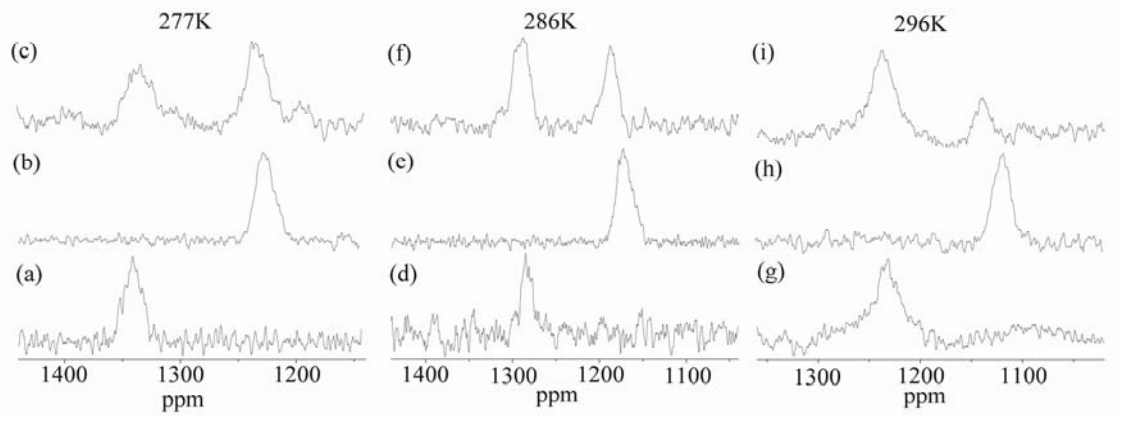

Figure 4.15. ^{31}P NMR spectra of aqueous solutions of (a) **4.2** (b) **4.2a** and (c) **4.2** (in the presence of 2.8mM LiCl) at 277K; (d) **4.2** (e) **4.2a** (f) **4.2** (in the presence of 2.8mM LiCl) at 286K; (g) **4.2** (h) **4.2a** (i) **4.2** (in the presence of 2.8mM LiCl) at 296K.

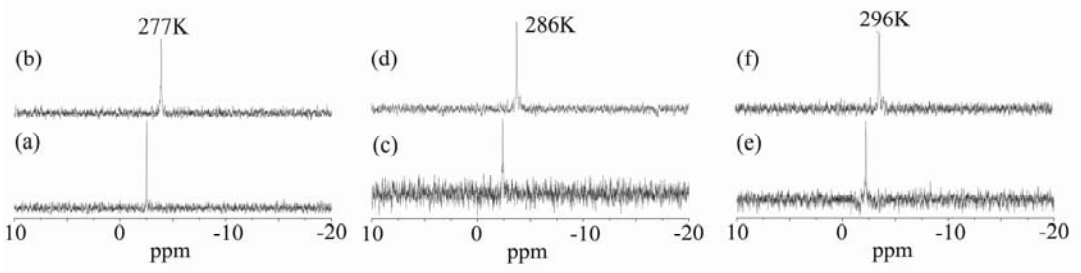

Figure 4.16. ^{31}P NMR spectra of (a) **4.4** and (b) **4.4a** in D_2O at 277K; (c) **4.4** and (d) **4.4a** in D_2O at 286K; and (e) **4.4** and (f) **4.4a** in D_2O at 296K.

4.3.4 Magnetic Susceptibility

The temperature dependence of magnetic susceptibility χ_m for **4.1, 4.2**, and **4.3** was investigated in the range 2-300 K with an applied field of 1000 Oe. The $\chi_m T$ product versus T for **4.1** is shown in **Figure 4.17**. Since Co(II) ion has a $^4T_1$ high-spin ground state in an octahedral environment, the significant orbital contribution results in a deviation of the room-temperature effective magnetic moment per Co_2 unit (6.38 emu K mol^{-1}) from the expected spin-only value for two Co(II) ions (S = 3/2, g = 2.0).[103] Upon cooling from room temperature, the $\chi_m T$ value decreases continuously until it reaches a minimum of 5.03 emu K mol^{-1} at 30 K. Such a decrease is due to strong spin-orbit coupling of Co(II) ion, from which six Kramers doublets result. Below 30 K, the $\chi_m T$ value increases abruptly to a maximum of 5.78 emu K mol^{-1} at 6 K. Taking account of the orthogonality of the magnetic orbitals in Co_2O_{10} unit, the increase of $\chi_m T$ should be indicative of ferromagnetic interactions in the Co(II)-Co(II) dinuclear entities. Then, the $\chi_m T$ value decreases again to 4.34 emu K mol^{-1} at 2 K; this is attributed to that the fact that the d electrons only populate the lowest Kramers doublet at very low temperature. The susceptibility data (see in **Figure 4.18**) for **4.1** could be fit with the Curie-Weiss

equation from 25 to 300K, giving C = 6.84 emu K mol^{-1} and θ = -18.42 K. To simplify the model, the Heisenberg spin-coupled Hamiltonian $\hat{H} = -2J\hat{S}_1 \cdot \hat{S}_2$ was applied to simulate the susceptibility data above 50 K, where J is the in interaction parameter between the Co(II) ions; a Weiss constant was introduced as well. The best-fit parameters obtained are J = 4.90 cm^{-1}, g = 2.71, θ = -30.23 K and $R = 9.1\times10^{-4}$ (the error factor R is defined as $\sum[(\chi_m T)_{obs}-(\chi_m T)_{calc}]^2/\sum[(\chi_m T)_{obs}^2]$). The J value is comparable to those of previously reported cobalt compounds.[104,105]

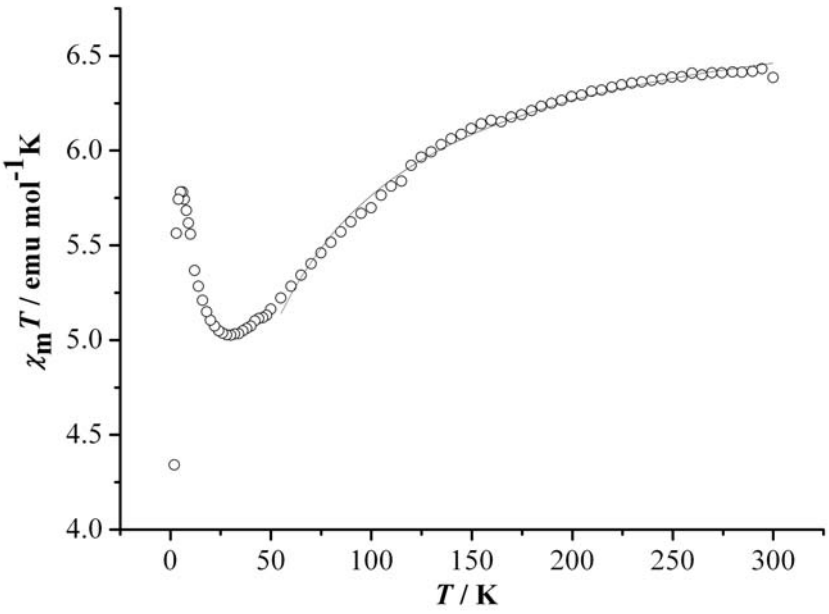

Figure 4.17. Temperature dependence of $\chi_m T$ for **4.1**. The solid lines correspond to the best-fit curves using the parameters described in the text.

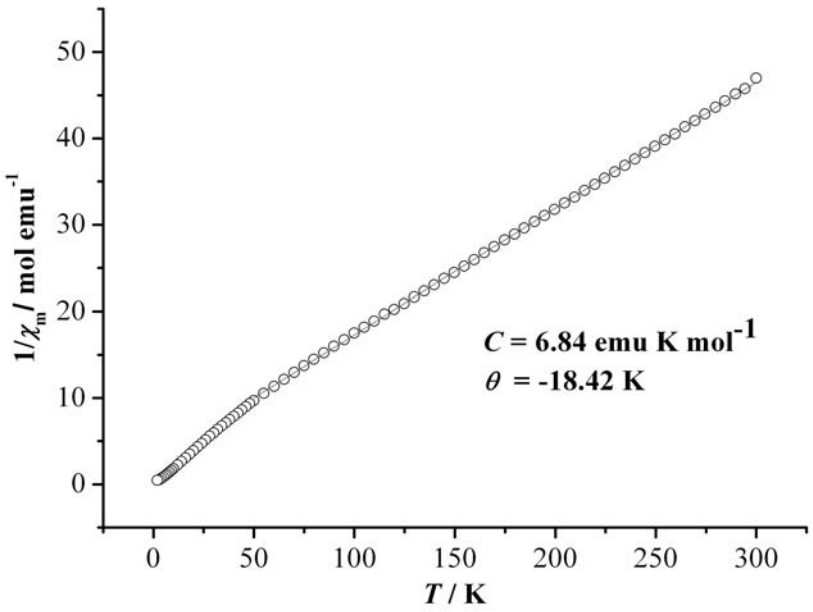

Figure 4.18. Temperature dependence of $1/\chi_m$ for **4.1**. The solid line is the best fit.

The magnetic properties of **4.3** in the form of a $\chi_m T$ versus T plot are shown in **Figure 4.19**. The $\chi_m T$ value stays basically at 9.16 emu K mol^{-1} from room temperature down to about 100 K, close to the expected value (8.75 emu K mol^{-1}) for two isolated spin-only Mn(II) center (s = 5/2, g = 2.0) in an octahedral field. Below 50 K, the $\chi_m T$ value suddenly drops down to 0.85 emu K mol^{-1} at 2K indicating a typical curve shape of the occurrence of an antiferromagnetic interaction in the Mn(II)-Mn(II) dinuclear entities. The $1/\chi_m$ versus T plot (see in **Figure 20**) for **4.3** could be fit with the Curie-Weiss equation from 25 to 300K, producing C = 9.61 emu K mol^{-1} and θ = -13.84 K, the negative Weiss constant indicating the occurrence of a dominant antiferromagnetic interaction between the neighbor Mn(II) atoms. The experimental data could be fitted to a

Heisenberg spin Hamiltonian ($S_1 = S_2 = 5/2$) spin-coupled model assuming $\hat{H} = -2J\hat{S}_1 \cdot \hat{S}_2$, where J is the intradimer interaction parameter between Mn(II) ions. By using least-squares methods, a satisfactory fit of the data was obtained with parameters, $J = -1.09$ cm^{-1} and $g = 2.07$. The agreement factor $R = \sum(\chi_m T_{obs} - \chi_m T_{calc})^2 / \sum(\chi_m T_{obs})^2$ is 1.0×10^{-4}. The J value is similar to that found in other manganese polyoxotungstate compounds.[106] The results indicate the presence of weak antiferromagnetic interaction between the neighboring Mn(II) centers within the cluster.

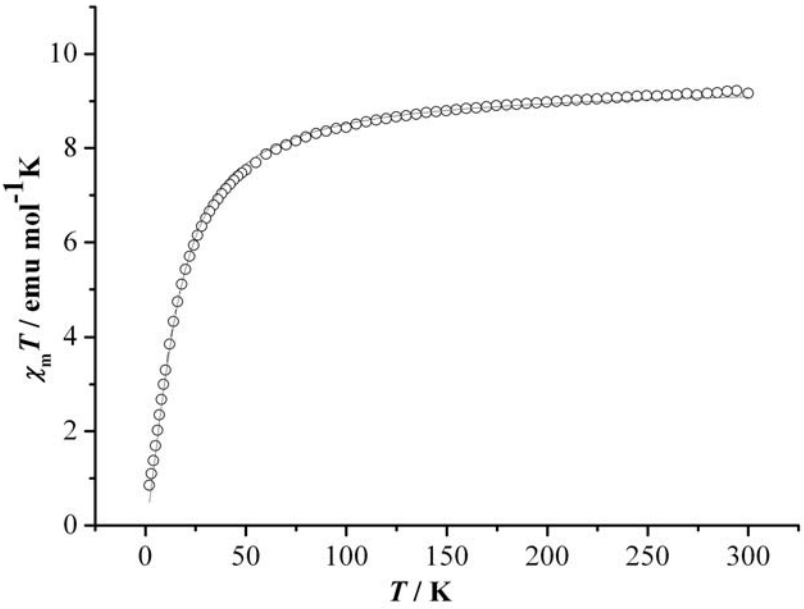

Figure 4.19. Temperature dependence of $\chi_m T$ for **4.3**. The solid line corresponds to the best-fit curve using the parameters described in the text.

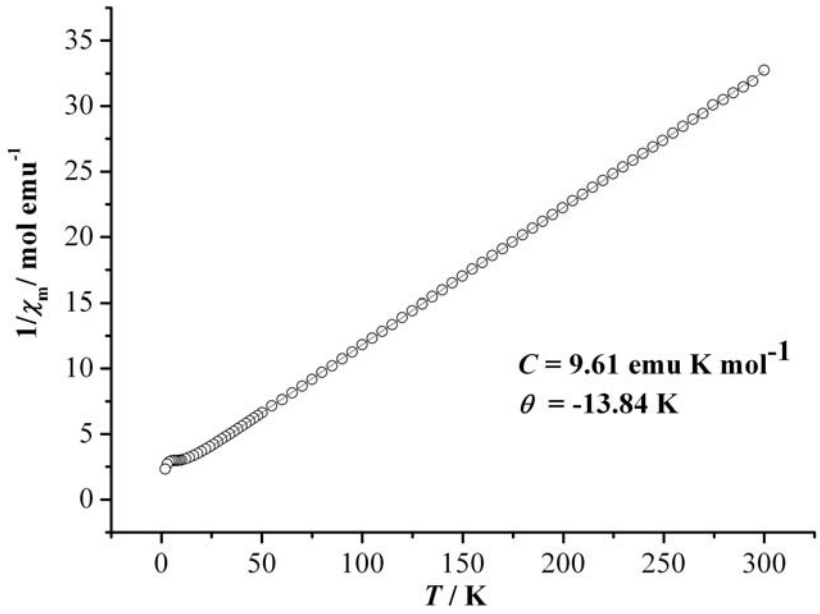

Figure 4.20. Temperature dependence of $1/\chi_m$ for **4.3**. The solid line is the best fit.

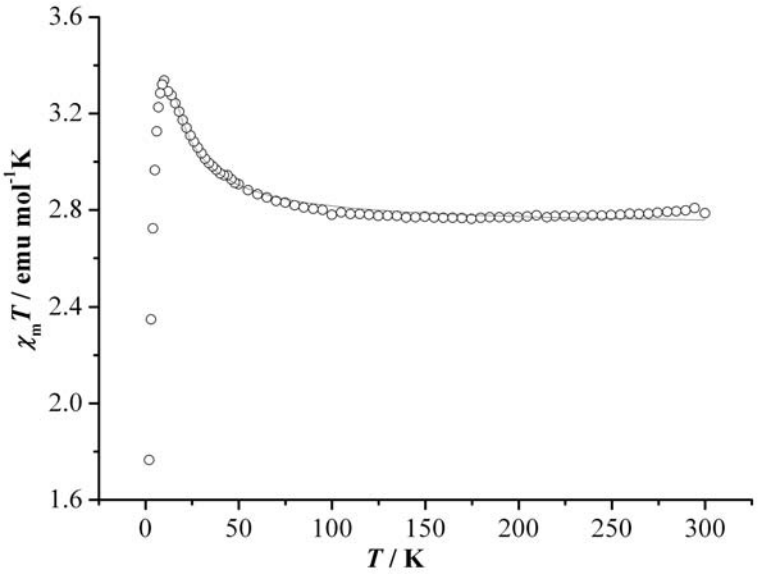

Figure 4.21. Temperature dependence of $\chi_m T$ for **4.2**. The solid lines correspond to the best-fit curves using the parameters described in the text.

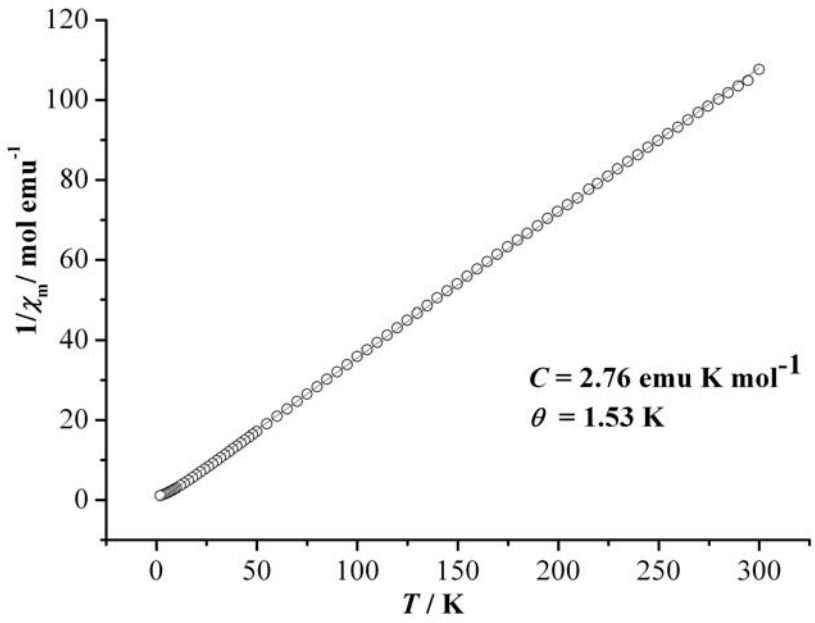

Figure 4.22. Temperature dependence of $1/\chi_m$ for **4.2**. The solid line is the best fit.

The magnetic properties of **4.2** were measured over the range 2 – 300 K and are shown in **Figure 4.21**. The experimental $\chi_m T$ values of **4.2** at room temperature is 2.78 emu K mol^{-1} per formula, which is larger than that expected for the total spin-only value for two Ni^{2+} ions (s = 2, g = 2.0). The $\chi_m T$ values increase from ambient temperature down to 10 K with a maximum of 3.34 emu K mol^{-1}, then decreasing sharply to 1.76 emu K mol^{-1} at 2 K. The increase of $\chi_m T$ indicates the presence of noticeable ferromagnetic interactions within the dinuclear entities, and the low-temperature drop may be attributed to secondary effects such as zero-field splitting (ZFS) and/or intermolecular antiferromagnetic interactions. The temperature dependence of the reciprocal susceptibilities ($1/\chi_m$) obeys the Curie–Weiss law with C = 2.76 emu K mol^{-1} and θ = 1.53 K (**Figure 4.22**), which supports

the presence of overall ferromagnetic coupling between the Ni^{2+} ions. To analyze the observed magnetic behavior, the isotropic exchange Hamiltonian $\hat{H} = -2J\hat{S}_1 \cdot \hat{S}_2$ was used for **4.2**, where J is the intradimer interaction parameter between Ni(II) ions; a Weiss constant was also introduced. The best parameters from fitting the data from 15 K to 300 K are J = 2.27 cm^{-1}, g = 2.08, C = 1.64 emu K mol^{-1} , θ = 2.41 K and $R = 3.6\times10^{-4}$ (the error factor R is defined as $\sum[(\chi_m T)_{obs}-(\chi_m T)_{calc}]^2/\sum[(\chi_m T)_{obs}^2]$). The J value is in agreement with that in other reported Ni polyoxotunstates.[107] The results confirm that the Ni···Ni interactions is ferromagnetic.

4.4 Conclusion

We have prepared a series of sandwich-type polytungstophosphates in which two different transition metal heteroatoms are sandwiched between two B-α-$PW_9O_{34}^{9-}$ units. All these polyanions have been fully characterized by FTIR, elemental analysis, and solution ^{31}P NMR spectroscopy. Compounds **4.1, 4.2, 4.2a 4.3,** and **4.4a** have been characterized by single crystal X-ray diffraction. The stabilities of all these compounds have been studied by solution ^{31}P NMR spectroscopy. None of these compounds are stable in aqueous solution; all will dissociate into metal ions and $PW_9O_{34}^{9-}$. The latter ultimately transforms into $PW_{11}O_{39}^{7-}$ and PO_4^{3-}. Complexes **4.1a** and **4.4a** convert primarily into the sandwich-type POMs with four transition metals in the belt; whereas, **4.3a** slowly decomposes into a mixture of polytungstates but no Ni-containing POMs. An investigation of the magnetic properties of **4.1, 4.2 and 4.3** indicates that the exchange interactions within the dinuclear entities are ferromagnetic in **4.1** (at 6-30K) and in **4.2** (2-300K). However, **4.3** exhibits an antiferromagnetic interaction between the two Mn^{2+} ions at 2-50K.

References

(1) Pope, M. T. *Heteropoly and Isopoly Oxometalates*; Springer-Verlag: Berlin, 1983.

(2) Pope, M. T.; Müller, A. *Angew. Chem. Int. Ed. Engl.* **1991**, *30*, 34.

(3) Hill, C. L. *Chem. Rev.* **1998**, *98*, 1.

(4) *Polyoxometalate Chemistry From Topology via Self-Assembly to Applications*; Pope, M. T.; Müller, A., Eds.; Kluwer Academic Publishers: Dordrecht, 2001.

(5) Yamase, T.; Pope, M. T. In *Nanostructure Science and Technology*; Lockwood, D. J., Ed.; Kluwer Academic/Plenum Publishers: New York, 2002; Vol. 2.

(6) Borrás-Almenar, J. J.; Coronado, E.; Müller, A.; Pope, M. T. *Polyoxometalate Molecular Science*; Kluwer Academic Publishers: Dordrecht, 2003; Vol. 98.

(7) Pope, M. T. In *Comprehensive Coordination Chemistry II: From Biology to Nanotechnology*; Wedd, A. G., Ed.; Elsevier Ltd.: Oxford, UK, 2004; Vol. 4, p 635.

(8) Cronin, L. In *Comprehensive Coordination Chemistry II: From the Molecular to the Nanoscale: Synthesis, Structure, and Properties*; McCleverty, J. A., Meyer, T. J., Eds.; Elsevier: Amsterdam, 2004; Vol. 7, p 1.

(9) Hill, C. L. In *Comprehensive Coordination Chemistry-II: From Biology to Nanotechnology*; Wedd, A. G., Ed.; Elsevier Ltd.: Oxford, UK, 2004; Vol. 4, p 679.

(10) *Polyoxometalates: From Platonic Solids to Anti-retroviral Activity*; Pope, M. T.; Müller, A., Eds.; Kluwer Academic Publishers: Dordrecht, Netherlands, 1993.

(11) Yamase, T.; Fujita, H.; Fukushima, K. *Inorg. Chim. Acta* **1988**, *151*, 15.

(12) Hill, C.; Weeks, M.; Hartnup, M.; Sommadossi, J.-P.; Schinazi, R. *Ann. N. Y. Acad. Sci.* **1990**, *616*, 528.

(13) Hill, C. L.; Weeks, M. S.; Schinazi, R. F. *Cjacs* **1990**, *33*, 2767.

(14) Yamase, T. In *Polymeric Materials Encyclopedia*; Salamone, J. C., Ed.; CRC Press: Boca Raton, 1996, p 365.

(15) Rhule, J. T.; Hill, C. L.; Judd, D. A.; Schinazi, R. F. *Chem. Rev.* **1998**, *98*, 327.

(16) Rhule, J. T.; Hill, C. L.; Zheng, Z.; Schinazi, R. F. In *Topics in Biological Inorganic Chemistry*; Clarke, M. J., Sadler, P. J., Eds.; Springer-Verlag: Heidelberg, 1999; Vol. 2: Metallopharmaceuticals, p 117.

(17) Seko, A.; Yamase, T.; Yamashita, K. *J. Inorg. Biochem.* **2009**, *103(7)*, 1061.

(18) Prudent, R.; Moucadel, V.; Laudet, B.; Barette, C.; Lafanechere, L.; Hasenknopf, B.; Li, J.; Bareyt, S.; Lacote, E.; Thorimbert, S.; Malacria, M.; Gouzerh, P.; Cochet, C. *Chem. & Bio.* **2008**, *15(7)*, 683.

(19) Mueller, C. E.; Iqbal, J.; Baqi, Y.; Zimmermann, H.; Roellich, A.; Stephan, H. *Bioorg. Med. Chem. Lett.* **2006**, *16(23)*, 5943.

(20) Hill, C. L. *J. Mol. Catal. A: Chem.* **2007**, *262*, 2.

(21) Hill, C. L.; Prosser-McCartha, C. M. *Coord. Chem. Rev.* **1995**, *143*, 407.

(22) Alhanash, A.; Kozhevnikova, E. F.; Kozhevnikov, I. V. *Catal. Lett.* **2008**, *120(3-4)*, 307.

(23) Moffat, J. B. *Metal-Oxygen Clusters: The Surface and Catalytic Properties of Heteropoly Oxometalates.*; Kluwer Academic/Plenum Publishers: New York, 2001; Vol. 9.

(24) Kozhevnikov, I. V. *Catalysis by Polyoxometalates*; Wiley: Chichester, England, 2002; Vol. 2.

(25) Okuhara, T.; Mizuno, N.; Misono, M. In *Advances in Catalysis* 1996; Vol. 41, p 113.

(26) Katsoulis, D. E. *Chem. Rev.* **1998**, *98*, 359.

(27) Kozhevnikov, I. V. *Chem. Rev.* **1998**, *98*, 171.

(28) Neumann, R. *Prog. Inorg. Chem.* **1998**, *47*, 317.

(29) Müller, A.; Das, S. K.; Kuhlmann, C.; Bögge, H.; Schmidtmann, M.; Diemann, E.; Krickemeyer, E.; Hormes, J.; Modrow, H.; Schindler, M. *Chem. Commun.* **2001**, 655.

(30) Mizuno, N.; Misono, M. *Chem. Rev.* **1998**, *98*, 199.

(31) Coronado, E.; Gomez-Garcia, C. J. In *Polyoxometalates: From Platonic Solids to Anti-Retroviral Activity*; Pope, M. T., Müller, A., Eds.; Kluwer Academic Publishers: Dordrecht, 1994, p 233.

(32) Coronado, E.; Gómez-García, C. J. *Chem. Rev.* **1998**, *98*, 273.

(33) Clemente-Juan, J. M.; Coronado, E. *Coord. Chem. Rev.* **1999**, *193-195*, 361.

(34) Clemente-Juan, J. M.; Clemente-León, M.; Coronado, E.; Forment, A.; Gaita-Ariño, A.; Gómez-García, C. J.; Martínez-Ferrero, E., Eds.; Kluwer Academic/Plenum Publishers:Norewell, MA, 2002.

(35) Clemente-Juan, J. M. M.; Coronado, E. F., A.; Gaita-Ariño, A., series; , Eds. In *NATO Science* Borrás-Alamenar, J. J., Coronado, E., Müller, A., Pope, M. T., Eds.; Kluwer Academic Publishers: Norwell, MA: 2003, p 273.

(36) Ouahab, L.; Golhen, S.; Triki, S. In *Polyoxometalate Chemistry* 2001, p 205.

(37) Bi, L.-H.; Kortz, U.; Keita, B.; Nadjo, L.; Borrmann, H. *Inorg. Chem.* **2004**, *43*, 8367.

(38) Hill, C. L.; Brown, R. B., Jr. *Casreact 104:168282; Cjacs* **1986**, *108*, 536.

(39) Lyon, D. K.; Miller, W. K.; Novet, T.; Domaille, P. J.; Evitt, E.; Johnson, D. C.; Finke, R. G. *Casreact 104:168282; Cjacs* **1991**, *113*.

(40) Mansuy, D.; Bartoli, J.-F.; Battioni, P.; Lyon, D. K.; Finke, R. G. In *Casreact 104:168282; Cjacs* 1991; Vol. 113, p 7222.

(41) Ruhlmann, L.; Canny, J.; Contant, R.; Thouvenot, R. *Inorg. Chem.* **2002**, *41*, 3811.

(42) Katsoulis, D. E.; Pope, M. T. *Casreact 104:168282; Cjacs* **1984**, *106*, 2737.

(43) Liu, J. G.; Ortega, F.; Sethuraman, P.; Katsoulis, D. E.; Costello, C. E.; Pope, M. T. *J. Chem. Soc., Dalton Trans.* **1992**, 1901.

(44) Anderson, T. M.; Zhang, X.; Hardcastle, K. I.; Hill, C. L. *Inorg. Chem.* **2002**, *41*, 2477.

(45) Liu, J. F.; Zhao, B. L.; Rong, C. Y.; Pope, M. T. *Acta Chimica Sinica* **1993**, *51*, 368.

(46) Qu, L.; Sun, Y.; Chen, Y.; Yu, M.; Peng, J. *Synth. React. Inorg. Met.-Org. Chem.* **1994**, *24*, 1339.

(47) Mizuno, N.; Hirose, T.; Tateishi, M.; Iwamoto, M. *J. Mol. Catal.* **1994**, *88*, L125.

(48) Meng, L.; Liu, J. F. *Chin. Chem. Lett.* **1995**, *6*, 453.

(49) Mizuno, N.; Nozaki, C.; Hirose, T.-o.; Tateishi, M.; Iwamoto, M. *J. Mol. Catal. A: Chem.* **1997**, *117*, 159.

(50) Liu, J. F.; Zhen, Y. G.; So, H. S. *Synth. React. Inorg. Met.-Org. Chem.* **1998**, *28*.

(51) Meng, L.; Zhan, X. P.; Wang, M.; Liu, J. F. *Polyhedron* **2001**, *20*.

(52) Jana, S. K.; Kubota, Y.; Tatsumi, T. *J. Catal.* **2008**, *255(1)*.

(53) Knoth, W. H.; Domaille, P. J.; Farlee, R. D. *Organometallics* **1985**, *4*, 62.

(54) Knoth, W. H.; Domaille, P. J.; Harlow, R. L. *Inorg. Chem.* **1986**, *25*, 1577.

(55) Finke, R. G.; Rapko, B.; Weakley, T. J. R. *Inorg. Chem.* **1989**, *28*, 1573.

(56) Xin, F.; Pope, M. T. *Casreact 104:168282; Cjacs* **1996**, *118*, 7731.

(57) Laronze, N.; Marrot, J.; Hervé, G. *Inorg. Chem.* **2003**, *42*, 5857.

(58) Robert, F.; Leyrie, M.; Hervé, G. *Acta Crystallogr.* **1982**, *B38*, 358.

(59) Boesing, M.; Noeh, A.; Loose, I.; Krebs, B. *Casreact 104:168282; Cjacs* **1998**, *120*, 7252.

(60) Kortz, U.; Al-Kassem, N. K.; Savelieff, M. G.; Kadi, N. A. A.; Sadakane, M. *Inorg. Chem.* **2001**, *40*, 4742.

(61) Botar, B.; Yamase, T.; Ishikawa, E. *Inorg. Chem. Commun.* **2001**, *4*, 551.

(62) Yamase, T.; Botar, B.; Ishikawa, E.; Fukaya, K. *Chem. Lett.* **2001**, 56.

(63) Mialane, P.; Marrot, J.; Riviére, E.; Nebout, J.; Hervé, G. *Inorg. Chem.* **2001**, *40*, 44.

(64) Kortz, U.; Nellutla, S.; Stowe, A. C.; Dalal, N. S.; van Tol, J.; Bassil, B. S. *Inorg. Chem.* **2004**, *43*, 144.

(65) Meng, L.; Liu, J. F. *Chin. Chem. Lett.* **1994**, *6*, 547.

(66) Finke, R. G.; Rapko, B.; Saxton, R. J.; Domaille, P. J. *Casreact 104:168282; Cjacs* **1986**, *108*, 2947.

(67) Bi, L.; Zhou, W.; Jiang, J.; Dong, S. *J. Electroanal. Chem.* **2008**, *624(1-2)*, 269.

(68) Kortz, U.; Mbomekalle, I. M.; Keita, B.; Nadjo, L.; Berthet, P. *Inorg. Chem.* **2002**, *41*, 6412.

(69) Mbomekalle, I. M.; Keita, B.; Nadjo, L.; Berthet, P. *Inorg. Chem. Commun.* **2003**, *6*, 435.

(70) Weakley, T. J. R.; Evans, H. T., Jr.; Showell, J. S.; Tourné, G. F.; Tourné, C. M. *J. Chem. Soc. Chem. Comm.* **1973**, *4*, 139.

(71) Casañ-Pastor, N.; Bas-Serra, J.; Coronado, E.; Pourroy, G.; Baker, L. C. W. *Casreact 104:168282; Cjacs* **1992**, *114*, 10380.

(72) Clemente-Juan, J. M.; Coronado, E.; Galán-Mascarós, J., J. R. ; Gómez-García, C. J. *Inorg. Chem.* **1999**, *38*, 55.

(73) Kortz, U.; Isber, S.; Dickman, M. H.; Ravot, D. *Inorg. Chem.* **2000**, *39*, 2915.

(74) Kortz, U.; Nellutla, S.; Stowe, A. C.; Dalal, N. S.; Rauwald, U.; Danquah, W.; Ravot, D. *Inorg. Chem.* **2004**, *43*, 2308.

(75) Bassil, B. S.; Dickman, M. H.; Kortz, U. *Inorg. Chem.* **2006**, *45*, 2394.

(76) Finke, R. G.; Droege, M. W. *Inorg. Chem.* **1983**, *22*, 1006.

(77) Finke, R. G.; Droege, M. W.; Domaille, P. J. *Inorg. Chem.* **1987**, *26*, 3886.

(78) Finke, R. G.; Lyon, D. K.; Nomiya, K.; Sur, S.; Mizuno, N. *Inorg. Chem.* **1990**, *29*, 1784.

(79) Gómez-García, C. J.; Borrás-Almenar, J. J.; Coronado, E.; Ouahab, L. *Inorg. Chem.* **1994**, *33*, 4016.

(80) Finke, R. G.; Weakley, T. J. R. *Journal of Chemical Crystallography* **1994**, *24*, 123.

(81) Kirby, J. F.; Baker, L. C. W. *Casreact 104:168282; Cjacs* **1995**, *117*, 10010.

(82) Crano, N. J.; Chambers, R. C.; Lynch, V. M.; Fox, M. A. *J. Mol. Catal. A: Chem.* **1996**, *114*, 65.

(83) Zhang, X.; Chen, Q.; Duncan, D. C.; Campana, C.; Hill, C. L. *Inorg. Chem.* **1997**, *36*, 4208.

(84) Müller, A.; Peters, F.; Pope, M. T.; Gatteschi, D. *Chem. Rev.* **1998**, *98*, 239.

(85) Song, W.; Wang, X.; Liu, Y.; Liu, J.; Xu, H. *J. Electroanal. Chem.* **1999**, *476*, 85.

(86) Zhang, X.; Anderson, T. M.; Chen, Q.; Hill, C. L. *Inorg. Chem.* **2001**, *40*, 418.

(87) Anderson, T. M.; Hardcastle, K. I.; Okun, N.; Hill, C. L. *Inorg. Chem.* **2001**, *40*, 6418.

(88) Gaunt, A. J.; May, I.; Collison, D.; Holman, K. T.; Pope, M. T. *J. Mol. Struct.* **2003**, *656*, 101.

(89) Kirby, J. F.; Baker, L. C. W. *Casreact 104:168282; Cjacs* **1995**, *117*, 10010.

(90) Zhang, X.; Hill, C. L. *Chem. Ind.* **1998**, *75*, 519.

(91) Mbomekalle, I. M.; Keita, B.; Nadjo, L.; Neiwert, W. A.; Zhang, L.; Hardcastle, K. I.; Hill, C. L.; Anderson, T. M. *Eur. J. Inorg. Chem.* **2003**, 3924.

(92) Keita, B.; Mbomekalle, I. M.; Lu, Y. W.; Nadjo, L.; Berthet, P.; Anderson, T. M.; Hill, C. L. *Eur. J. Inorg. Chem.* **2004**, 3462.

(93) Kim, K. C.; Pope, M. T. *Casreact 104:168282; Cjacs* **1999**, *121*, 8512.

(94) Kim, K.-C.; Gaunt, A. J.; Pope, M. T. *J. Cluster Sci.* **2002**, *13*, 423.

(95) Gaunt, A. J.; May, I.; Copping, R.; Bhatt, A. I.; Collison, D.; Danny-Fox, O.; Travis-Holman, K.; Pope, M. T. *J. Chem. Soc., Dalton Trans.* **2003**, 3009.

(96) Khoshnavazi, R.; Salimi, A.; Moaser, A. G. *Polyhedron* **2008**, *27*, 1303.

(97) Tan, R.; Wang, X.; Chai, F.; Lan, Y.; Su, Z. *Inorg. Chem. Commun.* **2006**, *9(12)*, 1331.

(98) Gaunt, A. J.; May, I.; Helliwell, M.; Richardson, S. *Casreact 104:168282; Cjacs* **2002**, *124*, 13350.

(99) Bruker AXS, I.; Analytical X-ray Sysems: Madison, WI, 2003.

(100) Bruker AXS, I.; Analytical X-Ray Sytems: Madison, WI, 2003.

(101) Bruker AXS, I. Madison, WI, 2003.

(102) SADABS, S., G.; 2.10 ed. **2003**.

(103) *Magnetic Properties of Transition Metal Compounds*; Carlin, R. L.; van Duyneveldt, A. L., Eds.; Springer-Verlag: New York, 1977.

(104) Bassil, B. S.; Nellutla, S.; Kortz, U.; Stowe, A. C.; Tol, J. v.; Dalal, N. S.; Keita, B.; Nadjo, L. *Inorg. Chem.* **2005**, *44*, 2659.

(105) Galan-Mascaros, J. R.; Gomez-Garcia, C. J.; Borras-Almenar, J. J.; Coronado, E. *Advanced Materials* **1994**, *6*, 221.

(106) Gómez-García, C. J.; Coronado, E.; Gómez-Romero, P.; Casañ-Pastor, N. *Inorg. Chem.* **1993**, *32*, 3378.

(107) Mbomekalle, I. M.; Keita, B.; Nierlich, M.; Kortz, U.; Berthet, P.; Nadjo, L. *Inorg. Chem.* **2003**, *42*, 5143.

CHAPTER 5

A New Polyoxometalate Structural Class: $Mn^{III}(HPW_7O_{28})_2^{13-}$

Abstract: A novel sandwich type polyoxometalate $Na_{13}[Mn^{III}(HPW_7O_{28})_2]\cdot 39H_2O$, **5.1,** has been synthesized and characterized by IR spectroscopy and elemental analysis. X-ray single crystal analysis was carried out on **5.1**, which crystallizes in the triclinic system, space group $P\bar{1}$, with a = 10.507(4) Å, b = 10.942(5) Å, c = 21.037(9) Å, α = 85.159(6)°, β = 77.896(5)°, γ = 67.212(5)°, and Z = 1. Compound **5.1** is composed of a high-valent manganese atom and two heptatungstophosphate units. Compound **5.1** is a sandwich POM with heptatungstophosphate ligands. This work demonstrates that heptatungstate can ligate a 3d metal and represents a rare case of polyoxometalate-based sandwich complex with a single bridging metal.

5.1 Introduction

d-Electron metal centers ligated by polyoxometalates (transition metal-substituted POMs or TMSPs) are a large family of highly modifiable metal-oxygen anionic clusters that continue to be the focus of considerable ongoing research.[1-8] The highly tunable nature of TMSPs, coupled with their chemically robust nature, has led to applications in catalysis,[9-19] molecular magnetism,[20-25] and medicine.[26-35] Sandwich-type compounds represent the largest subclass of TMSPs,[36] and their oxidative, thermal and hydrolytic stability have made them attractive as catalysts for the selective oxidation of organic substrates,[9-19,37-39] and most recently, water.[40-43] Mono, di, and trivacant Keggin and Wells-Dawson POM ligands such as $XW_{11}O_{39}^{n-}$, $XW_{10}O_{36}^{n-}$, and $XW_9O_{34}^{n-}$, X = P, As, Si, Ge, and $X_2W_{17}O_{61}^{n-}$, and $X_2W_{15}O_{56}^{12-}$, X = P, As, have been used extensively as precursors to prepare TMSPs.[44-69] However, TMSPs with heteropolyoxoanion units not derived from Keggin, Dawson, and Anderson derivatives are rare and their preparation remains a significant challenge. In 2005, Kortz *et al.* reported the complex

$[HXW_7O_{28}Ru(dmso)_3]^{6-}$ (X = P, As), the only structurally characterized POM with the heptatungstate ligands $[HPW_7O_{28}]^{8-}$ and $[HAsW_7O_{28}]^{8-}$.[70] Here, we report the synthesis, structure, magnetism and hydrolytic stability of a sandwich POM with heptatungstate ligands, $Na_{13}[Mn^{III}(HPW_7O_{28})_2]\cdot 39H_2O$ (**5.1**). This work demonstrates that heptatungstate can ligate a 3d metal and represents a rare case of a polyoxometalate-based sandwich complex with a single bridging metal.

5.2 Experimental

5.2.1 General Methods and Materials

All common laboratory chemicals were reagent grade, purchased from commercial sources and used without further purification. Elemental analyses for Mn, Na, P, and W were performed by Galbraith Laboratories, INC. (Knoxville, Tennessee). Infrared spectra (2% sample in KBr) were recorded on a Thermo Nicolet 6700 instrument. Electronic absorption spectra were acquired using Agilent 8453 spectrophotometer equipped with a diode-array detector. Thermogravimetric analysis (TGA) data were collected on Instrument Specialists Incorporated TGA 1000 instruments. Solution ^{31}P NMR measurements were made on a Varian INOVA 400 MHz spectrometer, referenced to 85% H_3PO_4 as an external standard.

5.2.2 Synthesis

$Na_2WO_4\cdot 2H_2O$ (5.00g, 15.2mmol) and Na_2HPO_4 (0.308, 2.2 mmol) was dissolved in 50 ml H_2O followed by addition of $Mn^{III}(CH_3COO)_3\cdot 2H_2O$ (0.295g, 1.1mmol). The pH was adjusted to 7.5 by adding 6M HCl dropwise and a brown solution formed. The solution was heated at 90 °C for 1h and then was allowed to cool to room temperature. KCl solid (0.3g) was added to the solution. Slow evaporation at room temperature after 6

days yields purple crystals suitable for X-ray diffraction (yield 1.7g, 34%). The numbers of counter cations and crystal water molecules were determined by both elemental analysis and thermogravimetric analysis (TGA). FT/IR data (cm^{-1}): 1104(s), 1067(s), 1008(s), 952(sh), 942(s), 905(s), 891(sh), 853(sh), 808(m), 728(sh), 668(s), 577(sh), 521(s). Elemental analysis calcd (%) for **1**, $H_{84}MnNa_{13}O_{97}P_2W_{14}$: Mn, 1.2; Na, 6.5; P, 1.3; W, 55.7. Found (%): Mn, 1.3; Na, 6.4; P, 1.2; W, 55.1.

5.2.3 X-ray Crystallography

X-ray analysis and crystal data for **5.1** at 173K: purple block, crystal size 0.37 x 0.36 x 0.34 mm^3, $H_{80}Na_{13}MnO_{95}P_2W_{14}$, Triclinic, space group $P\bar{1}$, a = 10.507(4), b = 10.942(5), c = 21.037(9) Å, V = 2180.2(16) $Å^3$, Z = 1, Mr = 4627.2, ρ_{calcd} = 3.435 $Mg•m^{-3}$; $\mu(Mo_{K\alpha})$ = 18.752 mm^{-1}; $0.99 \leq \theta \leq 30.39°$. Single crystal of **5.1** suitable for X-ray analysis were each coated with Paratone-N oil, suspended in a small fiber loop, and placed in a cooled gas stream on a Brüker D8 SMART APEX CCD sealed tube diffractometer. Diffraction intensities were measured using graphite monochromated Mo Kα radiation (λ = 0.71073 Å) at 173(2) K and a combination of φ and ω scans with 10 s frames traversing about ω at 0.3° increments. Data collection, indexing, and initial cell refinements were carried out using SMART;[71] frame integration and final cell refinements were done using SAINT.[72] The molecular structure of each complex was determined using Direct Methods and Fourier techniques and refined by full-matrix least squares.[73] A multiple absorption correction, including face indexed absorption correction, was applied using the program SADABS.[74] The largest residual electron density for each structure was located close to (less than 1.0 Å from) countercation and tungsten atoms and was most likely due to imperfect absorption corrections frequently encountered in

heavy-metal atom structures. All the heavy atoms, including Na, Mn, P and W were refined anisotropically. Scattering factors and anomalous dispersion corrections are taken from the International Tables for X-ray Crystallography. Structure solution, refinement, graphic and generation of publication materials were performed by using SHELXTL, V6.14 software. The refinement converged with R_1 = 0.0569 and wR_2 = 0.1767 for 11325 reflections with I > 2σ(I). Max/min residual electron density is 5.859/-7.349 e·Å^{-3}. The highest residual peaks are all associated with W atoms. Refinement details, structural parameters and selected bond lengths and bond angles are summarized in **Tables 5.1-5.2**. The corresponding CIF files are available as supplementary material.

Table 5.1. Crystal data and structure refinement for **5.1**

Complex	**5.1**
Molecular formula	$H_{78}MnNa_{13}O_{95}P_2W_{14}$
Formula weight ($g \cdot mol^{-1}$)	4588.27
Temperature (K)	172(2)
Radiation (λ, Å)	0.71073
Crystal system	Triclinic
Space group	$P\bar{1}$
a (Å)	10.507(4)
b (Å)	10.942(5)
c (Å)	21.037(9)
α (°)	85.159(6)
β (°)	77.896(5)
γ (°)	67.212(5)
V ($Å^3$)	2180.2(16)
Z	1
Density, $Mg \cdot m^{-3}$	3.435
μ, mm^{-1}	18.755
F(000)	1994
Crystal size (mm^{-3})	0.37 x 0.36 x 0.34
Reflections collected	36949
Independent reflections	12273[R(int) = 0.0650]
Absorption correction	Semi-empirical from equivalents
GOF	1.004
Final R indices [R>2σ(I)]	R_1[a] = 0.0569, wR_2[b] = 0.1767
R indices (all data)	R_1[a] = 0.0602, wR_2[b] = 0.1808
largest diff. peak and hole ($e \cdot Å^{-3}$)	5.859 and -7.349

[a] $R_1 = \Sigma||F_0| - |F_c|| / \Sigma|F_0|$;

[b] $wR_2 = \Sigma[w(F_0^2 - F_c^2)^2] / \Sigma[w(F_0^2)^2]^{1/2}$

Table 5.2. Selected bond lengths [Å] and angles [deg] for **5.1**

Bond lengths			
Mn(1)-O(23)#1	1.916(7)	Mn(1)-O(21)#1	1.932(6)
Mn(1)-O(23)	1.916(7)	Mn(1)-O(25)	2.177(6)
Mn(1)-O(21)	1.932(7)	Mn(1)-O(25)#1	2.177(6)
O(25)-P(1)	1.527(7)	O(26)-P(1)	1.596(6)
O(27)-P(1)	1.526(7)	O(28)-P(1)	1.539(6)
O(2)-W(1)	1.744(7)	O(3)-W(1)	1.957(6)
O(4)-W(1)	2.157(6)	O(5)-W(1)	1.733(7)
O(8)-W(1)	1.927(7)	O(11)-W(1)	2.238(6)
O(1)-W(2)	1.726(7)	O(3)-W(2)	1.956(6)
O(4)-W(2)	2.177(6)	O(6)-W(2)	1.767(7)
O(13)-W(2)	2.326(6)	O(7)-W(2)	1.926(7)
O(11)-W(3)	1.905(6)	O(12)-W(3)	1.717(6)
O(13)-W(3)	1.887(6)	O(17)-W(3)	1.958(6)
O(26)-W(3)#1	2.361(6)	O(18)-W(3)	1.921(6)
O(27)#1-W(4)	2.189(6)	O(8)-W(4)	1.946(6)
O(11)-W(4)	2.231(6)	O(9)-W(4)	1.760(7)
O(19)-W(4)	1.929(6)	O(10)-W(4)	1.754(8)
O(7)-W(5)	1.957(6)	O(14)-W(5)	1.752(7)
O(13)-W(5)	2.203(6)	O(15)-W(5)	1.734(7)
O(16)-W(5)	1.941(6)	O(28)#1-W(5)	2.246(6)
O(16)-W(6)	1.885(6)	O(17)-W(6)	1.957(6)
O(22)-W(6)	1.945(6)	O(24)-W(6)	1.730(7)
O(23)-W(6)	1.841(7)	O(26)-W(6)#1	2.339(6)
O(18)-W(7)	1.997(6)	O(21)-W(7)	1.840(7)
O(19)-W(7)	1.903(6)	O(22)-W(7)	1.924(6)
O(20)-W(7)	1.724(7)	O(26)-W(7)#1	2.347(6)

Bond Angles			
O(23)#1-Mn(1)-O(23)	180.0(4)	O(23)#1-Mn(1)-O(25)	88.0(3)
O(23)#1-Mn(1)-O(21)	88.2(3)	O(23)-Mn(1)-O(25)	92.0(3)
O(23)-Mn(1)-O(21)	91.8(3)	O(21)-Mn(1)-O(25)	89.2(3)
O(23)#1-Mn(1)-O(21)#1	91.8(3)	O(21)#1-Mn(1)-O(25)	90.8(3)
O(23)-Mn(1)-O(21)#1	88.2(3)	O(23)#1-Mn(1)-O(25)#1	92.0(3)
O(21)-Mn(1)-O(21)#1	179.998(1)	O(23)-Mn(1)-O(25)#1	88.0(3)
O(21)#1-Mn(1)-O(25)#1	89.2(3)	O(21)-Mn(1)-O(25)#1	90.8(3)

O(25)-Mn(1)-O(25)#1	179.999(2)		
O(27)-P(1)-O(25)	112.1(4)	O(27)-P(1)-O(26)	106.6(3)
O(27)-P(1)-O(28)	108.6(3)	O(25)-P(1)-O(26)	108.5(3)
O(25)-P(1)-O(28)	112.1(4)	O(28)-P(1)-O(26)	108.6(3)
O(5)-W(1)-O(2)	102.6(3)	O(2)-W(1)-O(4)	90.6(3)
O(5)-W(1)-O(8)	101.0(3)	O(8)-W(1)-O(4)	85.8(3)
O(2)-W(1)-O(8)	98.5(3)	O(3)-W(1)-O(4)	74.2(2)
O(5)-W(1)-O(3)	94.6(3)	O(5)-W(1)-O(11)	87.5(3)
O(2)-W(1)-O(3)	98.9(3)	O(2)-W(1)-O(11)	168.5(3)
O(8)-W(1)-O(3)	153.4(3)	O(8)-W(1)-O(11)	74.0(2)
O(5)-W(1)-O(4)	163.9(3)	O(3)-W(1)-O(11)	85.4(2)
O(4)-W(1)-O(11)	80.3(2)		
O(1)-W(2)-O(6)	103.9(3)	O(7)-W(2)-O(4)	80.9(3)
O(1)-W(2)-O(7)	98.5(3)	O(3)-W(2)-O(4)	73.7(2)
O(6)-W(2)-O(7)	102.5(3)	O(1)-W(2)-O(13)	169.6(3)
O(1)-W(2)-O(3)	100.0(3)	O(6)-W(2)-O(13)	84.0(3)
O(6)-W(2)-O(3)	95.9(3)	O(7)-W(2)-O(13)	73.0(2)
O(7)-W(2)-O(3)	149.8(3)	O(3)-W(2)-O(13)	85.5(2)
O(1)-W(2)-O(4)	95.7(3)	O(4)-W(2)-O(13)	77.4(2)
O(6)-W(2)-O(4)	159.2(3)		
O(12)-W(3)-O(13)	102.2(3)	O(18)-W(3)-O(17)	84.8(3)
O(12)-W(3)-O(11)	103.8(3)	O(12)-W(3)-O(26)#1	171.4(2)
O(13)-W(3)-O(11)	92.4(3)	O(13)-W(3)-O(26)#1	83.3(2)
O(12)-W(3)-O(18)	99.1(3)	O(11)-W(3)-O(26)#1	82.4(2)
O(13)-W(3)-O(18)	157.7(3)	O(18)-W(3)-O(26)#1	74.8(2)
O(11)-W(3)-O(18)	88.7(3)	O(17)-W(3)-O(26)#1	73.5(2)
O(12)-W(3)-O(17)	100.1(3)	O(12)-W(3)-Na(5)	31.1(2)
O(13)-W(3)-O(17)	85.1(3)	O(13)-W(3)-Na(5)	74.0(2)
O(11)-W(3)-O(17)	155.9(3)	O(11)-W(3)-Na(5)	117.58(19)
O(17)-W(3)-Na(5)	84.8(2)	O(18)-W(3)-Na(5)	124.7(2)
O(26)#1-W(3)-Na(5)	149.77(16)		
O(10)-W(4)-O(9)	102.4(3)	O(10)-W(4)-O(27)#1	87.6(3)
O(10)-W(4)-O(19)	99.2(3)	O(9)-W(4)-O(27)#1	169.8(3)
O(9)-W(4)-O(19)	94.5(3)	O(19)-W(4)-O(27)#1	82.4(2)
O(10)-W(4)-O(8)	95.5(3)	O(8)-W(4)-O(27)#1	83.1(3)
O(9)-W(4)-O(8)	97.1(3)	O(10)-W(4)-O(11)	162.6(3)
O(19)-W(4)-O(8)	158.8(3)	O(9)-W(4)-O(11)	92.6(3)
O(8)-W(4)-O(11)	73.8(2)	O(19)-W(4)-O(11)	88.0(2)
O(27)#1-W(4)-O(11)	77.6(2)		
O(15)-W(5)-O(14)	102.9(3)	O(14)-W(5)-O(13)	93.2(3)

O(15)-W(5)-O(16)	96.8(3)	O(16)-W(5)-O(13)	88.5(2)
O(14)-W(5)-O(16)	94.4(3)	O(7)-W(5)-O(13)	75.3(2)
O(15)-W(5)-O(7)	96.2(3)	O(15)-W(5)-O(28)#1	89.4(3)
O(14)-W(5)-O(7)	95.7(3)	O(14)-W(5)-O(28)#1	167.6(3)
O(16)-W(5)-O(7)	161.3(3)	O(16)-W(5)-O(28)#1	82.7(2)
O(15)-W(5)-O(13)	162.6(3)	O(7)-W(5)-O(28)#1	84.0(3)
O(13)-W(5)-O(28)#1	74.8(2)		
O(24)-W(6)-O(23)	102.5(3)	O(23)-W(6)-O(26)#1	84.2(2)
O(24)-W(6)-O(16)	101.9(3)	O(16)-W(6)-O(26)#1	79.5(2)
O(23)-W(6)-O(16)	93.8(3)	O(22)-W(6)-O(26)#1	75.7(2)
O(24)-W(6)-O(22)	102.3(3)	O(17)-W(6)-O(26)#1	74.0(2)
O(23)-W(6)-O(22)	87.6(3)	O(24)-W(6)-Na(8)	34.2(3)
O(16)-W(6)-O(22)	154.9(3)	O(23)-W(6)-Na(8)	73.5(3)
O(24)-W(6)-O(17)	99.1(3)	O(16)-W(6)-Na(8)	121.2(3)
O(23)-W(6)-O(17)	157.6(3)	O(22)-W(6)-Na(8)	83.2(2)
O(16)-W(6)-O(17)	87.4(3)	O(17)-W(6)-Na(8)	124.4(2)
O(22)-W(6)-O(17)	82.1(3)	O(26)#1-W(6)-Na(8)	149.9(2)
O(24)-W(6)-O(26)#1	173.0(3)		
O(20)-W(7)-O(21)	102.4(3)	O(19)-W(7)-O(18)	84.3(3)
O(20)-W(7)-O(19)	102.8(3)	O(22)-W(7)-O(18)	82.9(3)
O(21)-W(7)-O(19)	93.5(3)	O(20)-W(7)-O(26)#1	174.5(3)
O(20)-W(7)-O(22)	100.5(3)	O(21)-W(7)-O(26)#1	81.8(2)
O(21)-W(7)-O(22)	89.5(3)	O(19)-W(7)-O(26)#1	80.2(2)
O(19)-W(7)-O(22)	155.2(3)	O(22)-W(7)-O(26)#1	75.9(2)
O(20)-W(7)-O(18)	101.7(3)	O(18)-W(7)-O(26)#1	73.9(2)
O(21)-W(7)-O(18)	155.6(3)		1.932(6)

Symmetry transformations used to generate equivalent atoms: #1 -x+1,-y+2,-z+1; #2 -x+1,-y+1,-z+1; #3 x,y-1,z; #4 x-1,y,z; #5 -x+1,-y+1,-z; ;#6 x,y+1,z; #7 -x,-y+2,-z+1; #8 x+1,y,z; #9 -x,-y+1,-z+1

5.3 Results and Discussion

5.3.1 Synthesis

Complex **5.1** is prepared from reaction of $Na_2WO_4{\cdot}2H_2O$ and Na_2HPO_4 followed by addition of $Mn^{III}(CH_3COO)_3{\cdot}2H_2O$ and isolated before decomposition by addition of potassium ion (see Experimental section for details). In the one other report of heptatungstate, this defect POM was prepared both by reaction of $Na_2WO_4{\cdot}2H_2O$ and Na_2HPO_4 and from transformation of A-$PW_9O_{34}^{9-}$ or $P_2W_5O_{23}^{6-}$.

5.3.2 Structure

Single crystal X-ray diffraction shows that **5.1** contains the structurally novel polyanion, $[Mn_{III}(HPW_7O_{28})_2]^{13-}$ (**1** for convenience), constituted by a high-valent manganese sandwiched between two symmetry-equivalent heptatungstate polyanions, $[HPW_7O_{28}]^{8-}$ (**1** has overall C_{2h} symmetry; Figures 1a and 1b). The manganese ion is coordinated to each polyoxoanion unit by two Mn-O-W bonds and one Mn-O-P bond. The bond distances between central Mn^{III} ion and the symmetry-distinct oxygens are quite different (1.916(7), 1.932(7), and 2.177(6) Å), confirming the presence of a Jahn-Teller distorted d^4 Mn^{III} ion; both d^3 Mn^{IV} and h.s. d^5 Mn^{II} centers don't display such distortions. The heptatungstate polyanion, $[HPW_7O_{28}]^{8-}$, framework can be considered as containing two belts; one is an edge-shared W_3O_{13} triad, a very common feature in polyanion chemistry, and the other is constituted by four edge-shared WO_6 octahedra which are corner sharing via two P-O-W bonds to a PO_4 tetrahedron. These two belts are also connected by four corner-sharing W-O-W bonds. Bond valence sum (BVS) calculations for **5.1** indicate that the bridging oxygen, O4, between W1 and W2 (**Figure 1**)

is monoprotonated as it is in the published complex, $[HPW_7O_{28}Ru(dmso)_3]^{6-}$. [12] The value for Mn is 3.2 consistent with the +3 oxidation state.

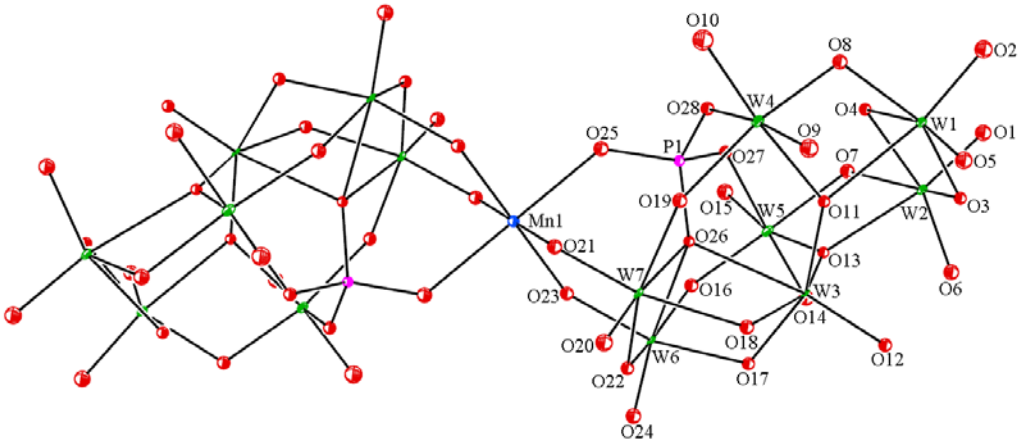

(a)

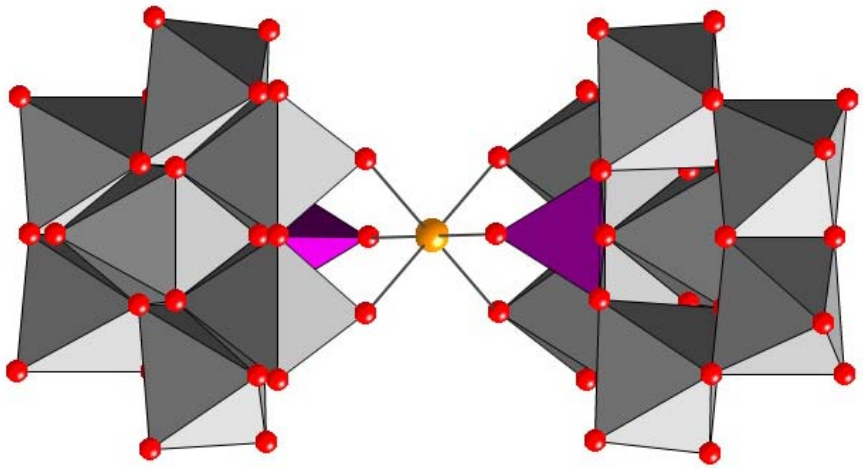

(b)

Figure 5.1. (a) An ADP plot (30% probability ellipsoids) of $[Mn^{III}(HPW_7O_{28})_2]^{13-}$ in $Na_{13}(HPW_7O_{28})_2 \cdot 39H_2O$ with atom numbering. (b) Polyanion **1** in polyhedral notation, showing the C_{2h} symmetry (Mn^{III} is in ball-and-stick notation; gray, W; purple, P; orange, Mn^{III}).

5.3.3 IR Characterization

The infrared spectrum of **5.1** (**Figure 2**) shows a split ν_3 vibrational mode of the central PO_4 indicating a lowering of the symmetry of the central PO_4 below T_d. The peaks in the low energy regime (<1000 cm^{-1}) are attributed to the characteristic $\nu(W–O_d)$, $\nu(O_b–W–O_b)$ and $\nu(W–O_c)$ absorptions.

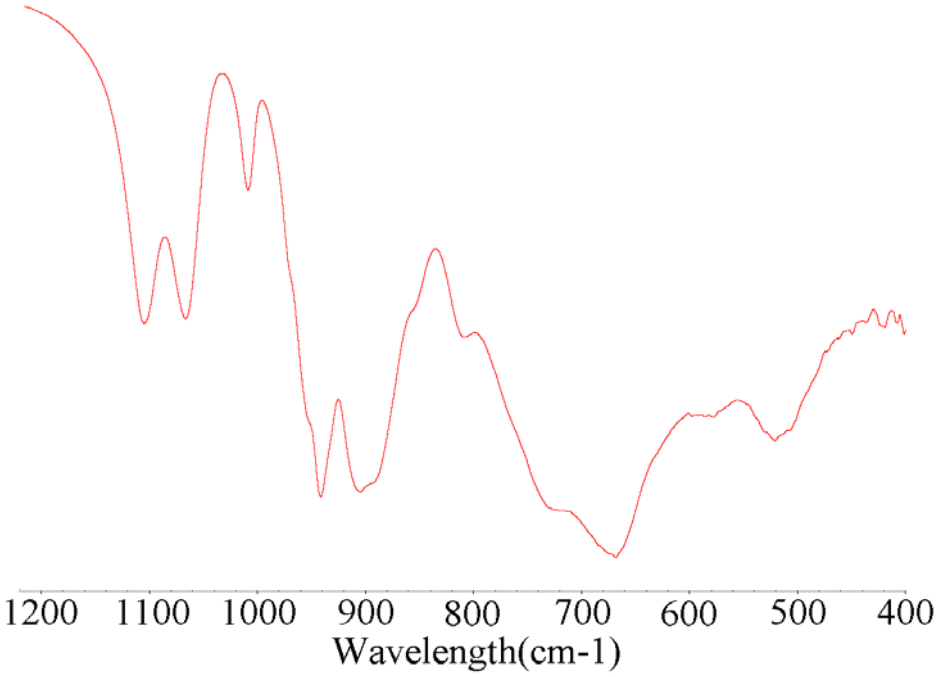

Figure 5.2. IR spectra of **5.1**. Sample is ca. 2 wt % in KBr.

5.3.4 Cation exchange of 5.1

Significantly, $PW_7O_{28}^{8-}$ has the highest negative charge density of any polytungstate (see Table 3) and by extension $[Mn^{III}(HPW_7O_{28})_2]^{13-}$ (**1**) has one of the highest charge densities of any TMSP complex. The solution metathesis chemistry of **5.1** reflects this. Although **5.1** decomposes slowly in aqueous solution (see below), it lives sufficiently long for both the standard precipitation and extraction metathesis reactions to be conducted. However, both fail because of the very high polyanion charge densities: the smaller quaternary cation salts of **1** such as (*n*-Bu_4N)**1** are too water soluble to precipitate and the larger hydrophobic quaternary cations such as *n*-$Hept_4N^+$ do not extract **1** into toluene. The inability to make solutions of **1** in organic solvents precludes assessment of the homogeneous catalytic oxidation properties of **1** in such media.

5.3.5 Solution chemistry of 5.1

Both UV-vis and ^{31}P NMR were used to study the stability of **5.1** in aqueous solution. The isosbestic point in the Uv-vis spectra (**Figure 5.3**) shows that **5.1** decays cleanly to another species initially. This decay is exponential with a pseudo-first-order rate constant of $7.3\pm0.1 \times 10^{-3}$ s^{-1}. Despite the paramagnetism of **5.1** (see below), its instability in solution can also be studied by ^{31}P NMR spectroscopy. A solution of **5.1** in D_2O at ambient temperature decomposes in 10 min to form a new paramagnetic species plus $HPW_7O_{28}^{8-}$ (**Figure 5.4**). **Figures 5.7a and 5.7b** give the spectra of the products after 24h at two different acquisition and delay times confirming the presence of the paramagnetic product. The initial $HPW_7O_{28}^{8-}$ product transforms first into A-α-$PW_9O_{34}^{9-}$, $P_2W_5O_{23}^{6-}$ and $PW_{11}O_{39}^{7-}$ and finally, after 24h, into only $PW_{11}O_{39}^{7-}$ (**Figures 5.5, 5.6a, 5.6b, 5.7a and 5.7b**). Despite efforts, we have not yet been able to identify the

paramagnetic product; however, its spectral properties rule out the known Mn-containing POMs: $Mn_4(H_2O)_2(B\text{-}\alpha\text{-}PW_9O_{34})_2^{10-}$, $MnPW_{11}O_{39}^{5-}$, $[(Mn(OH_2)_2)_3(A\text{-}\alpha\text{-}PW_9O_{34})_2]^{12-}$ and $[((MnOH_2)Mn_2PW_9O_{34})_2(PW_6O_{26})]^{17-}$ (**Figure5. 8**).

Table 5.3. Charge density (negative charge/total atoms) on polyoxoanions

Polyoxoanion		Charge density (negative charge/atoms)
$PW_{12}O_{40}^{3-}$		0.057
$PW_{11}O_{39}^{7-}$	$AsW_{11}O_{39}^{7-}$	0.137
$PW_{10}O_{36}^{7-}$	$AsW_{10}O_{36}^{7-}$	0.149
$PW_9O_{34}^{9-}$	$AsW_9O_{34}^{9-}$	0.205
$PW_7O_{28}^{9-}$	$AsW_7O_{28}^{9-}$	0.250
$SbW_9O_{33}^{9-}$	$AsW_9O_{33}^{9-}$	0.209
$SbW_{11}O_{39}^{7-}$		0.137
$TeW_9O_{33}^{8-}$		0.186
$SiW_{12}O_{40}^{4-}$	$GeW_{12}O_{40}^{4-}$	0.075
$SiW_{11}O_{39}^{8-}$	$GeW_{11}O_{39}^{8-}$	0.157
$SiW_{10}O_{36}^{8-}$	$GeW_{10}O_{36}^{8-}$	0.170
$SiW_9O_{34}^{10-}$	$GeW_9O_{34}^{10-}$	0.227
$AlW_{12}O_{40}^{5-}$		0.094
$AlW_{11}O_{39}^{9-}$		0.176
$BW_{12}O_{40}^{5-}$		0.094
$BW_{11}O_{39}^{9-}$		0.176
$P_2W_{21}O_{71}^{6-}$		0.064
$P_2W_{20}O_{70}^{10-}$	$As_2{}^{V}W_{20}O_{70}^{10-}$	0.109
$P_2W_{19}O_{69}^{14-}$		0.156
$As_2{}^{V}W_{20}O_{71}(H_2O)_3^{12-}$		0.118
$As^{III}{}_2W_{21}O_{69}(H_2O)^{6-}$		0.063
$As^{III}{}_2W_{20}O_{68}(H_2O)^{10-}$		0.108
$As^{III}{}_2W_{19}O_{67}^{14-}$		0.159
$P_2W_{18}O_{62}^{6-}$	$As_2W_{18}O_{62}^{6-}$	0.073
$P_2W_{17}O_{61}^{10-}$	$As_2W_{17}O_{61}^{10-}$	0.125
$P_2W_{15}O_{56}^{12-}$	$As_2W_{15}O_{56}^{12-}$	0.164
$P_2W_{12}O_{48}^{14-}$	$As_2W_{12}O_{48}^{14-}$	0.226
$Nb_2W_4O_{19}^{4-}$	$V_2W_4O_{19}^{4-}$	0.150
$NbW_5O_{19}^{3-}$	$VW_5O_{19}^{3-}$	0.120

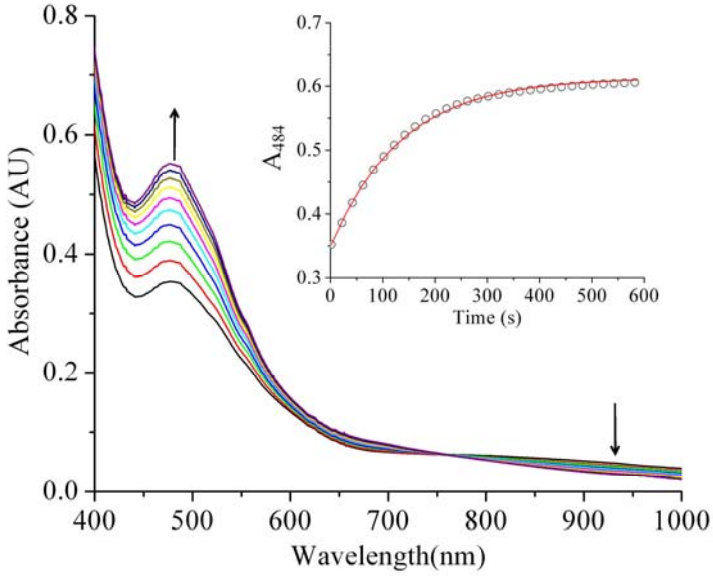

Figure 5.3. Time profile of electronic absorption spectra of 2.4 mM **5.1** in water at 25 °C showing the decay of **5.1**. For clarity, not all spectra are shown in this figure. The monomolecular reaction rate constant obtained from fitting of the absorbance at 484 nm is 7.3±0.1 × 10^{-3} s^{-1}. The fitting at 484 nm is shown in the inset: experimental points -(o); the fitting curve-(solid red line).

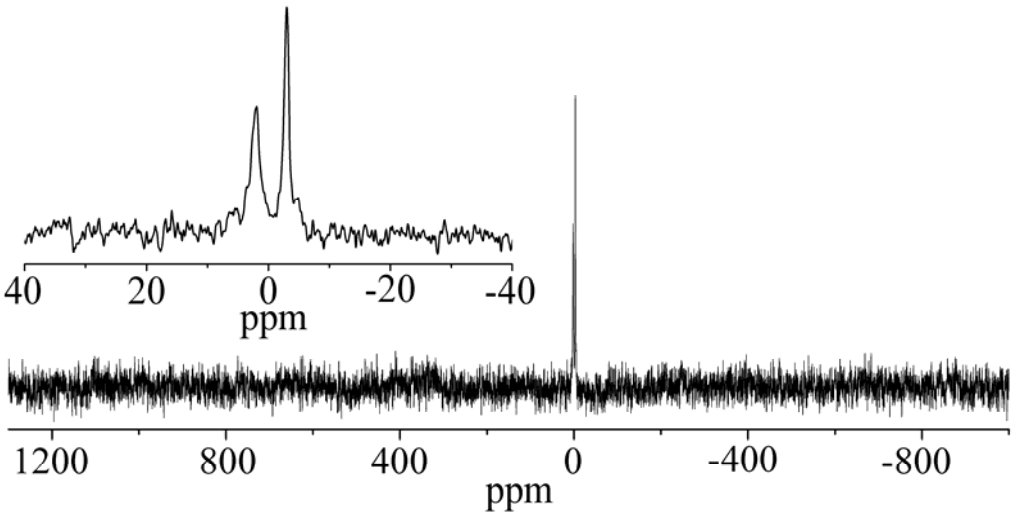

Figure 5.4. ^{31}P NMR of **5.1** in D_2O 10 min after dissolution (paramagnetic acquisition parameters: acq. time: 24 ms; line broadening: 100 Hz; relaxation delay: 0 s).

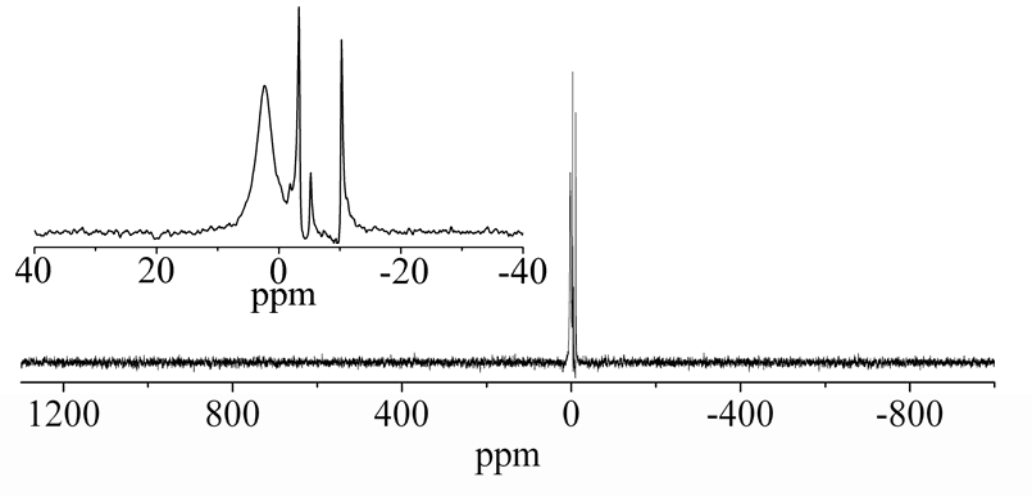

Figure 5.5a. ^{31}P NMR of **5.1** in D_2O 2h after dissolution (paramagnetic acquisition parameters: acq. time: 24 ms; line broadening: 100 Hz; relaxation delay: 0 s).

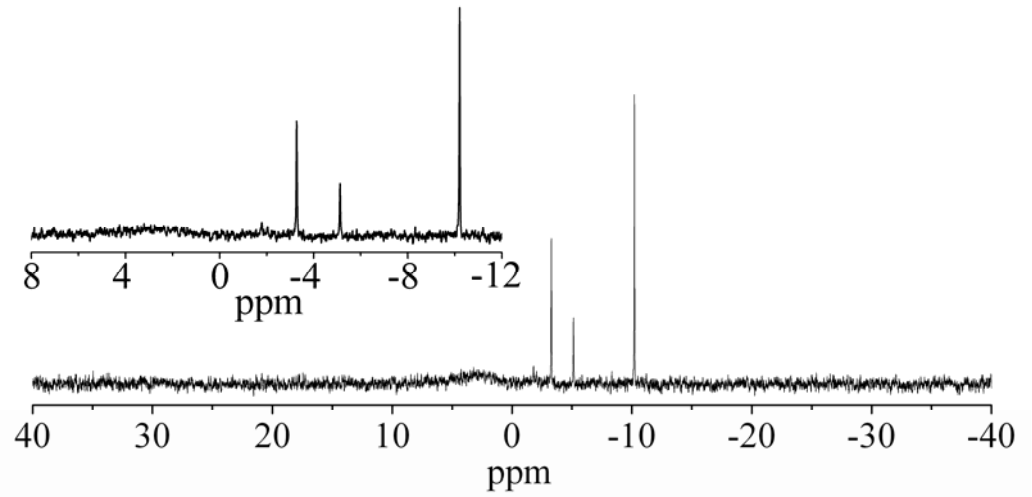

Figure 5.5b. ^{31}P NMR of **5.1** in D_2O 2.0 h after dissolution (diamagnetic acquisition parameters: acq. time: 1.2 s; line broadening: 3 Hz; relaxation delay: 0.4 s).

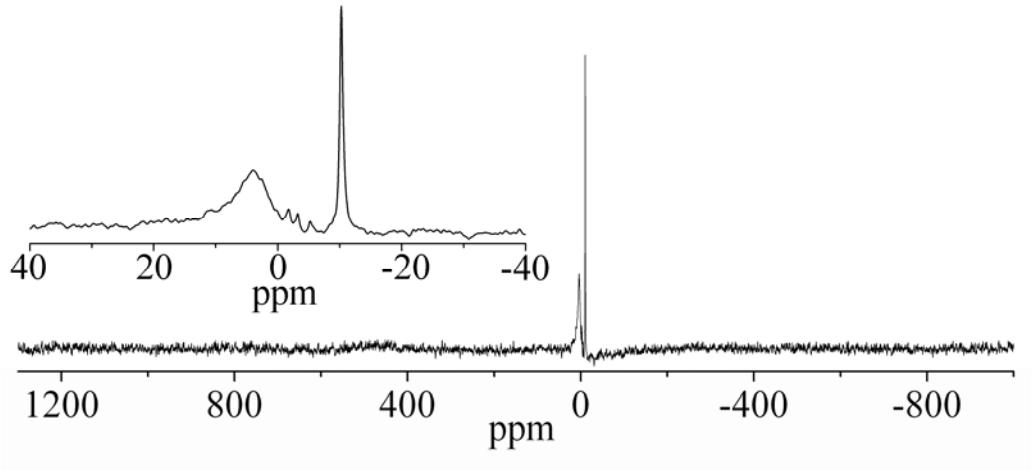

Figure 5.6a. ^{31}P NMR of **5.1** in D_2O 4h after dissolution (paramagnetic acquisition parameters: acq. time: 24 ms; line broadening: 100 Hz; relaxation delay: 0 s).

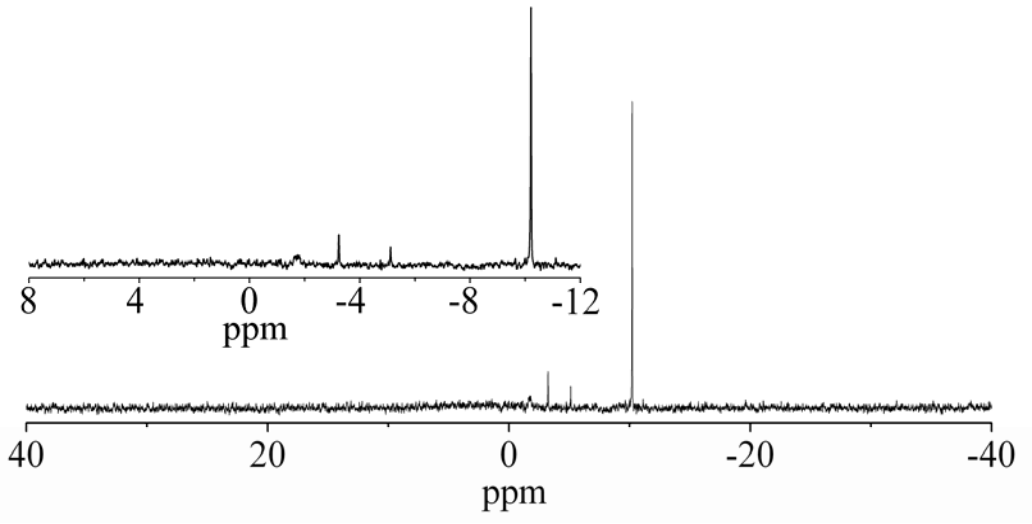

Figure 5.6b. ^{31}P NMR of **5.1** in D_2O 4h after dissolution (diamagnetic acquisition parameters: acq. time: 1.2 s; line broadening: 3 Hz; relaxation delay: 0.4 s).

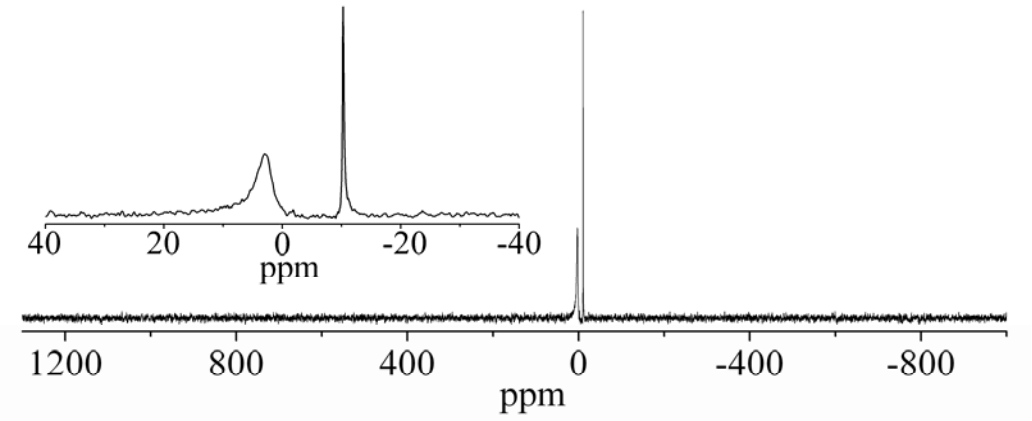

Figure 5.7a. ^{31}P NMR of **5.1** in D_2O 24h after dissolution using paramagnetic data acquisition parameters (acq. time: 24 ms; line broadening: 100 Hz; relaxation delay: 0 s)

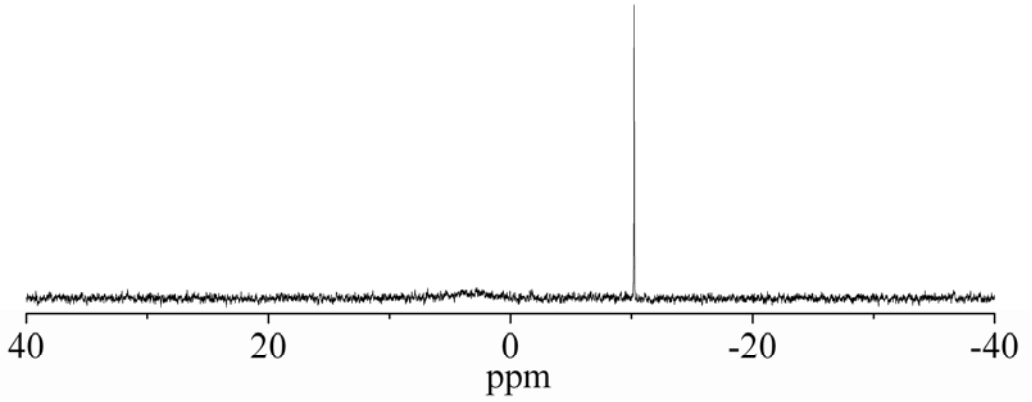

Figure 5.7b. ^{31}P NMR of **5.1** in D_2O 24h after dissolution using diamagnetic parameters (acq. time: 1.2 s; line broadening: 3 Hz; relaxation delay: 0.4 s).

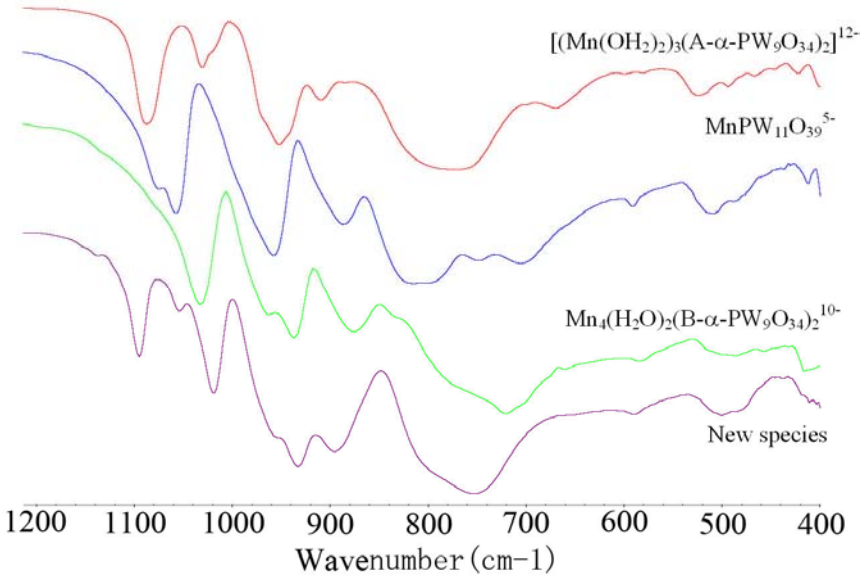

Figure 5.8. FTIR spectra of Mn-containing polytungstophosphates.

5.3.6 Magnetic property of 5.1

Figure 5.9 gives the temperature dependence (2-300K) of the magnetic susceptibility, $\chi_m T$ of **5.1** with an applied field of 1000 Oe. The $\chi_m T$ value at room temperature is 2.96 emu K mol^{-1}, in accord with the expected value (3.00 emu K mol^{-1}) for one isolated spin-only Mn^{III} center (s = 2, g = 2.0). Upon cooling, $\chi_m T$ decreases smoothly from 300 K to 50 K, then drops abruptly to 1.81 emu K mol^{-1} at 2 K, indicating the presence of an antiferromagnetic interaction between the magnetic centers. The $1/\chi_m$ versus T plot (**Figure 5.9 inset**) for **5.1** could be fit with Curie-Weiss equation from 2 to 300K, affording C = 2.98 emu K mol^{-1} and θ = -3.29. The small negative Weiss constant indicates an expectedly weak antiferromagnetic interaction between the well separated nearest Mn(III) atoms in adjacent **1** polyanions.

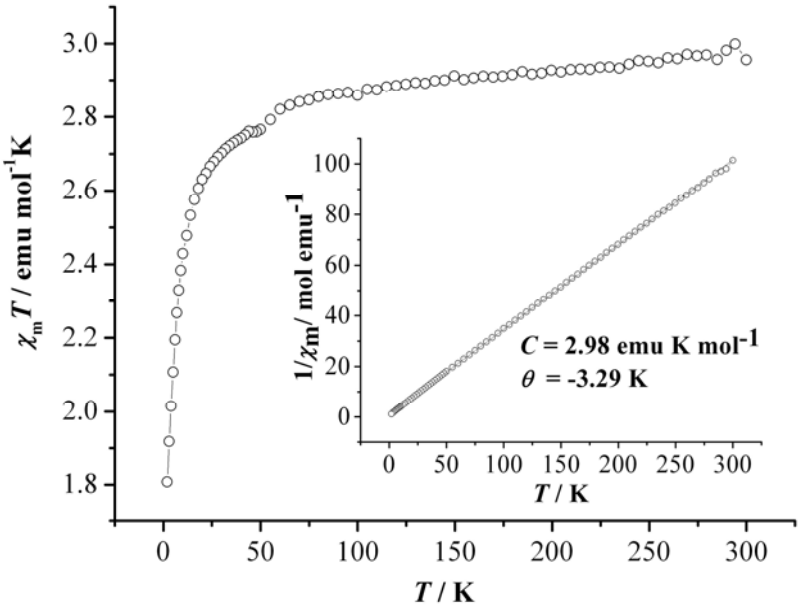

Figure 5.9. Temperature dependence of $\chi_m T$ for **5.1**. Inset: temperature dependence of $1/\chi_m$ for **5.1**. The solid lines are the best fits to the Curie-Weiss law.

5.4 Conclusions

Sandwich-type POM **5.1,** constructed from heptatungstophosphate $[HPW_7O_{28}]^{8-}$ units and Mn^{III} ion has been synthesized and characterized by infraed spectroscopy, elemental analysis, and X-ray crystallography. The stability of **5.1** was studied by both UV-vis spectroscopy and ^{31}P NMR spectroscopy. Compound **5.1** demonstrates that heptatungstate can ligate a 3d metal and represents a rare case of polyoxometalate-based sandwich complex with a single bridging metal.

References

(1) Pope, M. T.; Müller, A. *Angew. Chem. Int. Ed. Engl.* **1991**, *30*, 34.

(2) Hill, C. L. *Chem. Rev.* **1998**, *98*, 1.

(3) *Polyoxometalate Chemistry From Topology via Self-Assembly to Applications*; Pope, M. T.; Müller, A., Eds.; Kluwer Academic Publishers: Dordrecht, 2001.

(4) Yamase, T.; Pope, M. T. In *Nanostructure Science and Technology*; Lockwood, D. J., Ed.; Kluwer Academic/Plenum Publishers: New York, 2002; Vol. 2.

(5) Borrás-Almenar, J. J.; Coronado, E.; Müller, A.; Pope, M. T. *Polyoxometalate Molecular Science*; Kluwer Academic Publishers: Dordrecht, 2003; Vol. 98.

(6) Pope, M. T. In *Comprehensive Coordination Chemistry II: From Biology to Nanotechnology*; Wedd, A. G., Ed.; Elsevier Ltd.: Oxford, UK, 2004; Vol. 4, p 635.

(7) Cronin, L. In *Comprehensive Coordination Chemistry II: From the Molecular to the Nanoscale: Synthesis, Structure, and Properties*; McCleverty, J. A., Meyer, T. J., Eds.; Elsevier: Amsterdam, 2004; Vol. 7, p 1.

(8) Hill, C. L. In *Comprehensive Coordination Chemistry-II: From Biology to Nanotechnology*; Wedd, A. G., Ed.; Elsevier Ltd.: Oxford, UK, 2004; Vol. 4, p 679.

(9) Hill, C. L.; Prosser-McCartha, C. M. *Coord. Chem. Rev.* **1995**, *143*, 407.

(10) Okuhara, T.; Mizuno, N.; Misono, M. In *Advances in Catalysis* 1996; Vol. 41, p 113.

(11) Katsoulis, D. E. *Chem. Rev.* **1998**, *98*, 359.

(12) Mizuno, N.; Misono, M. *Chem. Rev.* **1998**, *98*, 199.

(13) Kozhevnikov, I. V. *Chem. Rev.* **1998**, *98*, 171.

(14) Neumann, R. *Prog. Inorg. Chem.* **1998**, *47*, 317.

(15) Müller, A.; Das, S. K.; Kuhlmann, C.; Bögge, H.; Schmidtmann, M.; Diemann, E.; Krickemeyer, E.; Hormes, J.; Modrow, H.; Schindler, M. *Chem. Commun.* **2001**, 655.

(16) Moffat, J. B. *Metal-Oxygen Clusters: The Surface and Catalytic Properties of Heteropoly Oxometalates.*; Kluwer Academic/Plenum Publishers: New York, 2001; Vol. 9.

(17) Kozhevnikov, I. V. *Catalysis by Polyoxometalates*; Wiley: Chichester, England, 2002; Vol. 2.

(18) Hill, C. L. *J. Mol. Catal. A: Chem.* **2007**, *262*, 2.

(19) Alhanash, A.; Kozhevnikova, E. F.; Kozhevnikov, I. V. *Catal. Lett.* **2008**, *120(3-4)*, 307.

(20) Coronado, E.; Gómez-García, C. J. *Chem. Rev.* **1998**, *98*, 273.

(21) Müller, A.; Peters, F.; Pope, M. T.; Gatteschi, D. *Chem. Rev.* **1998**, *98*, 239.

(22) Clemente-Juan, J. M.; Coronado, E. *Coord. Chem. Rev.* **1999**, *193-195*, 361.

(23) Ouahab, L.; Golhen, S.; Triki, S. In *Polyoxometalate Chemistry* 2001, p 205.

(24) Kögerler, P.; Muller, A. *J. Appl. Phys.* **2003**, *93(10)*, 7101.

(25) Chilas, G. I.; Stylianou, M.; Kubicki, M.; Vaimakis, T.; Kögerler, P.; Keramidas, A. D.; Kabanos, T. A. *Inorg. Chem.* **2008**, *47(11)*, 4451.

(26) *Polyoxometalates: From Platonic Solids to Anti-retroviral Activity*; Pope, M. T.; Müller, A., Eds.; Kluwer Academic Publishers: Dordrecht, Netherlands, 1993.

(27) Yamase, T.; Fujita, H.; Fukushima, K. *Inorg. Chim. Acta* **1988**, *151*, 15.

(28) Hill, C.; Weeks, M.; Hartnup, M.; Sommadossi, J.-P.; Schinazi, R. *Ann. N. Y. Acad. Sci.* **1990**, *616*, 528.

(29) Hill, C. L.; Weeks, M. S.; Schinazi, R. F. *Cjacs* **1990**, *33*, 2767.

(30) Yamase, T. In *Polymeric Materials Encyclopedia*; Salamone, J. C., Ed.; CRC Press: Boca Raton, 1996, p 365.

(31) Rhule, J. T.; Hill, C. L.; Judd, D. A.; Schinazi, R. F. *Chem. Rev.* **1998**, *98*, 327.

(32) Rhule, J. T.; Hill, C. L.; Zheng, Z.; Schinazi, R. F. In *Topics in Biological Inorganic Chemistry*; Clarke, M. J., Sadler, P. J., Eds.; Springer-Verlag: Heidelberg, 1999; Vol. 2: Metallopharmaceuticals, p 117.

(33) Mueller, C. E.; Iqbal, J.; Baqi, Y.; Zimmermann, H.; Roellich, A.; Stephan, H. *Bioorg. Med. Chem. Lett.* **2006**, *16(23)*, 5943.

(34) Prudent, R.; Moucadel, V.; Laudet, B.; Barette, C.; Lafanechere, L.; Hasenknopf, B.; Li, J.; Bareyt, S.; Lacote, E.; Thorimbert, S.; Malacria, M.; Gouzerh, P.; Cochet, C. *Chem. & Bio.* **2008**, *15(7)*, 683.

(35) Seko, A.; Yamase, T.; Yamashita, K. *J. Inorg. Biochem.* **2009**, *103(7)*, 1061.

(36) Bi, L.-H.; Kortz, U.; Keita, B.; Nadjo, L.; Borrmann, H. *Inorg. Chem.* **2004**, *43*, 8367.

(37) Lyon, D. K.; Miller, W. K.; Novet, T.; Domaille, P. J.; Evitt, E.; Johnson, D. C.; Finke, R. G. *J. Am. Chem. Soc.* **1991**, *113*, 7209.

(38) Mansuy, D.; Bartoli, J.-F.; Battioni, P.; Lyon, D. K.; Finke, R. G. In *J. Am. Chem. Soc.* 1991; Vol. 113, p 7222.

(39) Ruhlmann, L.; Canny, J.; Contant, R.; Thouvenot, R. *Inorg. Chem.* **2002**, *41*, 3811.

(40) Geletii, Y. V.; Botar, B.; Kögerler, P.; Hillesheim, D. A.; Musaev, D. G.; Hill, C. L. *Angew. Chem. Int. Ed.* **2008**, *47*, 3896.

(41) Geletii, Y. V.; Huang, Z.; Hou, Y.; Musaev, D. G.; Lian, T.; Hill, C. L. *J. Am. Chem. Soc.* **2009**, *131*, 7522.

(42) Sartorel, A.; Carraro, M.; Scorrano, G.; Zorzi, R. D.; Geremia, S.; McDaniel, N. D.; Bernhard, S.; Bonchio, M. *J. Am. Chem. Soc* **2008**, *130*, 5006.

(43) Cao, R.; Ma, H.; Geletii, Y. V.; Hardcastle, K. I.; Hill, C. L. *Inorg. Chem.* **2009**, *48*, 5596.

(44) Weakley, T. J. R.; Evans, H. T., Jr.; Showell, J. S.; Tourné, G. F.; Tourné, C. M. *J. Chem. Soc. Chem. Comm.* **1973**, *4*, 139.

(45) Casañ-Pastor, N.; Bas-Serra, J.; Coronado, E.; Pourroy, G.; Baker, L. C. W. *J. Am. Chem. Soc.* **1992**, *114*, 10380.

(46) Clemente-Juan, J. M.; Coronado, E.; Galán-Mascarós, J., J. R. ; Gómez-García, C. J. *Inorg. Chem.* **1999**, *38*, 55.

(47) Kortz, U.; Isber, S.; Dickman, M. H.; Ravot, D. *Inorg. Chem.* **2000**, *39*, 2915.

(48) Kortz, U.; Nellutla, S.; Stowe, A. C.; Dalal, N. S.; Rauwald, U.; Danquah, W.; Ravot, D. *Inorg. Chem.* **2004**, *43*, 2308.

(49) Bassil, B. S.; Dickman, M. H.; Kortz, U. *Inorg. Chem.* **2006**, *45*, 2394.

(50) Finke, R. G.; Droege, M. W. *Inorg. Chem.* **1983**, *22*, 1006.

(51) Finke, R. G.; Droege, M. W.; Domaille, P. J. *Inorg. Chem.* **1987**, *26*, 3886.

(52) Weakley, T. J. R.; Finke, R. G. *Inorg. Chem.* **1990**, *29*, 1235.

(53) Gómez-García, C. J.; Borrás-Almenar, J. J.; Coronado, E.; Ouahab, L. *Inorg. Chem.* **1994**, *33*, 4016.

(54) Finke, R. G.; Weakley, T. J. R. *Journal of Chemical Crystallography* **1994**, *24*, 123.

(55) Kirby, J. F.; Baker, L. C. W. *J. Am. Chem. Soc.* **1995**, *117*, 10010.

(56) Crano, N. J.; Chambers, R. C.; Lunch, V. M.; Fox, M. A. *J. Mol. Catal. A.* **1996**, *114*, 65.

(57) Zhang, X.; Chen, Q.; Duncan, D. C.; Campana, C.; Hill, C. L. *Inorg. Chem.* **1997**, *36*, 4208.

(58) Song, W.; Wang, X.; Liu, Y.; Liu, J.; Xu, H. *J. Electroanal. Chem.* **1999**, *476*, 85.

(59) Zhang, X.; Anderson, T. M.; Chen, Q.; Hill, C. L. *Inorg. Chem.* **2001**, *40*, 418.

(60) Anderson, T. M.; Hardcastle, K. I.; Okun, N.; Hill, C. L. *Inorg. Chem.* **2001**, *40*, 6418.

(61) Gaunt, A. J.; May, I.; Collison, D.; Holman, K. T.; Pope, M. T. *J. Mol. Struct.* **2003**, *656*, 101.

(62) Botar, B.; Geletii, Y. V.; Kögerler, P.; Musaev, D. G.; Morokuma, K.; Weinstock, I. A.; Hill, C. L. *J. Am. Chem. Soc.* **2006**, *128*, 11268.

(63) Botar, B.; Kögerler, P.; Hill, C. L. *Inorg. Chem.* **2007**, *46*, 5398.

(64) Hussain, F.; Bassil, B. S.; Bi, L.; Reicke, M.; Kortz, U. *Angew. Chem., Int. Ed. Engl.* **2004**, *43*, 3485.

(65) Bassil, B. S.; Nellutla, S.; Kortz, U.; Stowe, A. C.; Tol, J. v.; Dalal, N. S.; Keita, B.; Nadjo, L. *Inorg. Chem.* **2005**, *44*, 2659.

(66) Bassil, B. S.; Kortz, U.; Tigan, A. S.; Clemente-Juan, J. M.; Keita, B.; deOliveira, P.; Nadjo, L. *Inorg. Chem.* **2005**, *44*, 9360.

(67) Peacock, R. D.; Weakley, T. J. R. *J. Chem. Soc. A* **1971**, 1836.

(68) Zhang, C.; Robertha, C.; Howell, K. B.; Scotland, F. G.; Perez, L. T.; Lynn, C. F. *Inorg. Chem.* **2004**, *43*, 7691.

(69) Kato, C. N.; Shinohara, A.; Hayashi, K.; Nomiya, K. *Inorg. Chem.* **2006**, *45*, 8108.

(70) Bi, L.-H.; Dickman, M. H.; Kortz, U.; Dix, I. *Chem Comm* **2005**, 3962.

(71) Bruker AXS, I.; Analytical X-ray Sysems: Madison, WI, 2003.

(72) Bruker AXS, I.; Analytical X-Ray Sytems: Madison, WI, 2003.

(73) Bruker AXS, I. Madison, WI, 2003.

(74) SADABS, S., G.; 2.10 ed. **2003**.